NPP Sounding Group Evaluation Report

L. Larrabee Strow (UMBC), William Blackwell (MIT/LL), Evan Fishbein (JPL),
Bjorn Lambrigtsen (JPL)[1], and Hank Revercomb (UW-SSEC)

Tuesday 9th April, 2013

[1] B. Lambrigsten's contributions are appended to this report.

1 Executive Summary

The performance of the Cross-track Infrared Sensor (CrIS) and Advanced Technology Microwave Sounder (ATMS) flying on Suomi-NPP, and the quality of the NOAA IDPS products derived from these sensors are evaluated here. Both sensors are performing extremely well in orbit, clearly producing Sensor Data Records (SDRs) sufficiently accurate for Numerical Weather Prediction (NWP) applications. Further, it is clear that the CrIS instrument is very well suited to continue, and in several ways to improve on, the high accuracy climate record from high resolution IR spectra begun by the AIRS instrument on the NASA EOS Aqua platform. This being said, a number of small liens on the the CrIS and ATMS SDRs produced by the NOAA/IDPS will limit their utility for climate research, and further analysis of the SDRs (and their associated algorithms) is still needed for a full understanding of the climate quality of these records.

The performance of the Cross-track Infrared Microwave Sounding Suite (CrIMSS) Earth Data Records (EDRs) is not on par with the SDRs. The NOAA/IDPS production of CrIMSS EDRs uses a version of the retrieval algorithm that includes little CrIS input, and thus here we only present an analysis of the IP microwave-only retrievals. The EDR algorithm is a Bayesian retrieval algorithm using a climatology background. At this time, the microwave-only products contain a significant contribution from the climatology background for complex reasons outlined in this report, limiting its usefullness for climate research. The EDR algorithm will be updated at the NOAA/IDPS to fully use the CrIS sensor in June 2013. A complete assessment of the full CrIS/ATMS IDPS EDRs will be made in the final year of the current Science Team.

The CrIS sensor records a large portion of the earth's thermal infrared emission, and is sensitive to a wide range of geophysical variables not retrieved within the NOAA/IDPS environment. We outline here how other EOS products produced by the Tropospheric Emission Spectrometer (TES, flying on AURA), the Measurements of Pollution in the Troposphere (MOPITT), and the Atmospheric Infrared Sounder (AIRS) can be extended into longer-term climatologies using CrIS. Finally, we suggest that the CrIS radiance record, combined with the AIRS record, *may* be able to achieve some of the (longwave) science goals of the CLimate Absolute Radiance and Refractivity Observatory (CLARREO) Decadal Survey mission, but with a data record starting in 2002.

1.1 Sensor and SDR Characterization

- The CrIS and ATMS instruments are working very well, and exceed performance requirements needed for Numerical Weather Prediction (NWP) applications.
- The CrIS instrument radiometric performance is at the minimum comparable to that of its EOS predecessor thereby allowing the valuable high spectral resolution climate record from AIRS to be continued through the lifetime of Suomi NPP and JPSS.
- Minor liens exist for both the ATMS and CrIS SDR products for NWP applications. The suitability for CrIS/ATMS for climate trending is encouraging, more work is needed to establish absolute accuracy, stability and a full understanding of radiometric differences between these instrument's SDRs and those from NASA EOS-AQUA.
- The IDPS algorithm for CrIS SDR radiance calibration meets the accuracy and latency requirements for weather applications, but the implementation is unnecessarily complex, expensive to modify, and sub-optimal for climate applications.
- ATMS has inter-channel correlations unlike the AMSU on EOS-AQUA, but similar to the MHS series of instruments.

- ATMS has mildly degraded radiometric calibration for stray sunlight illuminating the calibration target when crossing the terminator. This is at the 0.01% level and has not been shown to influence the EDR.
- The ATMS radiances have stripping in the G-band and narrow-bandwidth V-band channels. The ATMS calibration algorithm operates sub-optimally to reduce stripping and this degrades radiometric stability in a TBD manner.
- CrIS will be placed in high spectral resolution mode in June 2013, allowing better spectral calibration of the short-wave band, retrieval of carbon monoxide, and better water vapor retrievals. However, the NOAA/IDPS will only store the full-length interferograms generated in high-resolution mode and will not produce high-resolution SDRs in the IDPS.

1.2 CrIMSS IDPS EDR Products

- The IDPS EDR products may be adequate for climate process studies, but further maturation of the IDPS algorithm implementation is necessary. There is some concern that the use of EOFs to represent the EDR profiles is limiting EDR accuracy.
- The assessment of the climate quality of CrIS EDR data is currently in progress and no final conclusions can yet been drawn regarding the product performance.
- It is clear that any geophysical climatology that spans both AIRS and CrIS will require a single unified EDR algorithm since (a) the AIRS and CrIMSS algorithms make many different assumptions, use different forward radiative transfer models, and have different first-guesses, and (b) the AIRS L2 algorithm is under re-consideration to move it from a 3-hour “weather” retrieval to a climate-level retrieval.

1.3 CrIS/ATMS Additional Products

- CrIS is capable of providing a number of products not produced by the NOAA/IDPS such as carbon monoxide, methane, ammonia, sulphur dioxide and ash from volcanic eruptions, cloud properties, dust optical depths, and surface emissivity. CrIS and IASI may provide the only path to extend the time series of of several of the AURA-TES and TERRA-MOPITT products into the future for climate applications.
- The hardware performance of CrIS suggests that AIRS + CrIS will be able to substantially augment the longwave radiance climatology from CLARREO by extending the start date to 2002 when AIRS began operation. The intercalibration techniques for tying CrIS and AIRS to the CLARREO calibration with on-orbit verification to <0.1K 3-sigma have been demonstrated with AIRS, CrIS and IASI.
- ATMS precipitation and cloud water products should be included in a NASA EDR product.

1.4 IDPS Processing Limitation

- Even minor software version updates are difficult to make, using a very inefficient process.
- The data record is incomplete due to missing or corrupted RDRs (repair granule problems)
- CrIS calibration looks (blackbody, space) are not smoothed properly when repair granules occur
- Current inability to process full spectral resolution CrIS data, which will begin in June 2013
- Discontinuities in radiometric calibration due to software version changes, and due to calibration coefficient changes
- Discontinuities in spectral calibration, due to the way IDPS triggers updates in the spectral corrections at irregular intervals.
- Core SDR processing parameters not stored in the SDR output (metrology laser wavelength used to produce the SDR).

- The CrIS IDPS code has been massaged separately by *five* different vendors, organizations and is opaque, and missing key elements needed for climate-level production
- NOAA has no definitive plans at present to re-process CrIS, ATMS data.

1.5 Recommendations

Sounder Team Recommendations

1. Devote more resources to research involving CrIS to properly reflect its high value for climate applications, deriving from its high accuracy, stability and information content.
2. Process new (June 2013) full-length CrIS interferograms into SDR high-resolution spectra.
3. Investigations of climate characterization and trending based on the radiance spectra themselves should be encouraged, including radiance gridding and probability distribution function (PDF) climate products that can exploit the full information content and absolute accuracy of the IR spectral radiances.
4. Development of retrieval approaches that elucidate climate change signals without serious bias or imprint of a priori assumptions.
5. Develop a satellite climatology of temperature and water vapor derived from CrIS and AIRS using a common algorithm, following studies of several potential existing algorithms.
6. Develop additional products from NPP to continue the EOS AIRS, MOPITT, IASI, and TES records, in particular the retrieval of atmospheric greenhouse gases (CO, NH_3, SO_2, CH_4, CO_2, and O_3), clouds and cloud radiative forcing, volcanic ash and dust aerosols along with land, ice, and ocean surface properties in the thermal infrared at high spectral resolution.
7. Develop product-centric algorithms and data rather than sensor-centric algorithms and products when appropriate, specifically including the combination of CrIS, VIIRS, and ATMS for cloud and thermodynamic products.
8. Support a combined AIRS/AMSU, CrIS/ATMS, and IASI/AMSU climate analysis system that encourages open community cooperation and code sharing. This is essential for inter-comparison and testing of various approaches to validate climate products from these instruments.
9. Implement NASA processing of CrIMSS SDRs, EDRs and CDRs because of limitations of the IDPS products and our inability to affect refinement of the IDPS system in a timely manner. The following problems are of specific concern:
   (a) In-completeness of EDR minor gas product set, including CH_4, CO, NH_3, and CO_2. O_3 retrievals from CrIS should receive more attention, possibly simultaneously with OMPS retrievals.
   (b) In-completeness of EDR cloud product set, including cloud top height, amount, ice water path, liquid water path, cirrus effective radius and phase.
   (c) Complexity of the IDPS xDR products, such as excessive number of files (10,000 per day) and poor documentation.
   (d) Inadequate error characterization and poor Q/C in both the SDR and EDRs.
   (e) Possible climatology imprint on EDRs.
   (f) Incomplete or poor representation of phenomena in the radiative transfer algorithm, including surface emission/reflection and missing minor gases. Sort-wave non-local thermodynamic equilibrium (non-LTE) emission should be included to allow use of the short-wave for day-time retrievals.
   (g) Inability to handle full resolution CrIS spectra which provides water vapor into the TTL and carbon monoxide retrievals (to continue CO now produced by Aqua-AIRS, MOPITT, and TES).
   (h) Added complexity of reconciling Aqua and NPP climate data records due to processing differences which far exceed differences in instrument capabilities.
   (i) Expected in-adequate ATMS scan bias correction and other IDPS issues that require NASA-developed and processed ATMS SDRs.

2 Introduction

The Cross-track Infrared Sensor (CrIS) and Advanced Technology Microwave Sounder (ATMS) flying on Soumi-NPP are primary satellite instruments for measuring atmospheric temperature and moisture profiles for use in Numerical Weather Prediction (NWP). CrIS/ATMS provide sounding in the pm polar orbit, while EUMETSAT's METOP satellite series provides soundings in the am orbit using the Infrared Atmospheric Sounding Interferometer (IASI) and the Microwave Humidity Sounder (MHS).

The CrIS instrument was originally developed by the IPO for NPOESS and is manufactured by ITT/Excelis. ATMS development was managed by NASA/GSFC for the IPO, and was manufactured by Northrup Grumman. These instruments essentially replace the Atmospheric Infrared Sounder (AIRS) and the combination of the Advanced Microwave Sounding Unit (AMSU, comprised of two units and three scan systems) and the Humidity Sounder Brazil (HSB) on NASA's EOS-AQUA platform. From the perspective of NOAA/NESDIS, CrIS/ATMS replace the present NOAA operational instruments: the Advanced TIROS Operational Vertical sounders (ATOVS) and the NOAA MHS instrument.

We first present an overview of the ATMS and CrIS instruments in Sections 2.1 and 2.2, followed by a standard calibration/validation assessment of the ATMS and CrIS instruments in Section 3. Section 4 discusses NASA climate research needs that can be fulfilled with the CrIS/ATMS measurements and recommendations for achieving climate quality scientific results from these instruments.

2.1 ATMS Instrument

ATMS is the follow-on to the Advanced Microwave Sounding Unit (AMSU) and Humidity Sounder Brazil (HSB) microwave sounders that were part of the AIRS instrument package on EOS-AQUA. ATMS has heritage from AMSU-A, AMSU-B, HSB and MHS, but was designed to have a simpler scan system and antenna patterns. Whereas ATMS and HSB have three units and four antennas and scan systems, ATMS has one unit, one scan system and two antennas. Likewise, AMSU-A has heritage from the Microwave Sounding Unit (MSU) and together provide a nearly 40 year CDR of microwave brightness temperatures.

AMSU/MHS currently flying on NOAA-18/19 in afternoon orbits and on EUMETSAT's METOP-1/2 in morning orbits and the near coincident observations provide information on cross calibration and measurement capabilities.

ATMS has a total of 22 channels (13 of which have identical channels on AMSU-A/B, 6 of which have similar channels on AMSU-A/B - differing only by polarization or passband, and 3 are new and not measured by AMSU-A/B). These new channels include two 180 GHz water vapor sounding channels to improve vertical resolution and one near surface 52 GHz channel to improve boundary layer characterization. The ATMS 23.8 and 31.4-GHz channels have 5.2 degree full-width at half maximum (FWHM) beamwidth (compared to 3.3 degree FWHM for corresponding AMSU-A channels). The ATMS temperature sounding channels (channels 3 to 15) and an imaging channel near 89 GHz have 2.2 degree FWHM beamwidth (compared to 3.3 degree FWHM for corresponding AMSU-A channels). The ATMS G-band channels have 1.1 degree FWHM, as do corresponding channels for AMSU-B. The ATMS sampling interval is 1.11 degrees for all channels. AMSU-A sampling interval is 3.33 degrees and AMSU-B sampling interval is 1.11 degrees. ATMS measures 96 spots per swath (compared with 30 for AMSU-A and 90 for AMSU-B) and therefore has a wider swath ~2600 km compared with ~2200 km for AMSU-A/B).

HSB failed within nine months of launch and there is only six months of simultaneous MW and MW/IR combined water vapor profiles. However, this period has provided important insight into is sampling errors and strengths and limitations of hyperspectral IR-only soundings.

The ATMS TDR ("temperature data record") product is produced on the native observation grid (1.11 degree spacing in sensor scan angle). The SDR ("sensor data record") includes antenna pattern and/or bias corrections. Every TDR observation has a corresponding SDR bias-corrected observation. The rSDR ("re-sampled SDR") is a spatially filtered product that attempts to maximize the spatial coincidence with the CrIS fields of regard. For every swath, there are 96 footprints in the TDR (8/3 seconds per swath), 96 footprints in the SDR (8/3 seconds per swath), and 30 footprints in the rSDR (8 seconds per swath).

The ATMS raw data, antenna temperatures, and brightness temperatures (i.e., RDR, TDR, & SDR) received the "beta" data product maturity level approximately a month (Dec. 10, 2011) after ATMS activation. For the data product maturity level descriptions, see the NOAA-CLASS maturity definition

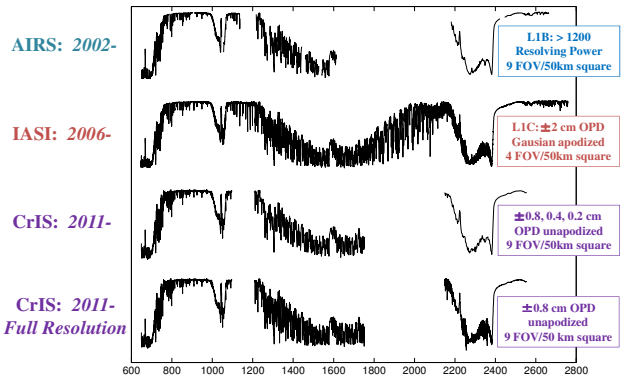

Figure 1: Comparison of brightness temperature spectra for CrIS, AIRS, and IASI.

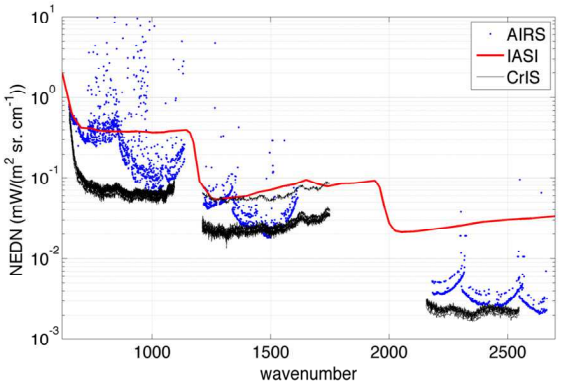

Figure 2: Comparison of CrIS radiance noise (NEDN) to that for AIRS and IASI. Note the low CrIS noise in the thermal infrared window and 15 micron CO_2 sounding band

document. CLASS also has a list of caveats for the ATMS SDR beta data products. The ATMS brightness temperatures re-sampled to the CrIS field of regards (rSDR) received the "beta" data product maturity level at the same time that the CrIS SDR received beta level on April 19, 2012. The ATMS raw data and antenna temperatures received the provisional data product maturity level on January 30, 2013. It is estimated that the ATMS data products will reach the final maturity level of validated/calibrated around the beginning of 2014.

2.2 CrIS Instrument

The Cross-track Infrared Sensor (CrIS) is the first NOAA operational hyperspectral infrared sounder, and represents the first major technology change for NOAA infrared sounders since their inception in the 1970's. AIRS on NASA's EOS-AQUA platform demonstrated the great utility of hyperspectral infrared sounders for numerical weather prediction (NWP) and indeed all large NWP centers assimilate AIRS radiances operationally. The IASI sounder(s) on EUMETSAT's Metop-1/2 satellites started operation in 2007, providing measurements in the 9:30 am/pm polar orbit.

CrIS started producing science quality SDRs on Jan. 20, 2012, although due to a number of software issues the IDPS processing system did not produce CrIS SDRs until April 2. However, the CrIS Calibration Algorithm and Sensor Testbed (CCAST, a Matlab-based SDR code jointly developed by the Univ. Wisconsin and UMBC) was used to produce CrIS SDRs immediately on Jan. 20. Subsequently, the NG IDPS simulator (termed ADL) was also used by several groups to generate CrIS SDRs using software almost identical to the IDPS. Initial calibration of CrIS was completed in several weeks, namely fine-tuning of the 27 detector non-linearity corrections, establishing the exact off-axis position of each detector, and spectral calibration of the Neon lamp used to calibrate the interferometer metrology laser.

Further evaluation of the CrIS SDRs confirmed the existence of significant offsets in the radiances relative to the interferometer scan direction. The vendor, Excelis/ITT, confirmed that these offsets could be reduced with a new on-board FIR (finite impulse response) filter that is used to restrict the bandwidth of the downloaded interferograms to the spectral region of interest. This new filter was installed on April 18, 2012. Initial validation showed that this new filter did improve the interferometer scan-direction striping, but significant striping remains. The CrIS SDR validation studies in this report use the IDPS SDR data generated after April 18.

Although this report primarily addresses the use of CrIS/ATMS as a follow-on to AIRS/AMSU, we include some discussion of IASI since it is the sister instrument to CrIS covering the *am* orbit. EUMETSAT is flying an AMSU on METOP-1/2, very similar to the AMSU flown with AIRS. (Note, the 2nd IASI is presently operating in check-out mode on METOP-2.)

The CrIS sensor on NPP, and the IASI sensor(s) on METOP-1,2 are very similar to AIRS, although

both are based on interferometric spectrometers rather than a grating spectrometers such as AIRS. Figure 1 illustrates simulated spectra from all three hyperspectral sounders. AIRS has an approximately constant resolving power of $\nu/\Delta\,\nu \sim 1300$, while the unapodized resolution of both IASI (~ 0.5 cm^{-1}) and the full-resolution mode of CrIS (~ 0.625 cm^{-1}) are independent of wavenumber. Thus IASI and CrIS (in high-resolution mode) have higher spectral resolution than AIRS in the mid- and short-wave bands. However, noise must also be considered in any detailed comparisons, which will be covered later in this document.

Also noteworthy is the excellent noise performance of CrIS, even in the shortwave band (2150 to 2600 cm^{-1}). This comparison is made for warm scenes, but even for cold scenes the shortwave noise performance is comparable to that of AIRS. See Fig.2.

The CrIS interferometer has three focal planes, long-wave (LW), mid-wave (MW) and short-wave (SW), each with a 3x3 array of HdCdTe detectors. Interferograms are simultaneously recorded on all detectors, thus the CrIS record contains data spread evenly over these 9 detectors (which we will often call FOVs for fields-of-view). Because the raw spectral scale and Instrument Line Shape (ILS) for each FOV depend on geometry, there are significant differences among center, side and corner detectors. To simplify user applications, a physically well understood inversion algorithm is applied to normalize these different spectral properties to an ideal sinc ILS and a standardized spectral scale. Ensuring that all nine detectors on each focal plane have the same spectral, and radiometric response, to below 0.1K represented a large part of the CrIS pre- and post-launch calibration activities. This was not done properly for the METOP IASI sensor (four detectors per focal plane) and led NWP centers to only assimilate data from only one detector per focal plane, a very significant loss of data.

3 Evaluation of NPP CrIS/ATMS

3.1 ATMS SDR Evaluation

Microwave radiometers typically require empirical corrections for biases related to the scan angle, which are difficult to completely account for using TVAC data due to the complicated beam pattern and dependence on the satellite thermal environment. NOAA STAR, NOAA NCEP, and ECMWF have been monitoring the ATMS TDRs against simulated brightness temperature (e.g.,STAR) to evaluate the ATMS scan bias and calibration accuracy. They report that the scan biases are “much smoother than commonly found in AMSU-A”[1].

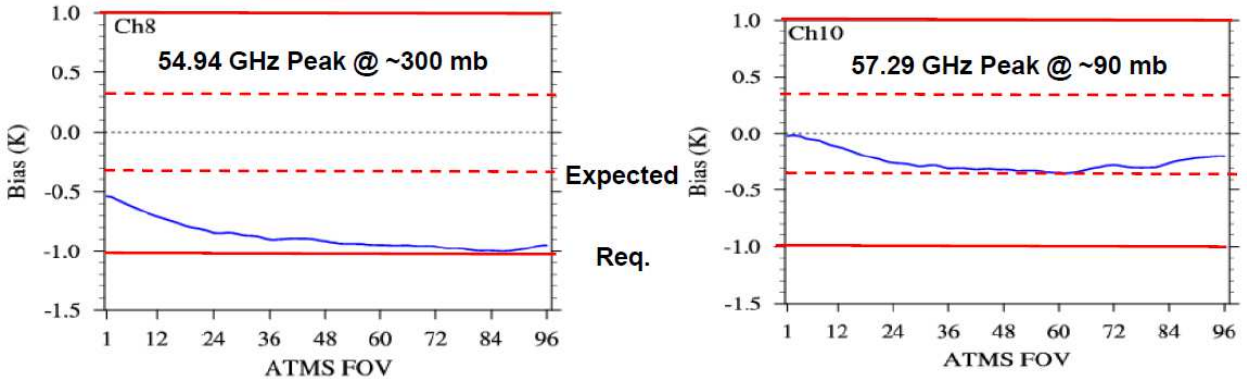

Figure 3: Calibration accuracy of ATMS antenna temperatures against requirements and expected performance based on NGES error budget.

A preliminary comparison of the vendor’s calibration accuracy error budget against the simulated brightness temperature bias is shown in Fig. 3. The ATMS bias is from NOAA STAR using clear-air ATMS antenna temperatures (TDR) over ocean against GPS radio occultation (GPSRO) retrievals converted to microwave brightness temperatures using NOAA’s in-house radiative transfer algorithm, CRTM (v 2.0.5). These two ATMS channels weighting functions peak near the part of the atmosphere that GPSRO

is most accurate. These comparisons will mature as the data products reach the validated/calibrated maturity level. These results suggest that ATMS is operating as well or better than previous AMSU sensors in terms of scan bias performance.

We now examine several radiometric calibration problems with ATMS and begin to address their potential impact on NASA climate science.

The ATMS antenna temperature to brightness temperature conversion process (i.e., TDR to SDR) involves corrections due to sidelobes in the antenna pattern (as measured during pre-launch testing). Furthermore, recent analyses of on-orbit spacecraft maneuver data suggest that reflector imperfections may introduce brightness temperature errors approaching several tenths of a Kelvin. Work is underway to better characterize the potential radiative impact of an imperfect reflector and to devise corrections based on the spacecraft maneuver data. This work is discussed in some detail in Section 3.1.4.

3.1.1 ATMS Calibration Striping

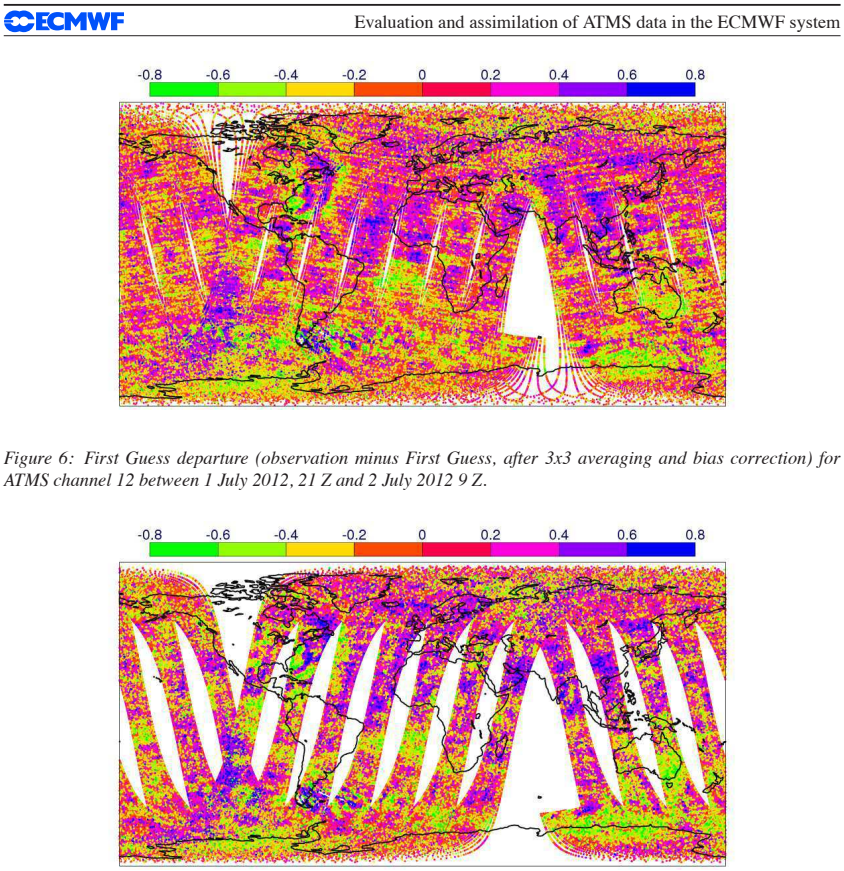

Figure 6: First Guess departure (observation minus First Guess, after 3x3 averaging and bias correction) for ATMS channel 12 between 1 July 2012, 21 Z and 2 July 2012 9 Z.

Figure 7: First Guess departure (observation minus First Guess, after 3x3 averaging and bias correction) for NOAA-19 AMSU-A channel 11 between 1 July 2012, 21 Z and 2 July 2012 9 Z. Only the scan positions considered for assimilation are shown here, ie, the outermost 3 scan positions on each side are not shown.

Figure 4: From ECMWF Technical Memo 689 (Dec. 2012) [1]

The NWP assimilation community has reported cross-track striping in "observation minus background" images with a magnitude on the order of 0.2K. The observations are re-sampled ATMS TDRs and the background is simulated brightness temperatures using NWP fields. AMSU TDRs for similar channels do not have striping. As an example, Fig. 4 is a pair of figures from an ECMWF Technical Memo [1] on their analysis of the ATMS striping. The first expected culprit was the filtering of the calibration

counts, but results from several organizations showed that the striping wasn't completely mitigated.

The striping was also seen in the sensor-level TVAC data (i.e., without spacecraft or other sensors). Further investigation is underway to eliminate the striping, but due to the striping existing to some extent in the sensor-level TVAC data, the latest culprit is the larger flicker noise of the MMIC LNA in the ATMS, which is not in the AMSU design. More sophisticated calibration algorithms are under investigation.

Another related topic from the NWP community is the higher ATMS inter-channel correlation than AMSU-A. The high inter-channel correlations were noted in the ATMS satellite-level TVAC testing (Fig. 5), and the ECMWF report Tech. Memo 689 [1] reported that ATMS had higher spatial and inter-channel error correlations that were "considerably larger" than AMSU-A as the AMSU-A were "largely negligible". The memo did mention that the covariance of the ATMS humidity sounding channels were "more consistent" with MHS, which has a spatial response and receiver design similar to ATMS. The memo continues by mentioning that such error correlations are ignored in the assimilation, and they presently deal with these non-diagonal observation covariance matrices by "considerable error inflation factors".

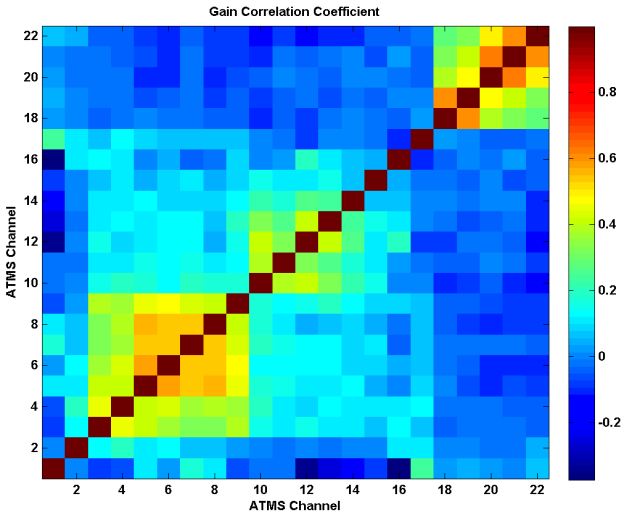

Figure 5: Correlation coefficient for ATMS estimated gain time series (periodic absolute calibration). The various receivers are clearly visible.

The ATMS SDR team and NWP community seems to be coming to the conclusion that the striping is an inherent part of the ATMS sensor with little that can be done to completely eliminate the striping within the SDR calibration algorithm. The ATMS SDR team is getting closer to agreeing on an approach to mitigate the striping to the degree possible by varying the calibration count filter length and shape. The decision is taking the NEDT, ADR, and inter-channel correlation coefficients into account. Fortunately, it looks like the final lengths won't require adding additional granules to the IDPS processing (i.e., less than 24 scans).

3.1.2 ATMS Solar intrusion of ICT

During the Early Orbit Checkout (EOC) of the S-NPP ATMS instrument, the Cal/Val team noticed that the Internal Calibration Target (ICT) had two temperature sensor (PRTs) measurements deviate from the other PRTs consistently at the same two points during an orbit. The most likely cause is solar intrusion of the ICT. The out of family PRTs are on the sun-side of the calibration target. There is a strong indication that direct solar intrusion causes a slight heating (0.15 Kelvin) of the "WG" band (Chan. 16-22) ICT as the NPP satellite enters the eclipse. This ICT temperature perturbation returns to nominal after about 30 minutes. The "KAV" band ICT has no direct solar intrusion due to the sun shade and varies by only ~ 0.05 Kelvin during these events. The worst-case temperature variation, however, is within the specified allowable temperature drift for the calibration target. The resulting BT bias error for this effect is likely 0.05K or less, but ICT gradients should be monitored throughout the mission to check for degradation

3.1.3 ATMS G-band Sideband Imbalance

The gain imbalance for multi-sideband ATMS channels was not measured for SNPP ATMS. Recent tests for J1 ATMS revealed that channel 18 (± 7 GHz) was imbalanced by ~ 5 dB and Chan. 19 & 20 were imbalanced by ~ 2.5 dB. If the J1 ATMS measurements are representative of SNPP ATMS behavior, this could result in a bias error of approximately 0.2 K and a systematic error of approximately 0.1 K RMS. This artifact was further analyzed using a simulation study with thousands of NOAA88b profiles. Figure 6 shows brightness temperature errors of this ensemble as a function of the degree (magnitude and

direction) of sideband imbalance. The solid lines indicate systematic bias errors and the error bars indicate random error.

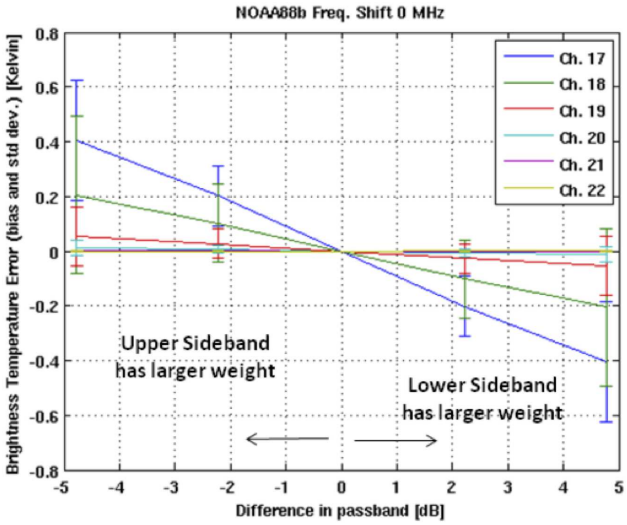

Figure 6: G-band passband and imbalance simulations (NOAA88b)

3.1.4 ATMS Rotating Flat Reflector Emissivity

The Suomi NPP spacecraft pitchover maneuver revealed that ATMS has a scan angle-dependent bias when viewing deep space, which is a homogeneous and unpolarized source that fills the entire ATMS Field of Regard. It was theorized that the bias was the result of higher than expected flat reflector emissivity [7]. SSMIS has a similar issue of high reflector emissivity [6]. For the ATMS configuration, the emissivity was polarization dependent, which resulted in a scan-dependent bias, with the quasi-vertical channels having a different bias shape than the quasi-horizontal channels. The ATMS calibration algorithm [2] was altered to account for the flat reflector emissivity, which required a value for the reflector's temperature and normal-incidence emissivity. The normal emissivity was empirically estimated by minimizing the scan bias during the pitchover maneuver, and the reflector's temperature was derived from ATMS telemetry. The model, calibration change, and estimated normal emissivity were verified using the ATMS thermal vacuum test data, which helped explain how two external targets with nearly identical physical temperature could have different counts (beyond the amount accounting for the small temperature difference).

The worst case impact of the flat reflector emissivity is during a cosmic background scene, so a simple sensor model was used to determine the error for the full dynamic range of the instrument. The results of using the simple model for the two worst cases (Chans. 1 and 16) are shown in Fig. 7. Based on an orbit worth of data, the channels median brightness temperature gives an error of ~ 0.4 Kelvin at nadir for the quasi-vertical polarized channels if the antenna temperatures are not corrected. The error is much smaller for the quasi-horizontal channels.

3.1.5 ATMS SVS Measurements Correlated with EVS measurements

Some of the ATMS channels had all four Space View Sectors (SVS) correlated with their Earth View Sector (EVS) measurements. It is expected that the SVS will measure some of the Earth's limb and the calibration algorithm accounts for this with a cold space bias correction, which was derived from the SVS (profile 1) antenna pattern measurements from the Compact Antenna Test Range (CATR). The cold space bias correction accounts for the Earth and spacecraft contamination in the antenna sidelobes, but the ATMS SDR algorithm bias correction is not a function of the nadir upwelling brightness temperature.

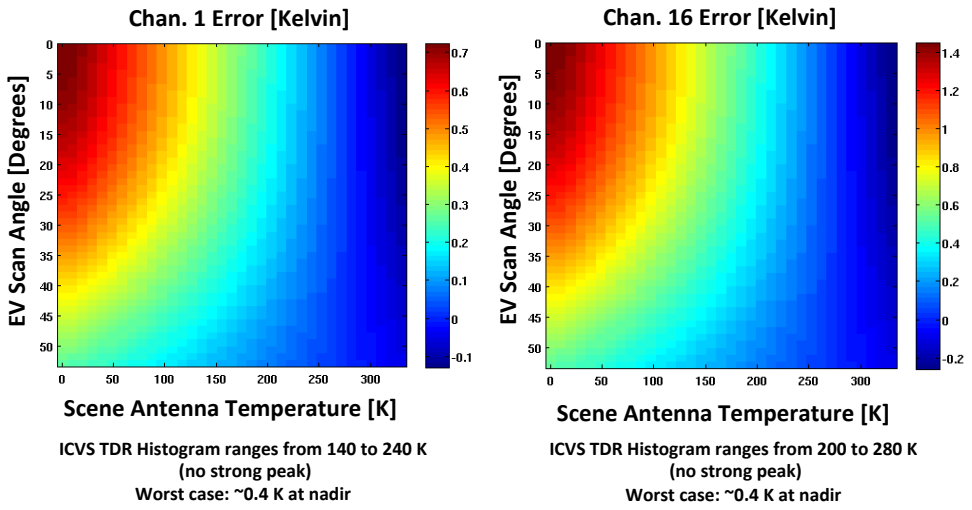

Figure 7: Error analysis of not correcting for the flat reflector emissivity. These two channels are quasi-vertical polarized channels.

Ch.	1	2	3	4	5	6	7	8	9	10	11
SP1 (6.66°)	0.569	0.379	0.167	0.174	0.196	0.128	0.051	0.023	0.034	0.008	0.058
SP2 (8.33°)	0.578	0.408	0.176	0.175	0.196	0.108	0.029	0.017	0.026	-0.002	0.068
SP3 (10.0°)	0.584	0.433	0.198	0.206	0.234	0.104	-0.072	-0.110	-0.060	-0.016	0.057
SP4 (13.33°)	0.571	0.391	0.168	0.179	0.202	0.084	-0.073	-0.099	-0.008	-0.055	0.038

Ch.	12	13	14	15	16	17	18	19	20	21	22
SP1	0.223	0.207	0.161	0.063	0.485	0.095	-0.006	0.012	0.027	0.007	-0.016
SP2	0.233	0.226	0.171	0.064	0.457	0.050	-0.034	-0.017	-0.014	-0.026	-0.040
SP3	0.228	0.217	0.168	0.060	0.466	0.008	-0.005	-0.011	0.024	0.016	0.006
SP4	0.221	0.221	0.168	0.057	0.506	-0.006	-0.014	0.031	0.015	0.004	-0.005

Table 1: Correlations of the four Space View Sectors for each channel.

It should be noted that the SVS counts were used to calibrate the nadir brightness temperature (or more exactly, the antenna temperature). The strongest correlations (0.4 - 0.5) were seen in the 23.8, 31.4, and 89-GHz channels, which were also the quasi-vertical and window channels. The calculated correlations can be found in Table 1. The lower V-band channels also had some correlation, but at 0.2. Choosing a SVS closer to the spacecraft and therefore further from the Earth's limb did not reduce the correlation. As a reality check, a spectral analysis was completed on the EVS, SVS, and ICT time series, and the EVS harmonics were seen in the SVS spectrum, but not the ICT spectrum.

3.2 CrIS SDR Evaluation

The CrIS radiometric accuracy has proven to be excellent and substantially exceeds the Suomi NPP program requirements that were established primarily for weather applications. As we summarize here, this instrument is very well suited to continue, and in several ways to improve on, the accuracy offered for establishing a valuable climate record from high resolution IR spectra began by the AIRS instrument on the NASA EOS Aqua platform. Much of the substantial calibration accuracy improvement of these spectrometers over lower resolution radiometers stems from the huge improvement in knowledge of

the spectral response functions.

3.2.1 CrIS Radiometric Accuracy and Stability

The on-orbit agreement between the nine CrIS FOVs after completion of "provisional" level analyses is shown in Fig. 8. The agreement among 6 of the FOVs is exceptionally good. The exceptions are SW pixels 3, 6, and 9; an anomaly that is still being studied. In general, these relative comparisons that inherently include some errors from the on-orbit comparison process are excellent and consistent with the expectations of pre-flight radiometric testing. This level of agreement between the nine FOVs was achieved by tuning the detector non-linearity coefficients using one day of data from Feb. 2012. The reference detector was FOV 5, which had the lowest non-linearity in TVAC testing.

Further analysis is needed to ensure that all nine FOVs have the same radiometric response for all scene temperatures. Any improvements can be easily included in SDR reprocessing. The absolute radiometric accuracy can be difficult to determine for all scene temperatures. Significant work remains to determine absolute accuracy of CrIS and AIRS. Eventually it *may* be necessary to make empirical adjustments to AIRS or CrIS in order to produce a climate radiance record. Fortunately, the SNO overlaps between CrIS and AIRS are numerous and should provide a very good measurements of radiometric calibration differences between these instruments. However, this is a non-trivial exercise and should not be undertaken until the inherent limitations of each sensor is well understood.

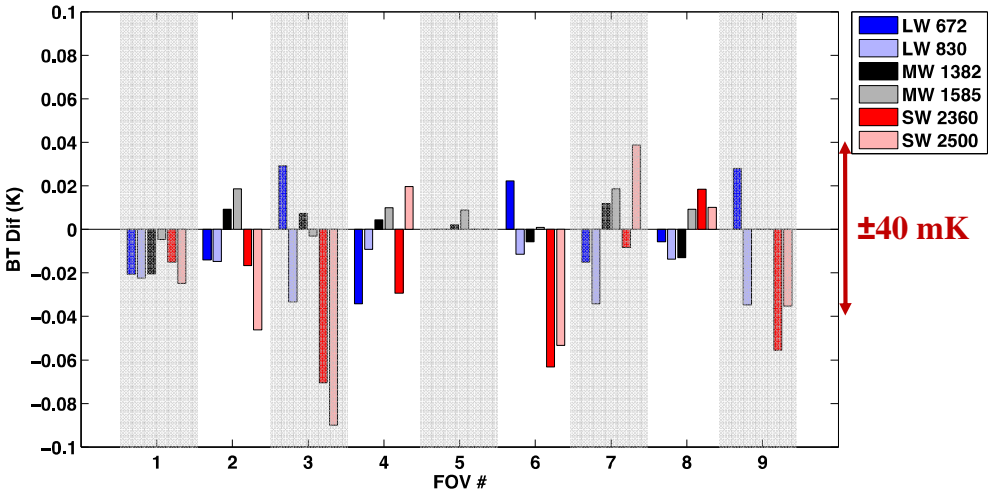

Figure 8: On-orbit brightness temperature comparisons among the nine CrIS FOVs for six sample wavenumbers. Most differences are less than ± 20 mK.

Vicarious calibration using well-known tropical sea surface temperatures for clear CrIS scenes suggests absolute accuracy in the 0.1-0.2K range, but this work is preliminary, although this level of agreement between observed and computed radiances is already near the limit of this approach for establishing absolute accuracy. Moreover, comparisons to sea-surface temperatures primarily tests the accuracy of the on-board blackbody rather than any non-linearity issues. More information on the CrIS radiometric accuracy awaits field campaigns flying a reference interferometer (S-HIS). However, as shown below, the agreement between CrIS, AIRS, and IASI is, on average, well below the 0.5K level.

It is too early to determine CrIS stability at the climate level, defined generally to be 0.01K/year. However, by examination of clear-scene tropical ocean time series of CrIS window channel radiances compared to sea-surface temperature products, we presently obtain a radiometric stability for 8 months of +0.005K ± 0.04K /year. Over time the uncertainty in this mean will decrease, especially once a full-year time series is available.

Drawing on the sensor characterization results to date, a preliminary estimate of the CrIS SDR in-flight Radiometric Uncertainty (RU) is shown in Fig. 9. Opposed to the pre-flight RU estimates from Thermal Vacuum blackbody views, the in-flight RU can vary depending on the magnitude and

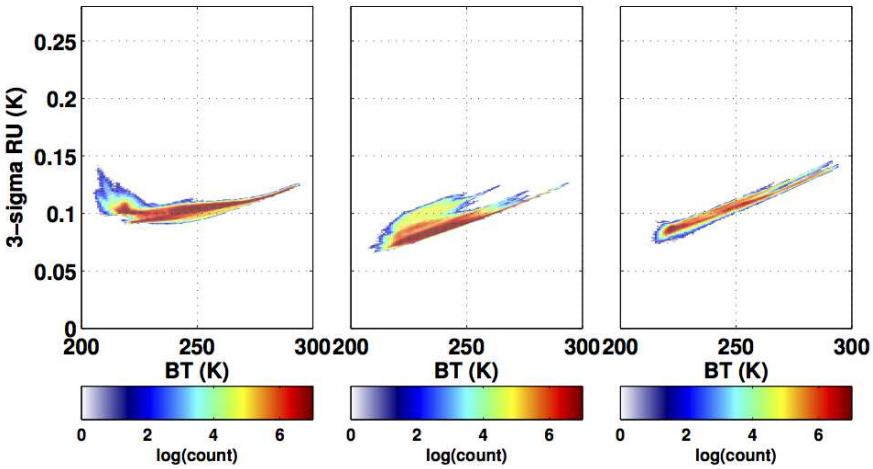

Figure 9: Sample of on-orbit 3-sigma Brightness Temperature uncertainty for 24 February 2012.

shape of the observed spectrum; this example is for an 8-minute granule from 24 February 2012 with a reasonable sample of clear sky spectra. It applies to all nine CrIS FOVs, because the FOV-to-FOV inter-comparison techniques for reducing non-linearity uncertainties on-orbit have already been applied.

3.2.2 CrIS Spectral Calibration Accuracy and Stability

Knowledge of the wavelength of the metrology laser that drives the CrIS interferometer is one key parameter for generation of accurate radiances. The solid-state metrology laser is temperature stabilized, but this temperature is expected to change slowly depending on the instrument baseline temperature. (To date CrIS instrument temperatures have been extremely stable, with a mean seasonal variability of only 0.5K/year with a far smaller secular trend.) The metrology laser is calibrated on-board using a Neon emission lamp co-aligned with the interferometer. The SDR algorithm uses the Neon wavelength to calibrate the metrology laser, and if the metrology laser moves by more than 2 ppm, new spectral calibration (and apodization) coefficients are re-computed. The CrIS vendor suggested updating the Neon calibration every month using up-welling spectra, since lifetime studies indicated that the Neon calibration system can drift slowly.

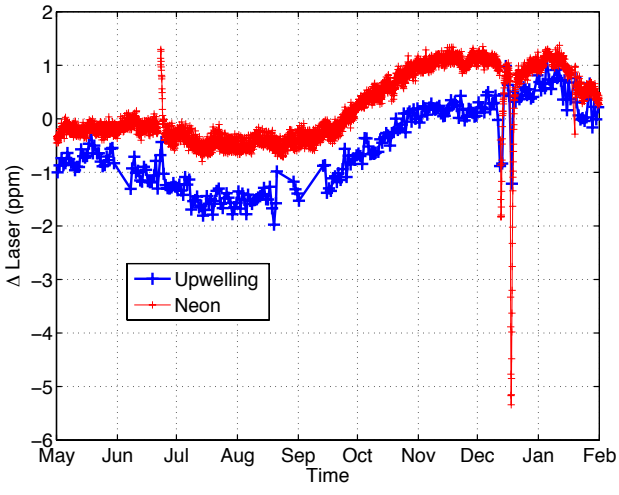

Figure 10: CrIS Neon lamp calibration of metrology laser with validation using up-welling radiances.

Figure 10 shows the calibration of the metrology laser by the Neon lamp (red curve) for much of the mission to-date. The blue curve is UMBC's measurement of the CrIS SDR frequency scale (translated to ppm offset from the metrology laser setting). First note that the CrIS frequency scale has drifted (seasonally it turns out) by only slightly more than 1 ppm in this time frame. The spikes in the Neon are real and due to known mission anomalies. We also note that the Neon calibration follows shifts in the metrology laser as confirmed using the observed atmospheric spectra. These drifts are in the CrIS radiances because the IDPS SDR software only switches to new frequency and apodization correction coefficients if the Neon lamp detects more than a 2 ppm shift in the metrology laser. In Dec. 2012 one can see that the metrology laser shifted by almost 6 ppm, while the up-welling spectra shifted by about 2 ppm, as it should based on the SDR 2 ppm trigger.

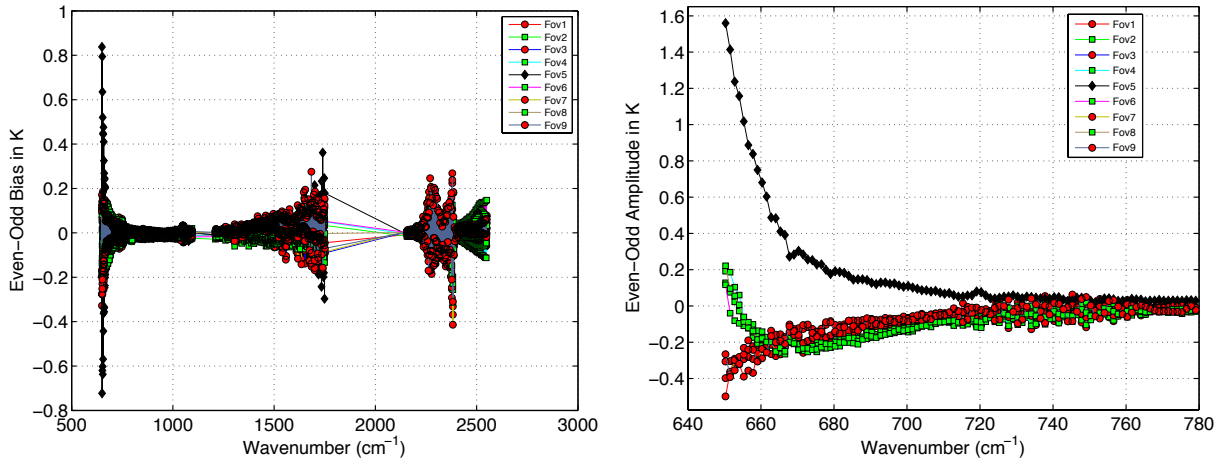

(a) Bias versus NWP calculations for each channel.

(b) Difference in bias between adjacent channels, long-wave only.

Figure 11: Brightness temperature striping with interferometer scan mirror direction.

(The blue curve is a daily average, and the true shift of the SDR spectra was indeed ~ 2ppm if not averaged.)

This discrete approach does introduce small discontinuities into the data stream, of up to 0.06K for some CO_2 channels (and one O_3 channel of up to 0.12K). This is indeed observable since the blue curve itself is based on an analysis of the SDRs. The > 2ppm events in this graph were quickly reversed, and thus of little importance. This is not guaranteed in the future, and is dependent ultimately on the CrIS optical bench temperature stability, which thus far has been extremely good.

Note that the AIRS frequency calibration exhibits slow multi-year drifts with superimposed drifts that vary with orbit position, and season of the year, on the order of 7 ppm. Although these drifts are easily measured (from the up-welling radiances) they are not corrected for in the L1b radiance record. Work is underway to correct for these errors in a new AIRS L1c radiance product.

3.2.3 CrIS Ringing

One of the largest unresolved errors in the CrIS SDR product can be characterized as a “ringing” artifact. This artifact can be as large as order ± 1 K for certain specific spectral regions of unapodized spectra, but is generally very much smaller. Also, studies in progress are pursuing techniques to minimize this effect.

Ringing is displayed as a saw-tooth artifact, varying every other spectral point between being too high and too small (for some regions of minimally sampled, unapodized spectra). For CrIS, some ringing should be expected and is not an artifact. i.e. it should also occur in a properly calculated spectrum, because of the way the instrument band limits the spectrum. Also, since ringing is largely eliminated by frequently used apodization functions, many users will not consider it to be a significant source of calibration error.

However, when imaging with unapodized spectra, ringing in CrIS can create a striping artifact. This occurs because some of the ringing artifact depends on the scan direction of the interferometer, which alternates between adjacent cross-track Field-of-Regards (3x3 FOV array).

Figures 11a and 11b summarize this behavior, which are derived from brightness temperature bias differences between observed and computed radiances (using ECMWF model data). Figure 11a plots the BT difference in the bias between the two interferometer scan directions. Figure 11b shows, for the long-wave band, the difference in this scan bias between adjacent channels (it oscillates with channel). While these differences are on the order of the noise for the corner and edge FOVs, they are very large for the center FOV (FOV 5) in the 3x3 detector focal plane, growing to about 1.5K near the band edge.

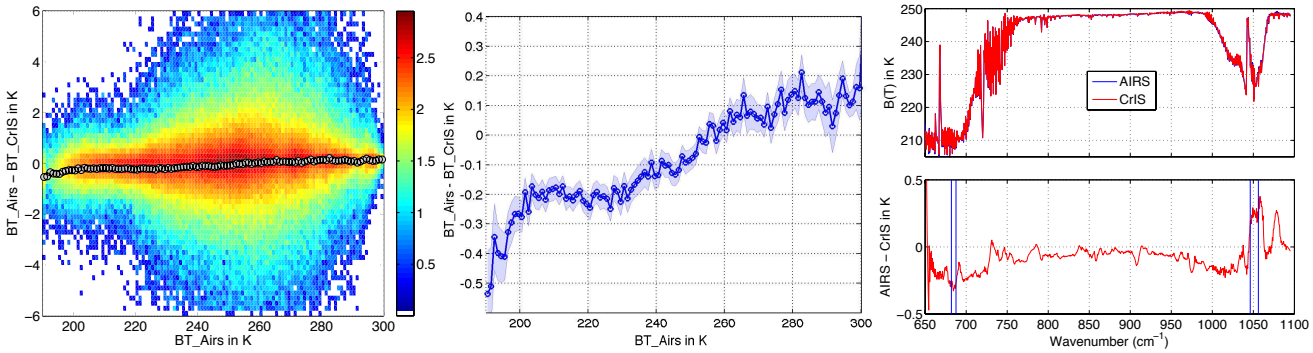

(a) 2-D histogram of AIRS-CrIS B(T) for the 960 cm^{-1} channel. Counts are shown with a log10 scale.

(b) Mean B(T) difference between AIRS and CrIS for the 960 cm^{-1} channel as a function of scene temperature. The shaded area represents the 2-σ uncertainty in the mean.

(c) AIRS minus CrIS SNO B(T) with AIRS converted to CrIS, long-wave.

Figure 12: Long-wave CrIS, AIRS SNOs

Note errors of up to 0.4K in the short-wave band. This is likely an apodization correction issue and not a radiometric calibration error. Studies to date indicate that the CrIS on-board FIR filter (used to filter the inteferogram to the target spectral region, and to reduce out-of-band noise) is the root cause of residual ringing and this striping.

3.2.4 CrIS Intercomparisons with AIRS and IASI

Presently all three operational hyperspectral sounders are operating (AIRS, IASI-1, CrIS, with IASI-2 being commissioned) providing ample opportunities for inter-comparisons. We concentrate here on comparisons using simultaneous nadir overpasses (SNOs), which are observations where two sensors observe the same scene at nadir within a tight spatial/temporal window. The UMBC SNO observations come from the Sounding PEATE, and use a window of 10 minutes, 8 km. Although the AIRS/CrIS SNO occurrence strongly peak in narrow bands near ± 80° latitude thousands of SNOs exist at all latitudes. The IASI/CrIS SNOs, however, all occur within about one degree of ± 78° latitude.

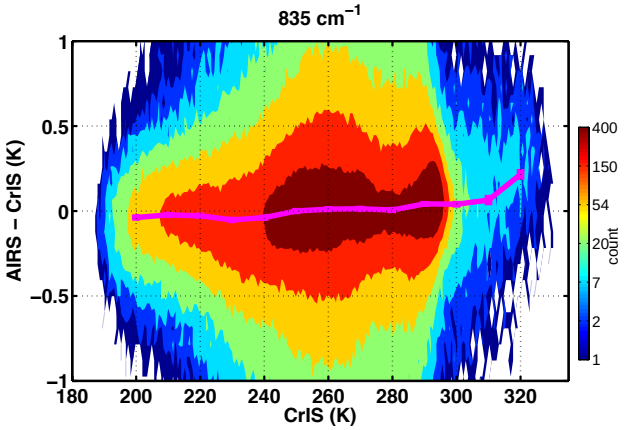

Figure 13: CrIS/AIRS SNO BT differences from UW SNO product.

We present here two views that inter-compare CrIS with either AIRS or IASI. The first view shows the spectrum of mean BT differences for all SNOs. The second view selects representative channels, and shows the SNOs (and their variability) as a function of the scene temperature. Given that the

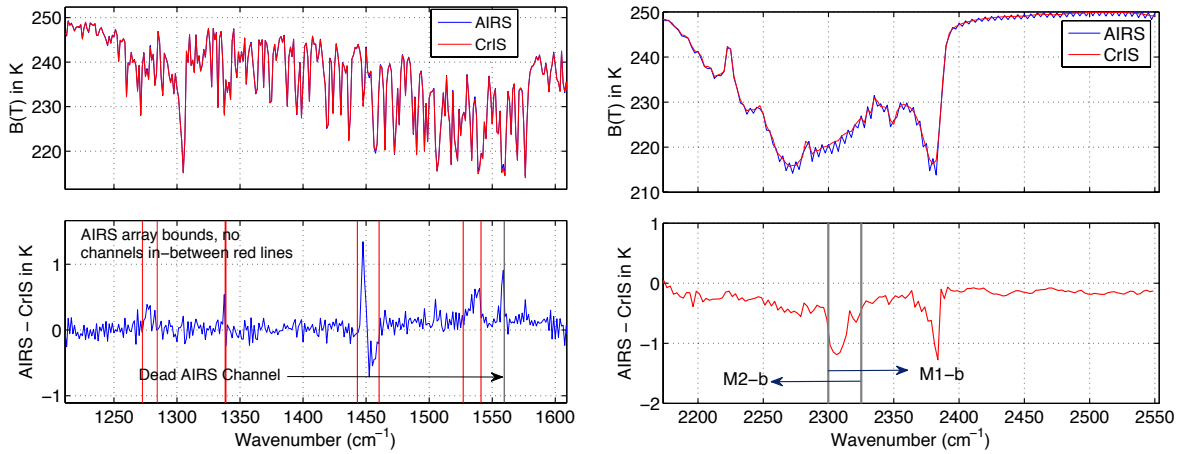

(a) AIRS minus CrIS SNO B(T) with AIRS converted to CrIS, midwave.

(b) AIRS minus CrIS SNO B(T) with AIRS converted to CrIS, shortwave. The AIRS to CrIS conversion is difficult at the ends of AIRS arrays, as denoted in this figure with vertical gray lines.

Figure 14: Mid- and short-wave CrIS, AIRS SNO Mean Differences

CLARREO mission is unlikely to begin in the foreseeable future, the best alternative for the present for thermal infrared climate trend observations is to use the AIRS/CrIS/IASI operational sensor record. It is remarkable that these three sensors already agree (with no adjustments, in the mean) to several tenths of a Kelvin. However, to produce a CLARREO-like record, we must ensure that these sensors agree as a function of scene type/temperature. Thus the importance of the second view just described, which highlights sensor calibration differences more clearly.

We concentrate here on the radiometric calibration differences between CrIS and AIRS. Here we have converted the AIRS radiances to the CrIS instrument line shape (ILS) with Hamming apodization.

Figure 12a shows the 2-D histogram of the SNO differences for the 960 cm^{-1} channel, showing the counts using a log10 scale, as a function of the AIRS observed B(T). Note the good agreement, with a very tight distribution about the mean.

Figure 12b shows the mean of Fig. 12a for the 960 cm^{-1} channel. These figures suggest that CrIS is slightly warmer then AIRS for colder scenes. The figures also point out that a total mean over all observing scene temperatures can lead to a misleading understanding of the radiometric differences of these two sensors.

The SNO differences shown in Figs.12-14 are UMBC results using the JPL Sounder Peate SNO data with no filtering (except for a limit on $100 < BT < 400$), which is extremely rare. The Atmospheres PEATE at UW also generates AIRS/CrIS SNOs, and the analysis of these data by D. Tobin and H. Revercomb (UW) uses a filtering approach based on the standard deviation (among channels) in the weighting of the mean SNOs. In addition, the UW SNOs have a larger time/space window which allows them to investigate hotter scenes. Figure 13 shows the UW SNO comparisons using the Atmospheres PEATE SNO product. Their sampling includes hotter scenes and shows about a 0.2K disagreement above 310K, with CrIS colder. However, they do *not* see the 0.3K difference seen by UMBC in Fig.12b near 200K. These differences highlight the present state of the SNO analysis, along with the possible need to determine better metrics for quality assurance. We are confident that these differences can be resolved in the future. Note that the statistics for these measurements are still uncertain at the BT extremes, which will improve as the number of SNO observations grows. However, the statistics for scenes away from these extremes are very good, and will eventually allow accurate "adjustments" of the radiances record should they be needed to obtain a CLARREO like record.

Figure 14 shows the difference between the mean SNOs for the mid-wave and short-wave band. One sees extremely good agreement at the 0.1-0.2K level. Histograms similar to that shown in Fig. 12a but

for the mid- and short-wave are similar, as the CrIS sensor becomes slightly warmer than AIRS as you go to colder scene temperatures.

Although the differences are rather dramatic for the short-wave channels observing very cold scenes it should be remembered that this represents a very small subset of the CrIS data. A *very* small radiometric DC offset could cause this behavior. Moreover, for all the SNO data presented here we can only, at present, state that AIRS and CrIS have some differences, we are not prepared to determine which sensor is correct, or better.

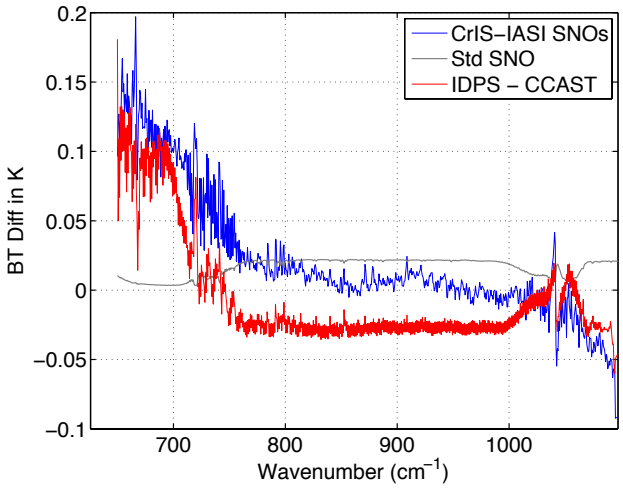

Figure 15: Mean SNO comparison between CrIS and IASI. Also shown is the difference between the IDPS SDR and the UW/UMBC CCAST SDR.

Figures 12c-14b show spectra of the B(T) differences between AIRS and CrIS for these SNOs. AIRS has been converted to CrIS channels. Some slight remaining problems in this conversion for the LW so they are spectrally smoothed out (running filter). The vertical lines in the bottom panel of some of these figures denote spectral regions where AIRS channels do not exist. We have applied the AIRS "L1c" conversion to all of the AIRS SNOs. This conversion removes "popping" data, and inserts estimated radiances into the spectral gaps where AIRS has no channels. Thus, one does not expect great agreement in these CrIS channels. The L1c is used so that channels close to the missing channels have an accurate AIRS to CrIS conversion.

Figure 12c shows excellent overall agreement between AIRS and CrIS, at the 0.1-0.2K level, but one must remember the earlier figures where we show that these SNO differences have a scene dependence, which partially invalidates these mean inter-comparisons (if the UMBC SNO results are correct, the UW SNO results do now show long-wave scene dependent differences between CrIS and AIRS).

The agreement in the mid-wave shown in Fig. 14a is extremely good, and shows a very small step of about 0.1K where AIRS switches detector arrays near 1460 cm^{-1}. In work not shown here, we generally find that CrIS is warmer than IASI (using SNOs) by about 0.1K in all bands.

An example of IASI/CrIS SNO inter-comparisons are shown in Fig.15, where we plot the mean SNO difference for the long-wave band. Here IASI has been converted to the CrIS ILS, which is very easy since both instruments are interferometers. The agreement is extremely good in the mean, as well as the standard error of the mean. Also shown in this figure is the difference between the UW/UMBC CCAST SDR algorithm and the IDPS CrIS SDR algorithm. We see about a 0.1K difference between these two algorithms, with the sign such that CCAST agrees better with IASI than the IDPS SDR algorithm. There are several things that could cause these differences, but more time is need to sort out the root cause of these differences. At this point we only know that our CCAST Science SDR algorithm agrees better with IASI than the IDPS SDR algorithm, we do not know which one is correct.

3.2.5 CrIS High Spectral Resolution Mode

The CrIS interferometer has a maximum optical path difference (OPD) of 0.8 cm, resulting in a sinc spectral resolution of 0.625 cm^{-1}. CrIS presently downloads the full interferogram in the long-wave, only 1/2 in the mid-wave band (0.4 cm OPD), and 1/4 in the short-wave band (0.2 cm OPD). While operation in this mode nominally meets NWP requirements, it completely removes any spectral structure from the short-wave band which contains the best lines for spectral calibration of the Neon lamp. In addition, in full resolution mode CrIS easily resolves the carbon monoxide (CO) lines near 2160 cm^{-1} with very good signal-to-noise allowing very competitive CO retrievals. Moreover, the CrIS am orbit provides better viewing conditions for CO retrievals (high surface temperature contrast) than the IASI pm orbit. Higher spectral resolution in the mid-wave band also allow better high altitude water vapor

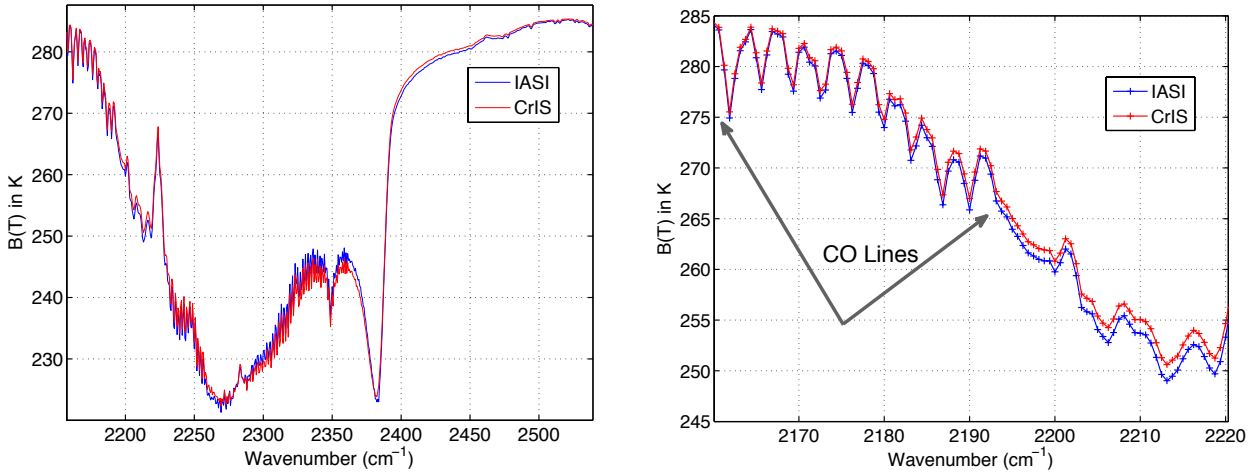

(a) CrIS/IASI observations, Hamming apodized.

(b) Zoom of Fig.16a near CO lines.

Figure 16: CrIS high-spectral resolution observations nominally coincident with IASI observations.

retrievals.

The JPSS Program Office has agreed to switch CrIS into high-spectral resolution mode in the June 2013 time-frame. One day's worth of high resolution data was taken on Feb.23, 2012; these data were converted to SDRs using the CCAST SDR algorithm, modified for these longer OPDs, and are presented here. On March 12, 2013 CrIS was again put into high resolution mode for five orbits in order to test the ability of the IDPS to produce full-length RDR interferogram files, which we also processed successfully with the CCAST SDR algorithm software. In June NOAA plans to produce full-length RDR interferogram files, but will truncate the interferograms back to their original lengths before feeding them into the IDPS SDR algorithm, thus the users will continue to see normal resolution SDRs in the NOAA/CLASS archive. This will allow NOAA to use the high-resolution RDRs, processed outside of CLASS, for calibration purposes. At present, NOAA has no plans to modify the IDPS CrIS SDR algorithm to produce high-spectral resolution SDRs, presumably due to the high cost of algorithm changes within the operation IDPS system.

Figures 16a and 16b show comparisons to IASI, (slightly) degraded to the CrIS high-spectral resolution. Since there is only one day of high-resolution data, SNO's are not possible. Here we selected a clear ocean IASI scene within several hundred km of a similar clear CrIS scene recorded four hours later, so exact agreement is not expected. However, we see very good general agreement, and inter-comparisons of BT bias versus ECMWF of these scenes indicate agreement in the 0.2K or better for mid-tropospheric channels where the ECMWF model is very good. Figure 16b zooms into the region of the CO lines that now appear in the CrIS spectra, containing about 9 individual CO emission/absorption lines. Note that for the same spectral resolution, CrIS NEDT is about 3X *lower* than IASI and approximately equal to AIRS NEDT in the CO spectral region. This strongly suggests that CrIS will be able to prove excellent CO retrieval products. Moreover, the 1:30 pm orbit should also provide better CO retrievals relative to the IASI 9:30 am orbit solely due to the higher thermal contrast at 1:30 pm.

As previously mentioned the CrIS high-spectral resolution interferograms (RDRs) were all processed to SDRs using the UW/UMBC CCAST SDR software. The most significant change to the SDR algorithm for high resolution mode is the apodization corrections for off-axis interferograms, which is larger than required for the other bands. However, we believe that this algorithm is working very well and is very close to producing identical radiances for all nine detectors in the focal plane. The CCAST software is capable of full data stream processing, although some standard I/O plumbing is needed as well as an independent high-quality geo-location routine. All of the CrIS first-light images shown by NOAA and NASA were processed using CCAST since the IDPS algorithm took several months to become operational.

Examples of CO "signals" from this one day of high-resolution mode will be shown in Section 4.4.1,

as well as other minor constituents.

3.3 CrIMSS EDRs

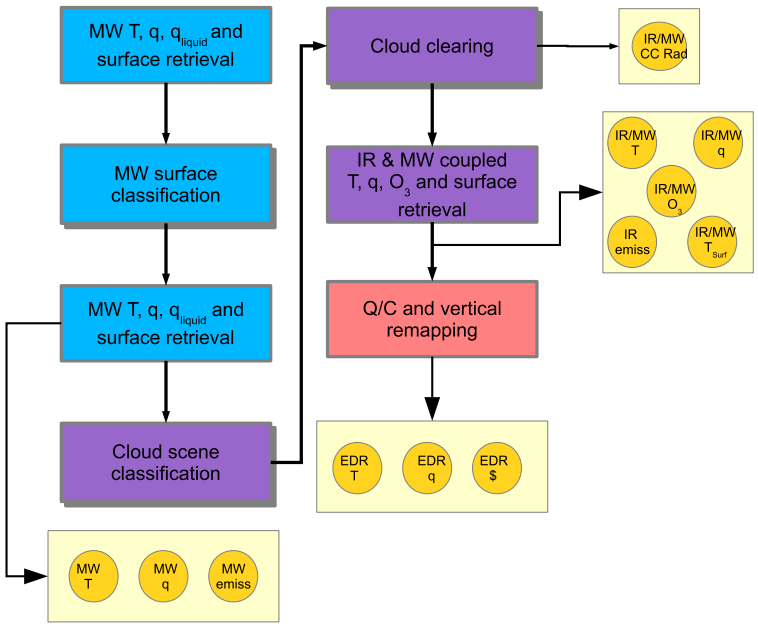

Figure 17: Data flow in the CrIMSS EDR processing. MW processing steps are indicated as blue squares, IR processing by violet squares and the EDR re-layering by the orange. Data products are represented by yellow circles.

The EDR data examined here were produced at the Suomi-NPP Interface Data Processing Segment (IDPS) and collected at the Sounder PEATE. The IDPS produces a layer averaged water vapor profile and temperature profile as its basic EDR, but produces intermediate products (IP) of high-resolution temperature, water vapor and surface products. Table 2 is a list of the IDPS CrIMSS products.

Figure 17 show the flow control in the CrIMSS EDR processing system. The first step is a generic MW retrieval with global a priori state and covariance matrix. The solution from this step is used to perform a second MW retrieval using a scene-type dependent a priori state and covariance matrix and profile representation.

The second MW retrieval produces a 101 level temperature and water mass mixing ratio vapor profiles, surface skin temperature, surface MW emissivity and total cloud liquid water and height of the liquid water cloud. The temperature and water vapor profiles are saved as microwave IPs, the cloud products are never saved and the surface products are overwritten if further processing in the combined retrieval is attempted. Next the scene is categorized based on the skin temperature, surface type and an inferred level of cloudiness. The clear sky radiance is inferred from the current surface and atmospheric state, cloud clearing is performed and a coupled surface property and temperature, water vapor and ozone profiles retrieval is performed. This final retrieval uses both the MW and cloud-cleared IR radiances and The coupling of errors between the MW radiances and the cloud-cleared radiances (which are derived from MW radiances) is not properly handled. Quality control (QC) is based on a threshold test on χ^2; either on the MW channels for the MW retrievals or the MW and cloud-cleared IR channels in the final state.

The height dependence of profiles and the spectral dependence of microwave surface emissivity are represented by empirical orthogonal functions (EOF). The EOFs are derived from a climatology sorted into eight categories:

1. global water, oceans and lakes under all conditions including ice covered,

Output	Description
AVTP EDR	Atmospheric vertical temperature profile EDR which consists of vertically averaged atmospheric temperature (K) for 42 layers
AVMP EDR	Atmospheric vertical moisture profile EDR which consists of vertically averaged atmospheric water mass mixing ratios (g/kg) for 22 layers.
PP EDR	Atmospheric vertical pressure profile EDR which consists of atmospheric pressure at 31 altitudes. (hPa)
AVTP Level IP	Second stage (MW + IR) temperature retrieval data at the OSS levels. (K)
AVMP Level IP	Second stage (MW + IR) moisture retrieval data at the OSS levels. (g/kg)
AVTP MW Level IP	First stage temperature retrieval data at the OSS levels. (K)
AVMP MW Level IP	First stage moisture retrieval data at the OSS levels. (g/kg)
IR Surface Emissivity IP	IR surface emissivity at the surface emissivity hinge points.
Ozone IP	Retrieved ozone profile at the OSS levels. (ppmv)
CrIS Cloud Cleared Radiance IP	Cloud cleared CrIS radiances. (mw/m2/str/cm-1)
MW Surface Emissivity IP	MW surface emissivity for each of the ATMS channels.
Skin Temperature IP	Skin temperature retrieval data (K)

Table 2: Output products of the CrIMSS algorithm (474-00065_OAD-CrIMSS-EDR_B).

2. ocean or lake covered by ice,
3. warm ocean or lake free of ice,
4. global land
5. land with a skin temperature between 200 and 240 K,
6. land with a skin temperature between 240 and 250 K,
7. land with a skin temperature between 250 and 280 K, and
8. land with a skin temperature above 280 K.

Generally EOF representations are not optimal for generating climate data sets because they do not have local support and introduce vertical or spectral correlations into the products which derive from the climatology and not the radiances. Figure 18 shows the height and scene dependence of the first four temperature profile EOFs. Because the retrieval uses a truncated scene-dependent set of EOFs, products from adjacent footprints from different scene types can have unphysical differences. Also signals are inserted into the profiles where ATMS or CrIS have no information, which may look reasonable, but have no observational basis and can be mistakenly interpreted by scientists.

The combined products depend on the quality of the MW products to estimate the cloud-cleared radiances and the combined MW-IR product will not be a CDR if the MW products are not CDRs as well. This report focuses on the MW products and how to proceed to MW-only CDRs. The NPP Team has not evaluated the CrIS Cloud Cleared Radiance IP listed in Table 2, which forms the input to the CrIS retrieval portion of the EDR algorithm (as is also done for AIRS). However, it should be noted that the CrIS Cloud Cleared Radiance IP *only provides cloud-cleared radiances for channels used in the CrIMS retrieval* and may not be useful for additional minor gas products.

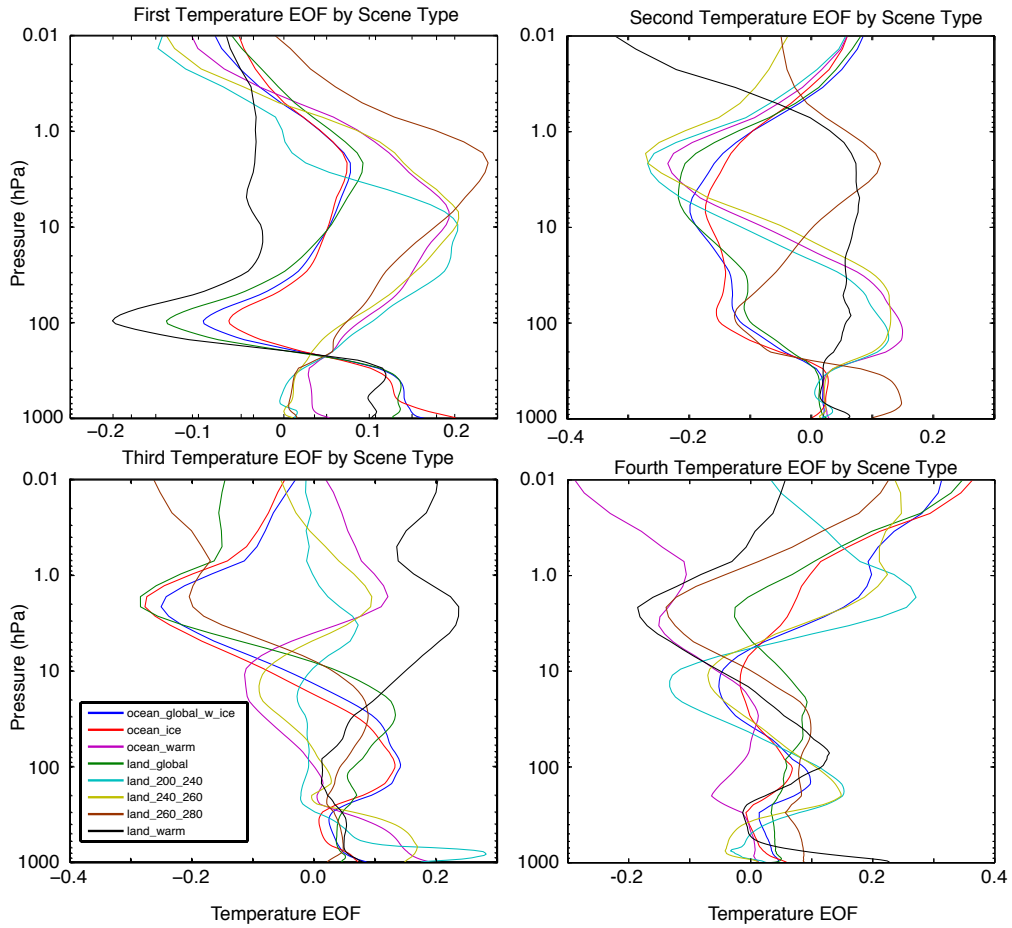

Figure 18: First four temperature EOF basis function, color-coded by scene type.

3.3.1 Microwave-only EDR Analysis

This section compares ATMS MW retrievals against analyzed products from the European Center for Medium Range Weather Forecasting (ECMWF) deterministic forecast.

Global statistics comparing temperature and water vapor profiles with sampled fields from global numerical weather forecasts provide an estimate of the product error characteristics. The ECMWF analysis is a particularly good product for these types of studies; having 91 levels extending from the surface to 0.01hPa, with better than 0.25°spatial resolution, and tends to match assimilated water vapor better than other products. While the ECMWF data is suitable for early analyses, it is generally not reliable in regions where model physics and parametrizations are poor, such as upper tropospheric water vapor, boundary layer lapse rates, regions with mesoscale convection or the summer polar stratosphere. Our comparisons will transition to using more accurate correlative data, such as research-grade radiosondes, balloon-born frost-point hygrometers, ozonesondes and GPS radio-occultations density profiles as the CrIMSS products mature, but that level of maturity has not been reached at this time.

A global comparison between ATMS and ECMWF temperature is shown in Figure 19a. The analysis is sampled at each footprint and log-linearly interpolated to the pressure levels of the IP product. Mean difference profiles are computed for all footprints (dotted lines) and QC'd profiles (solid line). The global accuracy of the CrIMSS products is bracketed by the mean difference, provided the ATMS and ECMWF errors are uncorrelated. The highest sounding MW channel peaks around 2hPa and ATMS has about 4km of vertical resolution. The mean difference is better than 1K in the region of sensitivity. QC reduces the difference slightly, but is is not significant. The standard deviations of the difference

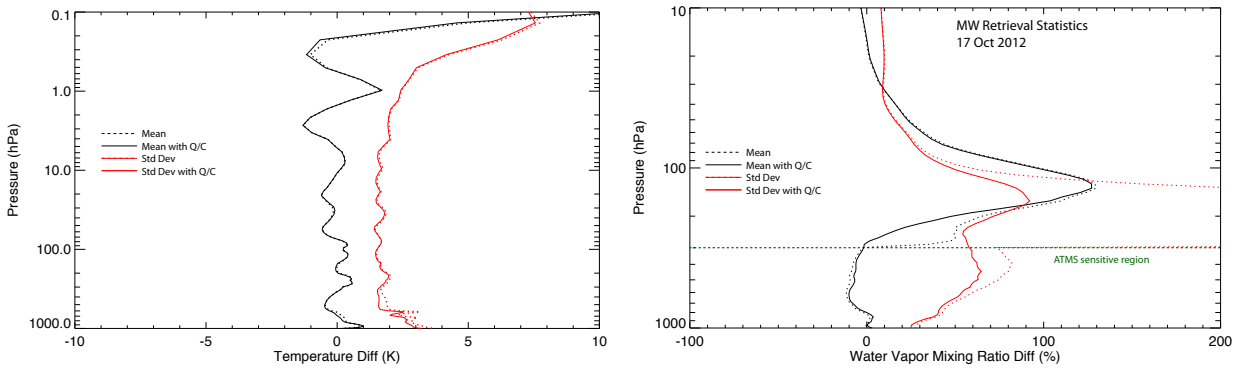

(a) Global mean statistics of MW IP temperature differenced with ECMWF temperature interpolated to the CrIMSS locations. The black curves are mean differences while the red curves are the standard deviation of the difference. Solid lines are with Q/C applied while dotted lines are without.

(b) Global mean statistics of MW IP water vapor differenced with ECMWF water vapor interpolated to the CrIMSS locations. Curves are delineated as in 19a.

Figure 19: Global mean statistics of MW IP temperature and H_2O.

are shown as red curves and provides an estimate of the CrIMSS + ECMWF precision. The standard deviation is better than 3K and the QC'd differences show a 0.5 K improvement near the surface and in the mid troposphere. Both the mean and standard deviations show poorer agreement near the surface in the planetary boundary layer. Profiles from microwave temperature sounders usually show a negative temperature bias around 200hPa because they can not resolve the sharp minimum of the tropopause. That this is not present here is suspicious and is discussed next.

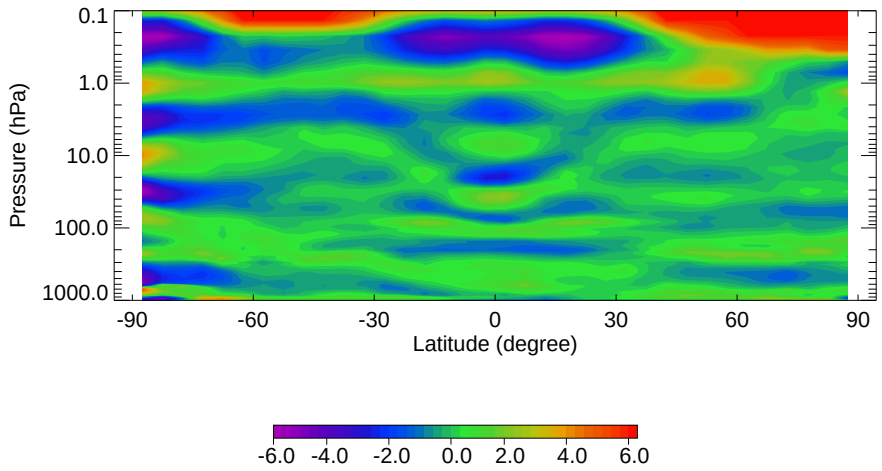

Figure 20: Zonal-mean cross section of the difference between CrIMSS MW temperature and ECMWF for 17 Oct 2012.

As was discussed earlier, using EOFs to represent profiles introduces "features" which make the products less suitable for climate research. One example is the representation of the tropopause. Since ATMS is not able to resolve the minimum of the tropopause, the absence of a negative bias suggests that external information is leaking into the temperature profile, and this most likely the EOF representation of the profile.

One way to examine this is to compare how the CrIMSS MW IP temperature characterizes the variability of the tropopause. Figure 20 shows the cross section of the mean temperature difference, binned in 5°latitude bins as a function of height. In the tropics where the tropopause moves upward

the CrIMSS tropopause remains at a fixed height and shows a cold bias below a warm bias. Similarly at high latitude where the tropopause moves downward, the CrIMSS tropopause does not follow it. Also we see a latitude dependent oscillation as large as 3K.

Global water vapor statistics are examined next in Figure 19b. Water vapor is compared in terms of percentage difference relative to the global mean ECMWF water vapor profile because water vapor varies by a factor of 1000 across the troposphere. A single global ECMWF profile is used to simplify interpreting horizontal structure and to prevent biasing the statistics from dry profiles. The highest-sounding ATMS water vapor sounding channel peaks around 300hPa and the largest increase in errors occurs where ATMS looses sensitivity. QC produces a large improvement in agreement in the region of no-sensitivity in the mean and standard deviation, and a large improvement in standard deviation in the region of sensitivity, but only a modest improvement in the mean difference.

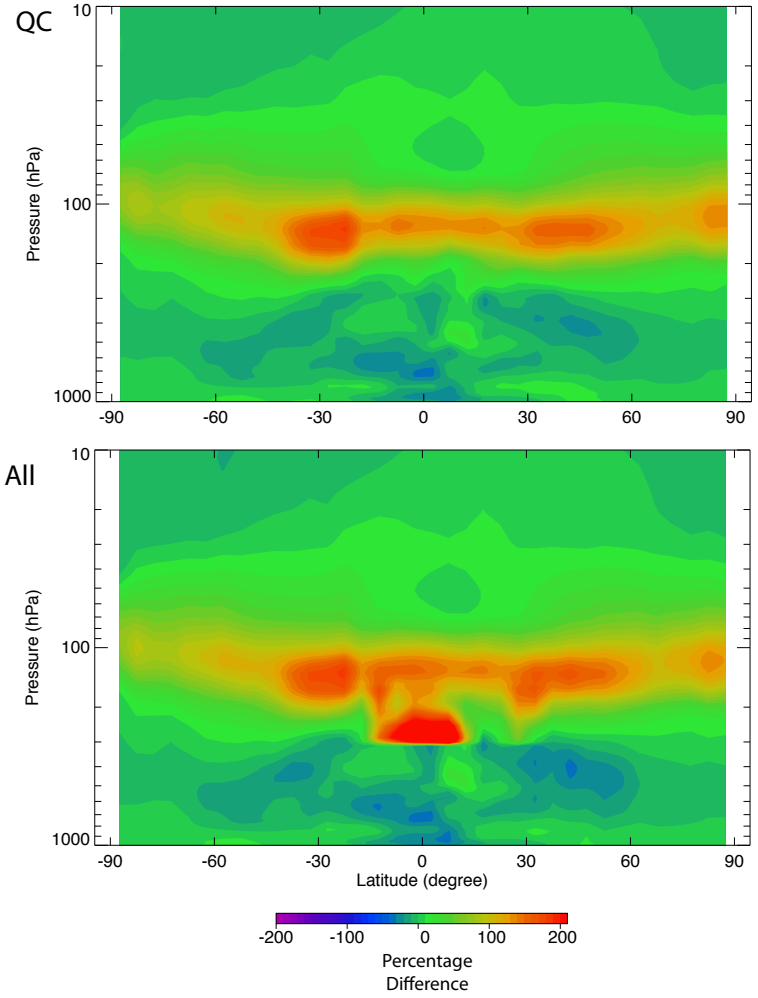

Figure 21: Zonal-mean cross section of the difference between CrIMSS MW water vapor and ECMWF for 17 Oct 2012.

An explanation of the large water vapor differences is seen in the water vapor zonal mean cross section shown in Figure 21. The top panel shows the QC'd data, the lower shows all data; the top panel shows large differences while the bottom panel show less. All of the large differences are located in the tropical upper troposphere where the air is cold and dry, but close to saturation. ATMS has sensitivity to temperature, but not to water vapor and the global a priori water vapor profile is physically too wet. The algorithm imposes a water vapor saturation constraint to minimize supersaturation in the upper troposphere, but has difficulty working because the problem is as much scene dependent as it is height dependent. The QC removes the high error cases, but this is surprising given that water vapor errors at

this level are unlikely to contribute to χ^2. A likely explanation has several sources including: the water vapor EOFs are correlating errors at this level with lower in the atmosphere, the a priori solution is very far from the true solution, and the a priori covariance matrix over-constrains the corrections required by the best radiance-fitting solution. Differences in the tropical lower troposphere are also lower (closer to zero) in the QC'd field and indicates that QC is biasing the data set towards the more dry tropical conditions. Several algorithm changes would include: more spatially and temporally-dependent a priori, looser a priori uncertainty, and use of a relative saturation parameter in place of water vapor mixing ratio, such as relative humidity or dew point depression temperature. The AIRS MW retrieval algorithm used relative humidity.

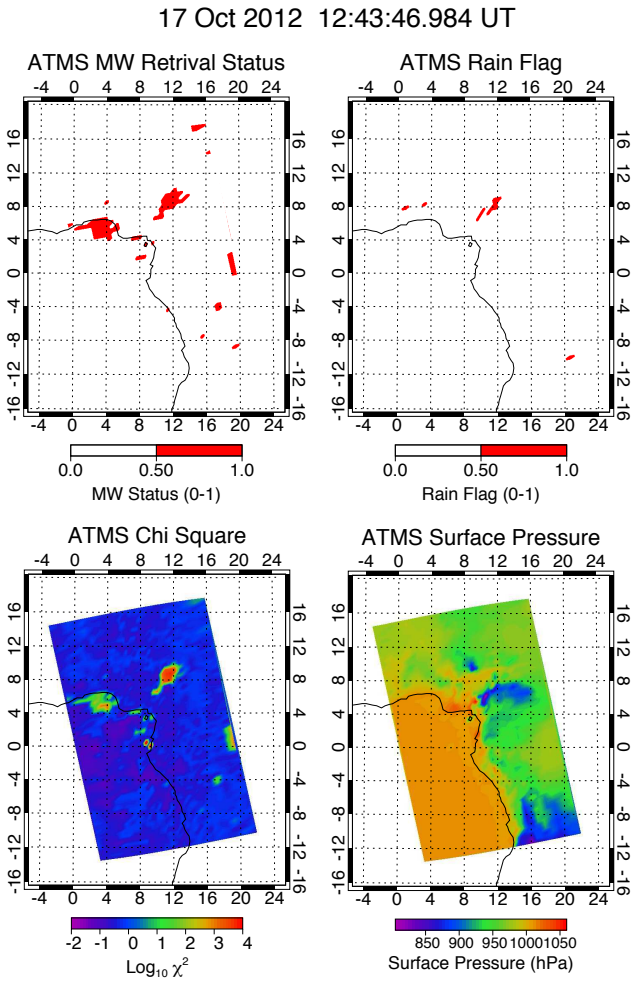

Figure 22: Mapped MW QC flag, rain flag, MW retrieval χ^2 and surface pressure. The center of the swath is at 0°N, 10°E and was observed on 17 Oct 2012 at 12:43:47 UT

The next set of figures show spatially mapped products which help to explore the usefulness of ATMS products to characterize processes and local climates. We show 8 minutes of data, 60 lines (1800 footprints) centered on the equator, including the West Africa and the Atlantic Ocean. Figure 22 shows the MW qc flag, rain detection flag, χ^2 and surface pressure. Although there are mountains in West Africa, there is no evidence that the product degrades at higher elevations. The profiles extend below the surface and the user must filter the IP profiles against surface pressure to remove subterranean data. Rain is detected at a few locations, but the regions of high χ^2 show are more indicative of rain.

Figure 23 shows maps of ATMS and ECMWF temperature at 100 and 800hPa spanning the Equatorial Western Africa coastline. The tropopause lies close to 100hPa and is affected by local atmospheric waves as shown in the ECMWF field. The ATMS field shows none of this, partly because it lacks vertical

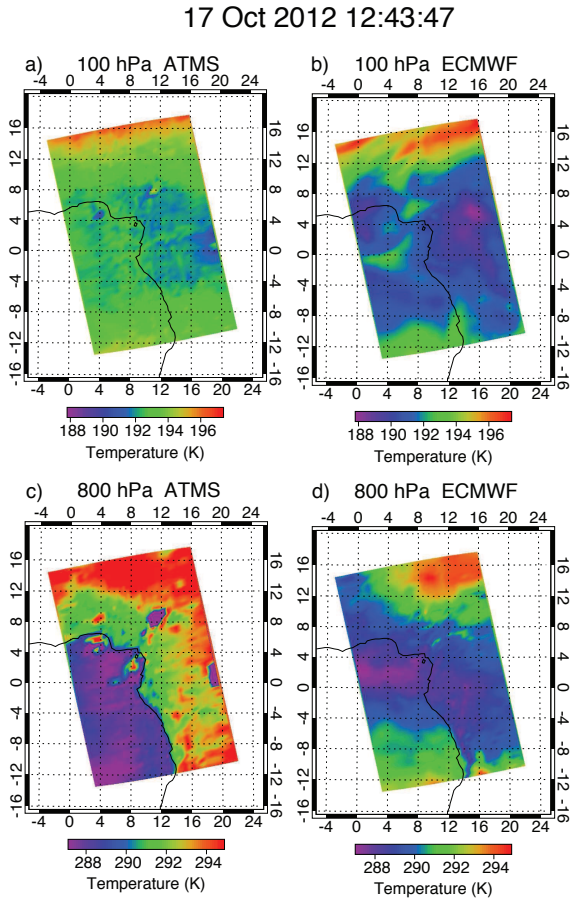

Figure 23: Mapped temperature at 100, and 800 hPa (top to bottom) from the ECMWF and ATMS left to right.

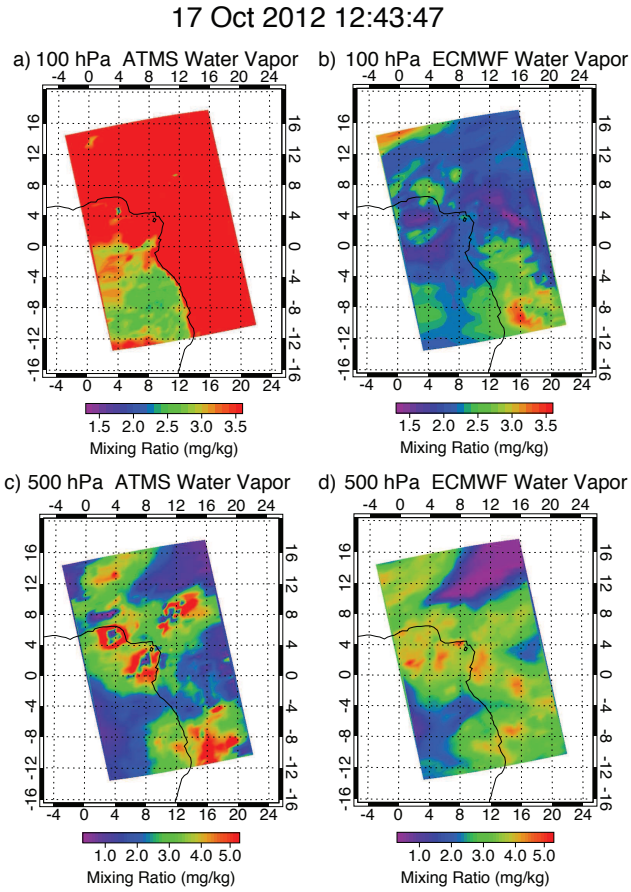

Figure 24: Mapped water vapor at 100, and 500 hPa (top to bottom) from the ECMWF and ATMS left to right.

resolution, but also because the retrieval system may be over-dampened. The lower panel at 800hPa, approximately 1.5km above the surface has a 3K temperature difference between water and land footprints (even inland lakes). This is certainly an artifact of the scene-type dependent EOF used in the retrieval. High χ^2 is poorly correlated with temperature differencs at 100 hPa and only slightly correlated in the regions of intensest raining; χ^2 is not a good discriminant of temperature quality in most situations.

Figure 24 shows ATMS and ECMWF water vapor on the 100 and 500 hPa levels. The 500hPa surfaces are qualitatively in agreement, but the ATMS map show regions of low water vapor ringed by high water vapor regions. These are regions where scattering from ice and rain droplets in precipitating mesoscale convection systems produce signals which can not be interpreted by the radiative transfer package. The rain flag detects some of the footprints containing rain, but χ^2 has better skill. ECMWF fields shows high water vapor in mesoscale convective systems, but the locations are control by subgrid scale processes poorly constrained by observations. Therefore, although both fields show "blobs" of high water vapor at 500 hPa, their locations are uncorrelated. The 100hPa ATMS water vapor shows coherent structure which are mostly independent of the structure seen in the ECMWF water vapor. ATMS has no sensitivity to water vapor at 100hPa and this structure arises from EOF representation of the profiles.

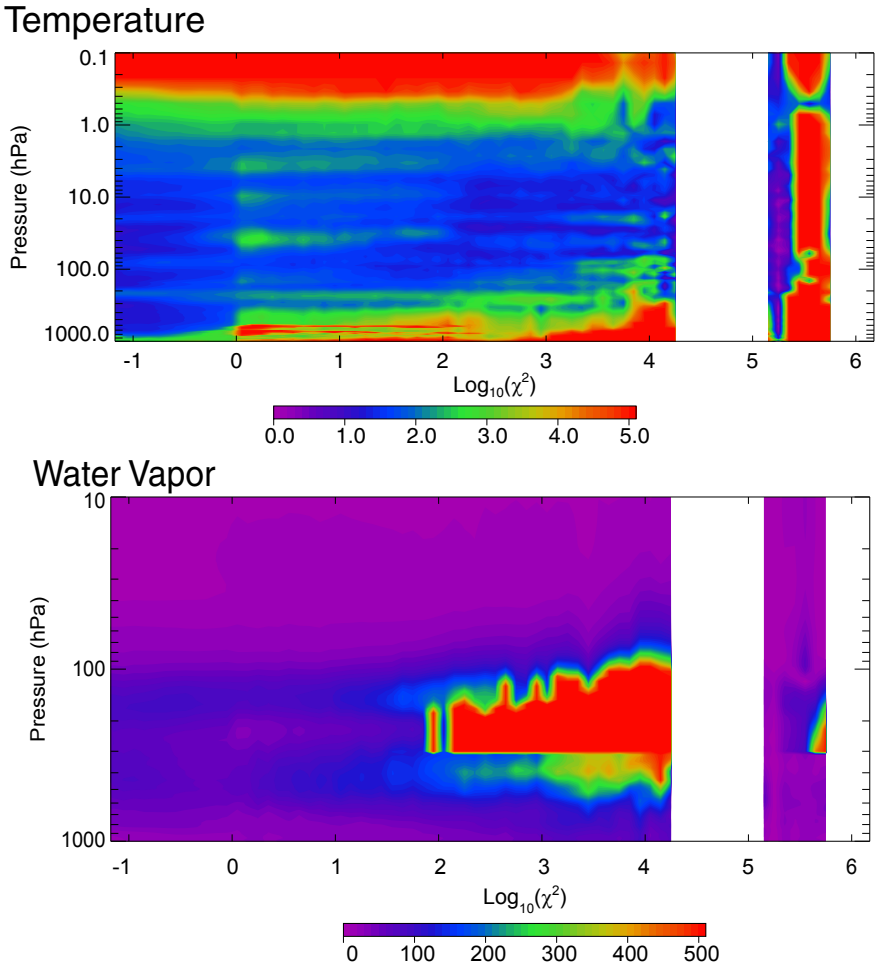

Figure 25: Standard deviations of differences between ATMS and ECMWF temperature (top) and water vapor (bottom) conditioned on χ^2. The χ^2 axis is in $\log_{10}\chi^2$.

Figure 25 examines the conditional probability of the standard deviation of differences between ATMS retrieved and ECMWF analyzed temperature and water vapor conditioned on χ^2. χ^2 is primarily influenced by brightness temperature differences in low noise surface channels and scattering in high frequency G-band channels. In both panels, the differences are uncorrelated with χ^2 except that

temperature shows a discontinous increase in difference across a χ^2 value of 1 and the tropical saturated upper troposphere where χ^2 is greater than 50. At a most levels the difference either independent of χ^2 or weakly dependent on it. For these reasons, we believe χ^2 is a poor Q/C detector and recommend high registered error obtained by propagating radiance residual or error covariance to a product error estimate.

3.3.2 Ozone IP

Ozone is an important AIRS/CrIS product and and could supplement the Ozone Mapper and Profiler Suite (OMPS) products on NPP by providing nighttime ozone, polar winter ozone, and some measure of tropospheric ozone. CrIS should easily be able to continue this product, possibly with improvements due to the far lower CrIS noise levels in the long-wave O_3 channels (compared to AIRS). Ozone is an intermediate product for the CrIMSS algorithm; but as yet the quality of this product has not been investigated by the NPP Sounder Team. We provide here in Fig. 26 a comparison done by the NOAA STAR Team (led by Larry Flynn) from the CrIMSS Provisional Review at NOAA, showing OMPS total ozone and the CrIS derived total ozone for Oct. 16, 2012. This figure at least shows good qualitative agreement, rigorous validation remains to be done. We do note that the impact of the excellent signal-to-noise of CrIS (relative to AIRS, for example) in the O_3 sounding region has yet to be explored. Synergy between the OMPS total column O_3 and CrIS derived O_3 should also be explored.

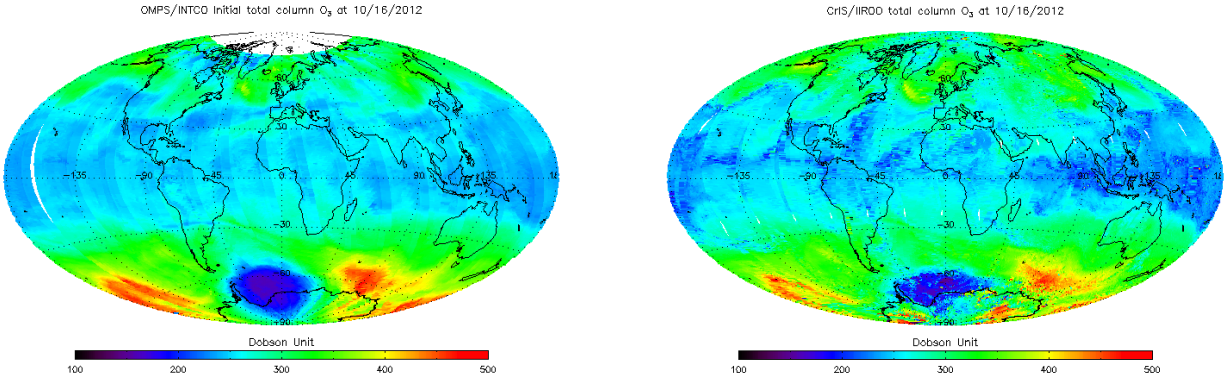

Figure 26: Left: OMPS, Right: CrIS total ozone, Larry Flynn, NOAA/NESDIS

3.3.3 EDR Validation Issues

At the time of this report (Spring 2013), the CrIMSS EDR products are in transition from “beta” to “provisional” status. The results presented here are a high level summary of results by the NPP science team members, some of whom are also JPSS Cal/Val team members. The top level conclusion is that the CrIMSS product has seen rapid improvements since launch in the very capable hands of the JPSS EDR Cal/Val team lead (Chris Barnet) at NOAA NESDIS working closely with the original CrIMSS algorithm innovator (Xiu Lu) at NASA LaRC. The result is that Mx 6.4 (Oct. 15, 2012 to current) is much improved in both bias, RMS, and yield (1% to 25% in MW+IR) over the previous version Mx6.3 and off-line evaluations of Mx7 suggest further improvements in yield (about 50% in MW+IR) will be obtained in the next IDPS version update (approx. Feb. 2013). Performance results are summarized in Fig. 31 in the Appendix of this report.

One possible criticism of the NOAA validation approach is over reliance on an NWP analysis field (in this case ECMWF) for the “truth” field. To mitigate this concern; the team members will be making assessments of the CrIMSS product against “independent” measurements. (Note, since many data types, including satellite data, are assimilated into NWP models and because NWP model fields are used in retrieval regression training, the term “independent” is used here in a qualitative sense only.) The independent measurements being used to assess the CrIMSS product for climate quality include 1)

Vaisala RS92 radiosondes launched co-incidentally with NPP overpasses (supported by JPSS Cal/Val), 2) the global radiosonde upper air network (supported by JPSS Cal/Val), 3) the COSMIC GPS RO network (analysis supported in part by JPSS Cal/Val), 4) Water vapor Raman Lidar (upper troposphere humidity) and total column water vapor (SUOMINET) (analysis supported by JPSS Cal/Val), 5) sea surface temperature using the Reynolds dataset, 6) cloud top temperature of convective clouds, and 7) aircraft validation campaigns using the NASA ER-2 and Global Hawk (supported by NOAA JPSS). None of these validation data are directly supported by the NPP science team project but all of these data are invaluable for the assessment of the climate quality of the NPP products. The detailed assessment following from these validation activities is just beginning, but is expected to be available for the next NPP assessment report in early 2014.

4 NASA Climate Research and Recommendations

The CrIS/ATMS system was designed primarily as a temperature and water vapor profiling instrument for weather forecasting, its powerful potential for climate applications has long been recognized and has been reinforced by the activities supporting the CLimate Absolute Radiance and Refractivity Observatory (CLARREO) Decadal Survey mission as a Tier 1 NASA priority. The *climate process studies* and diverse range of *climate product examples* developed by the AIRS Science Team and others, along with the potential to serve as part of a *climate benchmarking system* for decadal trend characterization a la CLARREO represent the diverse range of important climate applications of CrIS.

This report is the first assessment by the Suomi NPP Science Team of the overall quality for climate applications of the CrIS sounding measurements and products with recommendations for improvements. The overall question to be addressed is often summarized as: *Can Suomi NPP continue the EOS climate record*? To illustrate the nuances of this question, we offer a few short observations:

1. The basic sensor characteristics and measurement quality of CrIS are definitely capable of successfully continuing the high accuracy and information content data record of AIRS.
2. The operational SDR algorithms and processing are working reasonably after a year with many modifications, but will not serve the climate community well for performing required quality refinement and reprocessing. Code that is more transparent to developers, like the joint UW/UMBC CrIS Calibration Algorithm and Sensor Testbed (CCAST) is needed. It is important to realize that products based directly on measured radiances and brightness temperatures are fundamental climate records in their own right. It is also important to recognize that the existing AIRS L1B radiance record is not considered climate quality for many studies, and improvements such as the planned AIRS L1C code/products are still needed.
3. The IDPS CrIMSS EDR products are limited to profiles of temperature, water vapor, and pressure performed after cloud clearing with a specialized physical retrieval algorithm. Significant work remains to validation the IDPS EDRs for climate applications, but they are inherently incomplete for representing the full climate potential of CrIS due to a number of missing products. Further, discontinuities are to be expected when joined to the AIRS record. A common, high spectral resolution retrieval algorithm, specifically chosen for creating an unbiased climate record is needed to produce refined climate products from the 13:30 orbit starting in 2002.
4. To fully represent the potential of the infrared sounders on EOS and Suomi NPP, in addition to advanced sounder type high vertical resolution temperature and water vapor profiling, CrIS/AIRS climate products should include cloud properties, dust optical depth, trace gas distributions, and surface emissivity. Again, common algorithms for CrIS, IASI and AIRS are needed.
5. Given the absence of IR absorbing channels on the Suomi NPP imager, VIIRS, coordination between CrIS and VIIRS teams are needed to produce the best cloud products.

The basic climate products ultimately expected from CrIS can be characterized as Level 3 means, higher moments, and probability distribution functions from (1) Spectral Radiances and Brightness Temperatures (SDR-like reprocessed products), (2) Temperature and Water Vapor Profiles (EDR-like

reprocessed products), and (3) Other key products, including cloud properties, dust optical depth, trace gas distributions, and surface emissivity.

4.1 CrIS SDR Algorithm Limitations

The CrIS SDR algorithm currently running in IDPS is adequate to meet NWP needs. This is the result of on-going efforts by the Cal/Val team to identify and fix issues with the operational code. Initially, the IDPS software had several major issues, and it took several months after CrIS was powered on for IDPS to produce reasonable spectra, despite off-line codes such as CCAST and ADL/CSPP producing accurate spectra much earlier. The issues with the IDPS code and implementation ultimately trace back to the overall NPOESS structure, where the calibration algorithm experts were not included in the SDR algorithm development until only recently. Moreover, the IDPS CrIS SDR code base has undergone a long list of "owners", in chronological order: BOMEM, ITT, Northrup Grumman, Raytheon, and now NOAA/NESDIS. ITT Excelis, for example, are developing independent changes to the SDR algorithm for FM-2, and how these changes will flow into the IDPS algorithm are unknown, presumably via NOAA/NESDIS and then back to Raytheon with Northrup Grumman providing support. In short, this is an unwieldy, slow, and error-prone process that takes many months to years to produce a significant upgrade to the SDR algorithm.

Although the IDPS SDR algorithm is adequate for NWP applications, *the IDPS SDR code and processing and resulting SDR record is not adequate for climate needs*. The completeness and maturity of IDPS geo-located radiances are not adequate for the generation of optimum climate records for the following reasons:

- Difficulty/inefficiency of making even minor software version updates
- Incomplete data record due to missing or corrupted RDRs (repair granule problems)
- Calibration look smoothing problems associated with repair granules
- Current inability to process full spectral resolution CrIS data, which will begin in June 2013
- Discontinuities in radiometric calibration due to software version changes, and due to calibration coefficient changes
- Discontinuities in spectral calibration, due to the way IDPS triggers updates in the spectral corrections at irregular intervals.
- Core SDR processing parameters not stored in the SDR output (metrology laser wavelength used to produce the SDR).

The UW and UMBC have developed a SDR "science code", named CCAST, which is highly accessible, flexible, and faster than the vendor supplied IDPS code. A CCAST-based approach for generating reprocessed radiances is recommended for the development of reprocessed climate data records in order to preserve a direct traceability of the radiance record to SI standards (on orbit calibration and corresponding error budget). CCAST can also process the high-spectral resolution SDRs which were discussed earlier in this report. This reprocessed SDR radiance record should be performed by NASA to facilitate the close interaction of scientific experts with the climate products while avoiding the introduction of programming errors introduced by third party software vendors. We suggest that NASA adopt science code for the production of climate records and reject the vendor supplied IDPS code for this important purpose.

We expect climate products will be generated directly from AIRS/CrIS radiances, in order to preserve rigorous error estimates of climate change, as was planned for CLARREO. We recommend science team support for development of algorithms to generate appropriate Level 3 products, including means, higher moments, and probability distribution functions, along with uncertainty estimates.

4.2 ATMS SDR Algorithm Limitations

The liens discussed above on the ATMS calibration, taken together with current plans for the IDPS, necessitate an alternative processing approach for NASA ATMS climate data records. There are three

principal reasons for this. First, it is not clear that IDPS will reprocess data to exploit new and improved algorithms and calibration optimization. Second, calibration improvements such as those described in this report are not all planned for inclusion in the ATMS IDPS algorithms, to our knowledge. Third, an improved and expanded set of quality control is needed for a high-fidelity climate data record, and these data are not available in the IDPS records. Furthermore, an ATMS precipitation product has been produced and is now operational at the Sounder PEATE. This product has valuable climate applications and could be readily included in an expanded ATMS data record produced by NASA.

4.3 EDR Algorithm Limitations

The primary goal of the AIRS sounder on EOS-AQUA was to improve numerical weather prediction (NWP) by moving to a hyperspectral infrared (IR) instrument with thousands of high-spectral resolution channels. The AIRS instrument suite also included a microwave sounder, AMSU, and the Humidity Sounder Brazil (HSB). HSB provided microwave water channels (now available on NPP-ATMS), but if failed within six months. AIRS was the first operational hyperspectral IR sounder and was shown to have more impact on forecasts than any other single instrument at the time. (The sum of AMSU instruments together have a slightly larger impact as there are several operating at one time.)

The fundamental retrieval algorithms for the AIRS Level-2 products (or EDRs in NPP language) were developed with an emphasis on near real-time processing for NWP use, which also required independence from auxiliary data sets that are produced after the observations. Thus, the AIRS L2 retrieval has built-in limitations for climate-level reprocessing due to its heritage as a potential product for NWP. This self-imposed requirement on AIRS Level-2 and CrIS EDR processing algorithms places limitations on the retrieval algorithm that are often incompatible with production of climate data records (CDRs) of useful accuracy. This is especially true with regard to AIRS Level-2 and Level-3 error estimates and issues to do with sampling (due to clouds) in Level 3 products. *These same limitations apply to the NPP CrIMSS EDR products* since they are totally oriented towards weather forecasting rather than climate.

In practice, almost all large NWP centers assimilate AIRS radiances, not AIRS Level 2 retrievals. This is also the case with EUMETSAT's IASI hyperspectral sensor on METOP-1/2 and with CrIS on NPP. There are many reasons why NWP centers assimilate radiances rather than Level-2 retrievals, but can be broadly stated as the difficulty in characterizing the Level-2 errors. For AIRS, these errors are influenced by the prior information used in the retrieval and by the difficulty in evaluating errors in the cloud-cleared radiances are used for temperature (T(z)) and water vapor (Q(z)) profile retrievals. Note also that all major re-analysis products (MERRA, ERA-Interim, etc.) also ingest radiances from AMSU/AIRS/IASI, not Level 2 products or EDRs.

Recognizing these issues, the AIRS Project at NASA/JPL is planning to develop a new retrieval algorithm based using a Bayesian-based optimal estimation algorithm (OE) that is now the standard for NWP assimilation and for many minor-gas sounders (MOPITT, TES, IASI). This includes shedding the use of cloud-clearing, which can introduces errors that are extremely difficult to characterize within the retrieval. Although the issues are complex, removing the requirement to produce retrievals within 3-hours with little use of a-priori data should result in a superior climate record with known error characteristics and better sampling (by using a good a priori when the information content is not available from AIRS).

The selection and development of the proper microwave/hyperspectral retrieval methodology that provides objective, climate quality geophysical variables, without the imprint of possibly incorrect retrieval assumptions is of paramount importance. Bayesian optimal estimation is the "industry standard" across a wide range of earth science parameter retrieval applications. It is universally used for infrared minor gas retrievals (MOPITT, TES, IASI) except for AIRS (at present). However, we know of no existing optimal estimation retrieval using microwave + hyperspectral IR radiances for single field-of-view (meaning all cloud types). Although the TES retrieval uses OE, they only consider fields-of-view with minimal clouds, and their primary interest is minor gases, not temperature and water vapor profiles. OE properly combines a priori information with new information from the measurement. But, for cloudy IR radiances, the selection and handling of a priori information is exceedingly non-trivial. The IDPS CrIMSS algorithm provides a starting point for an OE algorithm, except that it continues to

use cloud-cleared radiances.

This suggests that the proper retrieval approaches *may* depend strongly on the science being examined. Thus, for minor gas retrievals using CrIS an OE approach is probably warranted since that community has in general not accepted minor gas retrieval products that do not also contain the mathematically rigorous information about retrieval errors and kernel functions that only OE provides. This approach is possible, in part, because minor gas retrievals are generally done using relatively cloud-free observations. However, the authors of this report are mixed in their opinions on the best climate-level retrieval methodology for temperature and water profiles, and cloud products. The overriding issue is to either avoid unknown a priori imprints in the retrievals, or characterize them sufficiently.

We recommend that the development of a new retrieval algorithm for AIRS/CrIS be structured to be as open a process as possible, since it is unlikely that a single group will have sufficient resources to produce a retrieval algorithm system that can generate all the products possible with CrIS/ATMS. At a minimum, open-source coding standards and processes, including configuration management, should be seriously considered. Development of climate-level algorithms for IR hyperspectral sensors has received little attention to-date, and will likely only be successful with full community involvement will heavy code re-use. Given the potential importance of the AIRS/CrIS radiance record as a climate change indicator in the coming years, and the recent directives from the Office of Science and Technology Policy (OSTP) for "Increasing Access to the Results of Federally Funded Scientific Research", we believe that a new model for code and data development and access, is warranted.

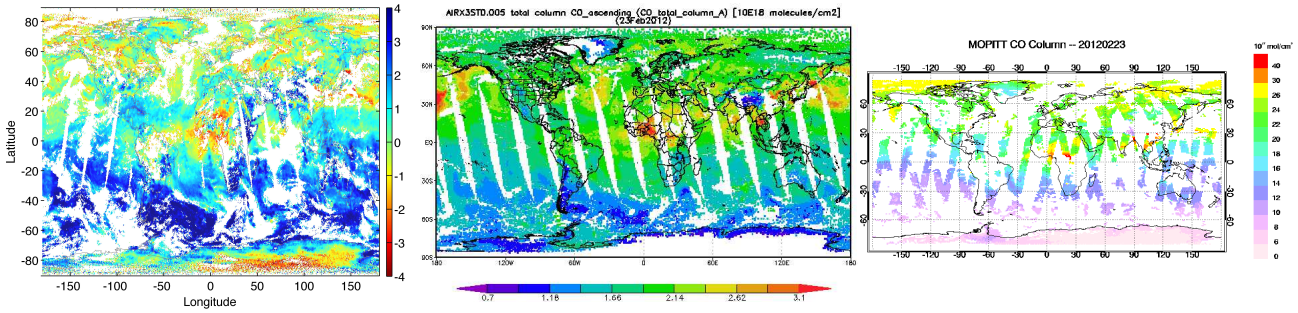

(a) CrIS CO Signal (in K) **(b)** AIRS CO **(c)** MOPITT CO

Figure 27: Carbon monoxide observations by CrIS, AIRS, and MOPITT on 2/23/2012.

4.4 Minor Gases

The capabilities for sounders such as AIRS and CrIS for minor gas and aerosol (dust, ash) retrievals has generally received very little attention. This is partially because AIRS was conceived as a weather sounder, and programmatically was not oriented towards ozone, and minor gas/aerosol retrievals. In addition, during the development and early years of AIRS, NASA was developing or flying other sensors that could possibly do slightly more accurate retrievals of CO, O_3, NH_3, and dust, ash such as MOPITT, TES, OMI, and MODIS (dust over ocean). Thus AIRS/CrIS have not been considered as minor gas/dust instruments and this has naturally made it difficult to attract both researchers, and funding, to build robust retrieval algorithms. (We do acknowledge, for example, that AIRS/CrIS CO will not be able to determine boundary layer CO, which has just started to become possible with MOPITT by use of the near-IR CO channels.)

Presently, there appears to be no follow-on missions for either MOPITT or TES. Although the latest EV-I selection is a pollution mission (TEMPO) the one major pollutant that TEMPO cannot measure is CO.

What is highly certain, though, is that the high-spectral resolution infrared radiance record, started in 2002 with AIRS, will continue for several decades or more, given the importance of IR sounding for operational weather forecasting. Therefore, if proper attention is paid to the operational sounder

record, many of the measurements pioneered by TES and MOPITT can be continued by NPP and JPSS-1/2 CrIS. The excellent radiometric stability of these instruments, and their extremely good intra-instrument radiometric agreement as highlighted in the report, also strongly suggests that the operational sounders will also be well suited to providing a very stable climatology of minor gases.

4.4.1 Carbon Monoxide

AIRS minor gas products distributed at the GSFC DAAC include CO, CH_4, upper-tropospheric CO_2. The CO product has been shown to be similar to the TES and MOPITT products, but with far greater global coverage. The TES mission is effectively over, and MOPITT will likely only last a few more years. Thus, CrIS represents the *only* way to continue those global time series for the *pm* orbit and produce multi-decadal records of atmospheric CO. As discussed earlier, once CrIS is placed into high-resolution mode, CO will be a very viable product, *if* the high-resolution SDRs are produced (no plans by NOAA as yet) and *if* a CrIS CO algorithm is developed and run.

Since only one day of CrIS high-resolution data exists to-date, there has been little reason to develop a CrIS CO algorithm. In order to demonstrate that CrIS has a good CO signal, we generated high-resolution SDRs from the full interferogram data of Feb. 25, 2012. These SDRs were matched to the ECMWF forecast data, and simulated CrIS radiances were computed using a single background value for the CO profiles. A *very crude* cloud detection algorithm was used, which let through a number of cloudy scenes in order to maximize global observations. Figure 27 shows the bias between observed and computed radiances for *a single CO_2 channel* (out of nine CO channels on CrIS). There has been no other data Q/A or masking done, so a number of false CO readings are shown, especially in the Antarctic, which can be easily corrected. However, it is clearly evident that a single CrIS CO channel has abundant CO information by comparing the CrIS CO signal to the AIRS and MOPITT CO products for that date.

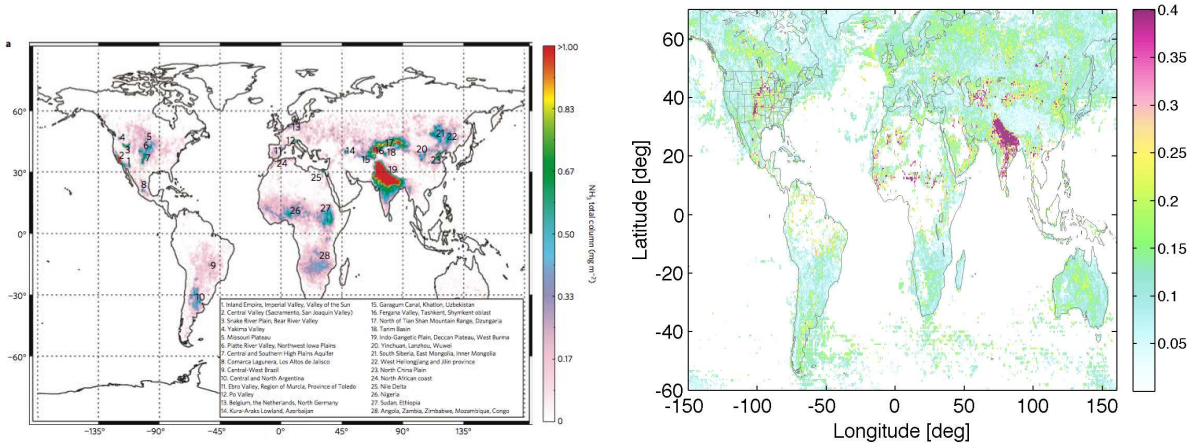

(a) Global yearly mean NH_3 from the METOP IASI sensor. **(b)** May 2012 average NH_3 B(T) /signal/ from CrIS.

Figure 28: Global comparison of IASI mean NH_3 to CrIS NH_3 B(T) signal.

4.4.2 Ammonia

The infrared thermal window near 10 microns contains strong NH_3 lines, which have been used by the AURA-TES team and the IASI team for numerous scientific studies. The NH_3 is primarily detected in the boundary layer and most studies have concentrated on agricultural emissions that are extremely important for understanding the nitrogen cycle and how it may change with increasing population. NH_3 is also produced by combustion, especially via forest fires. As previously mentioned, the TES record is effectively over, and has low coverage. The IASI NH_3 has generated very significant interest, see for

example [3] and [4]. However, AIRS and CrIS are capable of producing *better* NH_3 products due to (a) lower noise, especially CrIS, (b) the *am* orbit gives better sensitivity since the ground temperature is hotter. Of course NH_3 3 emissions are closely related to production of secondary particulate matter, leading to high aerosol production (and EPA PM 2.5 aerosol warnings).

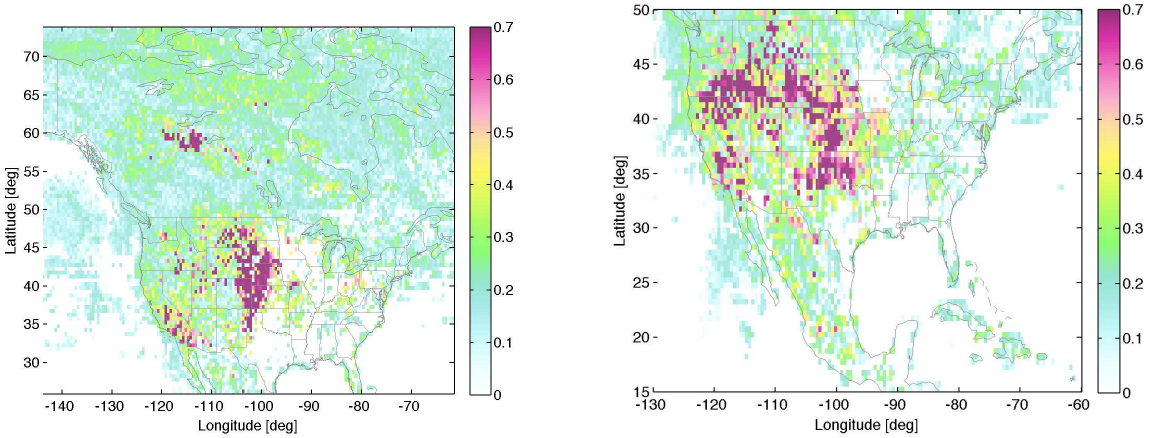

(a) Max NH_3 B(T) signal detected by CrIS in July 2012 for N. America. NH_3 emissions from both agricultural sources and wildfires are evident.

(b) Same as Fig. 29a but for August 2012 showing enhanced fire emissions of NH_3, especially in southern Idaho and Washington states.

Figure 29: Maximum NH_3 B(T) signals for July, August 2012.

Figure 28 shows the IASI derived mean global NH_3 yearly emissions, along with the CrIS mean NH_3 *signal* for the month of May 2012. The CrIS NH_3 *signal* is a double-difference, subtracting the bias between NWP computed radiances and observed radiances, for two channels, one sensitive to NH_3 and another nearby channel with no NH_3 sensitivity. Because we used a rather crude surface emissivity model, false readings can arise in some desert regions.

The ability of CrIS to see NH_3 emission from both agricultural and fire sources is shown in Fig.29 where we plot maximum NH_3 signal for both July and August 2012. Here we see both agricultural emission in the mid-west and near large feed-lots, then turning into extensive emissions from fires in August in southern Washington and Idaho. Also seen in July is NH_3 from fires in northern Canada (and in Siberia, but not shown.)

In general, there has been the opinion in the remote sensing community, both in the U.S. and in Europe, that CrIS has too low spectral resolution to do any atmospheric chemistry. This opinion is partially due to the lack of appreciation of the usefulness of the extremely low noise of CrIS, especially in the thermal infrared window. In addition, the community is generally not aware that CrIS can, and will, be run in high-spectral resolution mode start in June 2013. There *are* TES products that CrIS most likely cannot produce; for example HDO may be difficult for CrIS, even with higher spectral resolution in the mid-wave band.

4.4.3 Volcanic SO_2

The thermal infrared contains several SO_2 bands that can be used to detect volcanic SO_2 emission. This has been used extensively by the IASI community for tracking the fate of SO_2 and ask from numerous volcanic eruptions. Both AIRS and CrIS have similar (and possibly better) sensitivities to volcanic ash and SO_2, but these capabilities have barely been taken advantage of with AIRS, and there are no SO_2 retrievals under consideration for CrIS. Again, note that CrIS sensitivity to SO_2 will be enhanced when CrIS is switched to high resolution mode (the SO_2 band is in the mid-wave). In addition, the far lower noise of CrIS compared to either AIRS or IASI in the long-wave should enhance CrIS detection and tracking of volcanic ash compared to either AIRS or IASI.

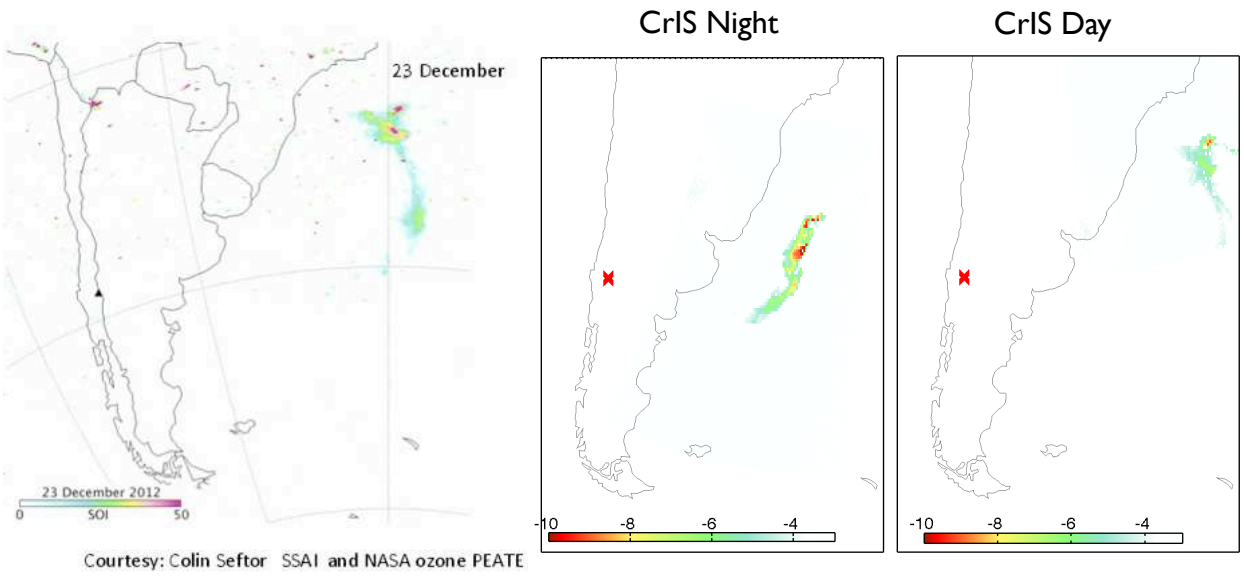

Figure 30: CrIS and OMG volcanic SO_2 on Dec. 23, 2012. Left is OMG, right is CrIS night, day. CrIS provides extra tracking information since retrievals can be done at night unlike OMG.

OMPS is also sensitive to SO_2, with better sensitivity to low altitude SO_2 due to shielding of that signal by water vapor in the thermal infrared. However, volcanic SO_2 is often ejected well above altitudes shielded by the water bands. However, OMG can only detect, track SO_2 and ash during the day, while CrIS can provide information day and night. Figure 30 shows detection of SO_2 by OMG on Dec. 23, 2012. On the right, we show the nighttime detection of the same volcanic eruption, not seen by OMG, along with the CrIS daytime detection of SO_2 which is similar in morphology and location to what is seen by OMG. Again, the CrIS SO_2 is just a B(T) bias *signal* relative to the bias of the CrIS radiances relative to radiances computed using NWP model fields.

4.4.4 Dust, Ash

Desert dust and volcanic ash have strong spectral signatures in the 10 micron thermal infrared window. Numerous studies have shown the capabilities of AIRS and IASI to measure dust/ash optical depths, and dust altitudes in optically thick regions. Moreover, thermal infrared radiances can monitor dust over bright land surfaces, unlike MODIS, as well as provide retrievals at night. IASI has been used extensively for tracking volcanic ash clouds partially for aircraft safety applications. There have been no systematic retrievals of either dust or ash for AIRS, even though their capabilities are well established. Moreover, several studies have shown that AIRS (and other sounders) retrievals are compromised in the presence of dust, which is generally ignored in the Level 2/EDR retrievals. This brings into question a rather significant number of retrievals under often interesting atmospheric regimes.

The hyperspectral sensors also provide some ability to differentiate the chemical composition of the dust/ash clouds, which may ultimately provide important information on the source of dust, which is difficult to do otherwise since MODIS cannot track dust clouds over bright desert surfaces. Dr. Nikolay Krotkov (NASA/GSFC), for example, is very interested in using CrIS for volcanic eruption research and monitoring.

4.5 Cloud Products

AIRS has demonstrated skill identifying cloudy footprints, estimating the clear sky radiance and determining the cloud properties. The AIRS version 6 processing produces the following cloud products:

- multi-layered cloud fraction,

- cloud-top pressure,
- cloud-top temperature,
- cloud liquid water path,
- cloud ice optical thickness,
- cloud ice effective diameter, and
- cloud thermodynamic phase.

The cloud top pressures are generally consistent with MODIS thermal IR cloud products, especially when MODIS cloud heights are derived using CO_2 slicing. The reduced VIIRS thermal IR channel set severely limits its ability to continue the MODIS cloud data set because of the absence of CO_2 channels on VIIRS. The cloud ice and phase products are new for AIRS Version 6, providing a very sensitive measurement of cirrus particles in the thermal IR window region that is only possible with hyperspectral spectra. CrIS is capable of producing all of these products with similar (or better) capability and can be retrieved from the CrIMSS cloud-cleared IP product, *if* all CrIS cloud-cleared radiance channels are saved, which is not the case in the IDPS system. The cloud liquid water path is currently generated in the microwave retrieval, but is not saved. The lack of cloud retrievals within the CrIMSS IDPS system thus represents a major deficiency in the continuation of climate products from AIRS.

4.6 Longwave CLARREO

The CLimate Absolute Radiance and Refractivity Observatory (CLARREO) mission, is a Tier 1 NASA priority Decadal Survey mission that is now on hold until later this decade. CLARREO had three components, a long-wave infrared interferometer not un-similar to CrIS (but with far-IR channels), a short-wave solar reflected sensor, and a GPS occulation sensor. Given the excellent performance, stability, and overlap between AIRS CrIS, and IASI there is considerable promise that these operational IR sensors could provide a CLARREO-like infrared product starting in 2002 that could continue for the foreseeable future.

This is possible because the radiances produced by the operational sensors are significantly better than specification. Moreover, within the JPSS CrIS program, changes to the CrIS hardware for the J1 mission will further improve the radiometric accuracy (new blackbody design for example). In addition, new approaches for measuring climate trends with hyperspectral sensors (such as PDFs, as mentioned earlier in this report) *may* lower the CLARREO requirements on accuracy. Although AIRS/CrIS provide two measurements/day for diurnal coverage, this can be further improved if IASI is also included.

This will require rather immediate efforts, especially with regard to AIRS, since several personnel most familiar with the details of the AIRS TVAC calibration are nearing retirement. Work is being done within the ROSES “Satellite Intercalibration Interconsistency Studies” and the ROSES “Science Definition Team for the CLARREO Mission” to address some of these issues. However, the full involvement of the AIRS and NPP CrIS Teams, and close collaborations with EUMETSAT for IASI, will be needed to make a CLARREO-like long-wave product from AIRS+CrIS+IASI. Note that both H. Revercomb and L. Strow have been long-standing members of EUMETSAT’s IASI Science Sounding Working Group (ISSWG) and have excellent working relationships with that team, including the IASI Project Office at CNES. Both H. Revercomb and L. Strow also serve on the CLARREO Science Definition Team.

5 Appendix

We present here a slide from the NOAA STAR CrIMSS EDR review that summarizes the NOAA EDR Cal/Val results. The CrIMSS requirements are the red dotted lines. The red lines are the errors for the Mx7 IDPS software release scheduled to become operational in June 2013. The assessment is made relative to the ECMWF forecast/analysis, and is global.

As stated earlier, about ~ 70% of the existing IDPS CrIMSS EDRs are derived solely from ATMS, with the remaining ~ 30% derived from some combination of ATMS and CrIS radiances. Since updates to the IDPS CrIMSS EDR software take 6+ months to install, NOAA used the IDPS simulator (ADL) with new

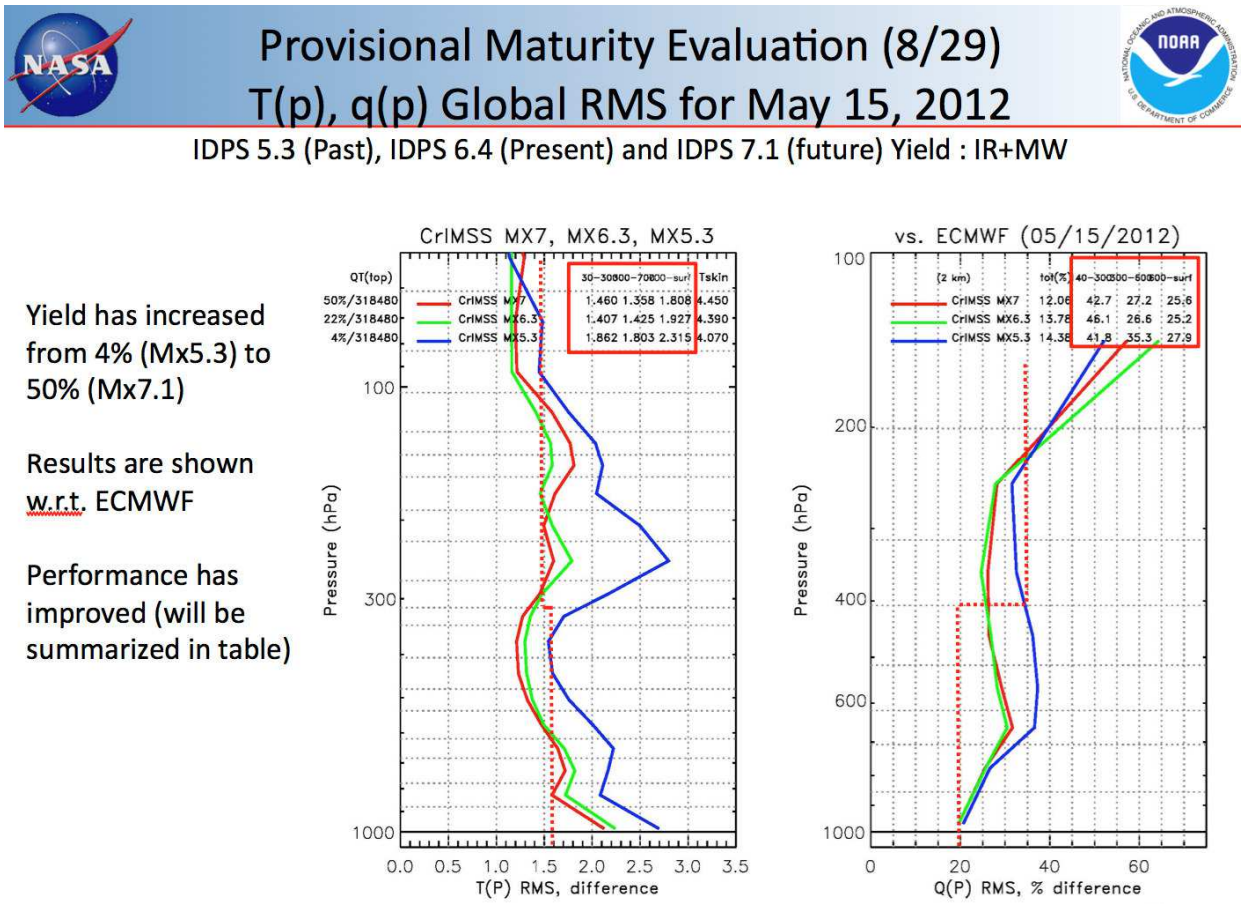

Figure 31: From NOAA CrIMSS EDR CalVal Assessment, C.Barnet. NOAA based EDR assessment on global statistics for 1 day for Mx7.1 software. Mx5.3 is a "past" version, Mx6.4 is the "current" version, and Mx7.1 is the "future" version, nominally June 2013.

updated EDR algorithms to compute one day's worth of EDRs, May 15, 2012. These results were used by NOAA for validation to bring the EDR to Provisional Status once the IDPS software install becomes operational.

Upcoming Publications

The on-orbit performance of CrIS/ATMS has been reported in numerous scientific conferences thus far, including the annual meetings of the American Meteorological Society, the American Geophysical Society (AGU), etc. AGU is planning a special issue for Suomi-NPP this year, which we form the initial basis for peer-reviewed assessment of CrIS/ATMS performance.

A good review of the wide range of products possible with hyperspectral sounders such as CrIS and AIRS can be found in [5].

References

[1] N Bormann and et.al. Evaluation and assimilation of the ATMS data in the ECMWF system. Technical Report 689, ECMWF, December 2012 2012.

[2] R Chu. Joint polar satellite system (jpss) advanced technology microwave sounder (atms) sdr radiometric calibration algorithm theoretical basic document (atbd). Technical report, NASA GSFC, 2007.

[3] Lieven Clarisse, Cathy Clerbaux, Frank Dentener, Daniel Hurtmans, and Pierre-François Coheur. Global ammonia distribution derived from infrared satellite observations. *Nature Publishing Group*, 2(7):479–483, June 2009.

[4] C L Heald, Jr J L Collett, T Lee, K B Benedict, F M Schwandner, Y Li, L Clarisse, D R Hurtmans, M Van Damme, C Clerbaux, P-F Coheur, S Philip, R. V. Martin, and H O T Pye. Atmospheric ammonia and particulate inorganic nitrogen over the United States. *Atmospheric Chemistry and Physics*, 12(21):10295–10312, 2012.

[5] Fiona Hilton, Raymond Armante, Thomas August, Chris Barnet, Aurélie Bouchard, Claude Camy-Peyret, Virginie Capelle, Lieven Clarisse, Cathy Clerbaux, Pierre-François Coheur, Andrew Collard, Cyril Crevoisier, Gaelle Dufour, David Edwards, Francois Faijan, Nadia Fourrié, Antonia Gambacorta, Mitchell Goldberg, Vincent Guidard, Daniel Hurtmans, Samuel Illingworth, Nicole Jacquinet-Husson, Tobias Kerzenmacher, Dieter Klaes, Lydie Lavanant, Guido Masiello, Marco Matricardi, Anthony McNally, Stuart Newman, Edward Pavelin, Sebastien Payan, Eric Péquignot, Sophie Peyridieu, Thierry Phulpin, John Remedios, Peter Schlüssel, Carmine Serio, Larrabee Strow, Claudia Stubenrauch, Jonathan Taylor, David Tobin, Walter Wolf, and Daniel Zhou. Hyperspectral Earth Observation from IASI: Five Years of Accomplishments. *Bulletin of the American Meteorological Society*, 93(3):347–370, March 2012.

[6] D. et.al. Kunkee. SSMIS radiometric calibration anomalies - part i: Identification and characterization. *"IEEE Trans. on Geoscience and Remote Sensing"*, 46(4):1017–1033, April 2008.

[7] R. Leslie and et.al. S-NPP advanced technology microwave sounder: Reflector emissivity model, mitigation, and verification. In *IGARSS 2013 Proceedings*, 2013. in review.

ATMS performance assessment

Interim report

April 2013

Bjorn Lambrigtsen

Van Dang, Mathias Schreier

Jet Propulsion Laboratory, California Institute of Technology

lambrigtsen@jpl.nasa.gov

Tel: 818 354 8932

Contents

Summary and Recommendations

Instrument performance

Findings

1. The instrument is largely performing to spec, but a few channels show anomalous behavior that needs to be further investigated
2. Radiometric sensitivity is better than specs for most channels
3. There is noticeable 1/f-noise in some channels
4. RDR statistical analysis does not reveal any significant anomalies, although radiometer count PDFs are not Gaussian
5. An exception is channel 17, which shows some anomalous behavior

Recommendations

1. The anomalous behavior of channel 17 should be fully characterized
2. Further analysis of non-gaussian count PDFs is needed
3. Pointing verification should be done
4. Analysis of lunar interference with calibration should be done

Calibration performance

Findings

1. 1/f-noise is noticeable in some channels and results in noisy calibration and resulting striping in TDRs/SDRs
2. Calibration coefficients exhibit orbital and other variability that cannot be fully accounted for by instrument temperature variations

Recommendations

1. TDR/SDR analysis needs to be repeated once NOAA has revised the calibration algorithms
2. Alternative calibration algorithms that would account for anomalous variability and meet climate stability requirements should be explored

Scan bias

Findings

1. There is substantial scan bias in most channels
2. The scan bias varies significantly from channel to channel
3. The scan bias is asymmetric

4. The scan bias varies along the orbit
5. The NOAA scan bias correction, which has not yet been determined, is expected to account for mean behavior only and is therefore unlikely to be adequate for producing climate quality ATMS SDR and IP/EDR products
6. The observed scan bias is largely explained by the scan bias model developed for Aqua/AMSU, but more analysis is needed to fully characterize the scan bias and develop a model that accounts for most of it

Recommendations

1. A climate-quality scan bias correction algorithm should be developed
2. This algorithm must account for scan-level variability; global or even orbital means will not be adequate
3. Residual bias rms error should not exceed 0.1 K

Calibration accuracy

Findings

1. Calibration accuracy appears to be dominated by the nadir component of scan bias
2. This is confirmed by SNO comparisons with NOAA-19, which is in the same orbit plane as NPP and therefore produces SNOs at all latitudes
3. PDFs of SNO-differences vs. mean scene temperature agrees with the Aqua scan bias model and indicates that a scene dependent bias correction must be applied to achieve climate quality calibration accuracy

Recommendations

1. A climate quality overall brightness temperature bias correction algorithm should be developed, in conjunction with a scan bias correction algorithm
2. Calibration bias estimates should be refined with analysis of vicarious uniform calibration scenes

Data processing

Findings

1. Only partial assessment of TDR processing has been possible so far, since the IDPS algorithms have not been fully mature
2. SDRs have not been available and have not yet be assessed
3. It is unlikely that IDPS TDR and SDR products will reach climate quality

Recommendations

1. NASA should process its own SDR products that implement adequate scan bias correction and calibration bias correction
2. It is possible that NASA may also need to process its own TDR products – pending an assessment of revised NOAA calibration algorithms
3. These steps will necessitate that NASA also process its own IP/EDR products
4. All ATMS IPs should be elevated to EDR status
5. A number of "missing" IPs should be added to the NASA product suite
6. The format of the data products should be updated to make the data more easily accessible; this applies particularly to RDRs, which are extremely difficult to access

The bottom line

- **Instrument performance**
  - Meets specs; Can generate climate quality data
  - Some 1/f-noise, but this can be mitigated in software
  - Considerable scan bias, as expected; must be mitigated in S/W
- **TDR/SDR data products**
  - Calibration algorithms still in flux due to “striping”
    - *JPSS may find adequate striping mitigation*
    - *If not, NASA may need to develop own strategy*
  - JPSS scan bias correction (TBD) may be adequate for NWP but not for NASA climate research
    - *If improved bias correction is not adopted by JPSS, NASA may have to process own TDR/SDR and subsequent IP/EDR products*
  - Error estimates: In progress
- **IP/EDR products**
  - Not yet mature enough to assess

Instrument performance appears to meet specifications in most regards, but our analysis of RDRs hint at anomalous behavior of some channels, particularly channel 17 but also several of the 183-GHz channels. The analysis is inconclusive at this time and requires further work.

For the most part channels exhibit random, gaussian noise, but here too there are anomalies that need to be further investigated.

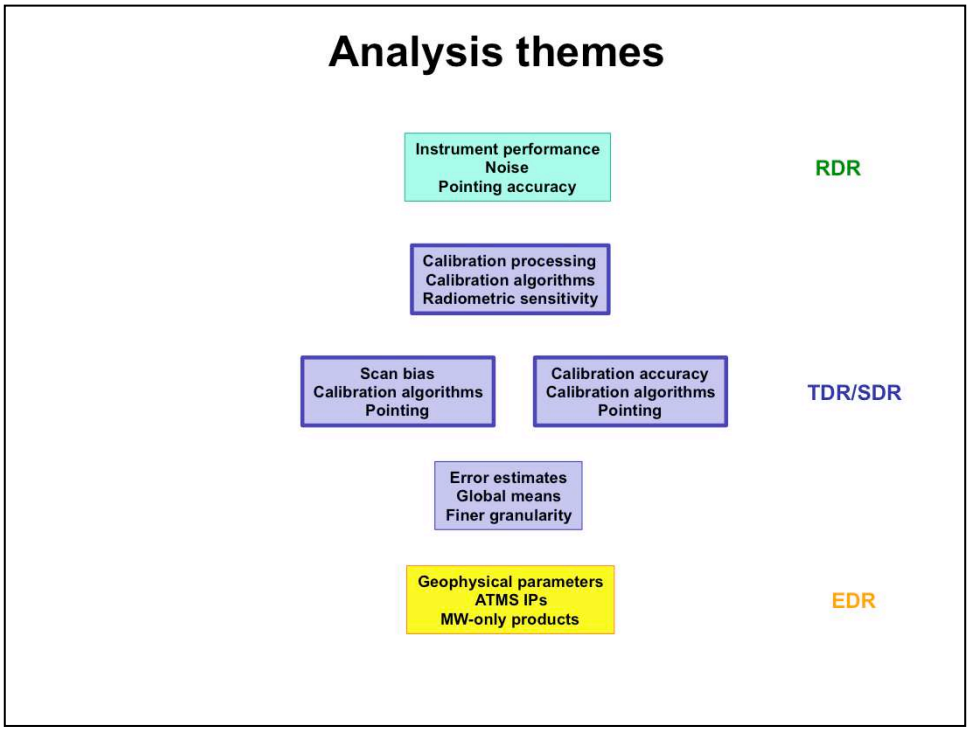

This is a graphical depiction of the general processing flow of ATMS data and the issues related to each product level that we have focused on or will focus on in further analysis

RDR analysis

- **The following pages illustrate analysis based on RDR data so far**
- **It does not yet include pointing analysis**

- **We note that RDR analysis is extremely time consuming and cumbersome due to the difficulties of reading RDR data**
  - **The RDR format is very difficult to deal with**
  - **Granules are too small**
  - **There is no standard reader available to the PEATE or Science Team**
  - **Existing readers are written in Matlab and extremely slow**
  - **It is nearly impossible to generate geolocated RDR data**
  - ***NASA must solve this problem!***

Repeating: NASA must solve the RDR reader problem

In general, the IDPS generated file structure is far from user friendly

Noise is better than specs

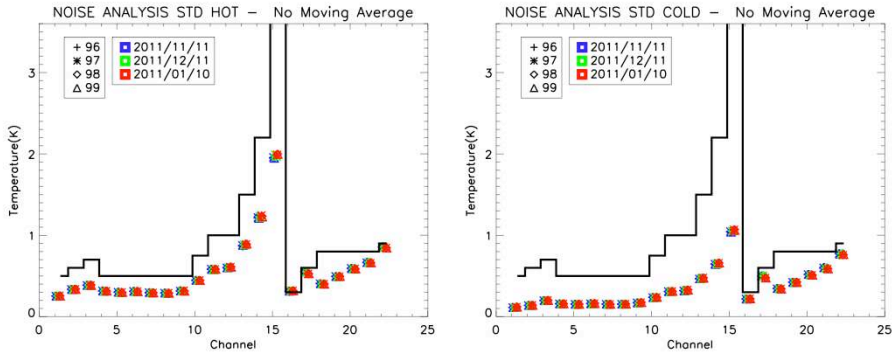

These plots show standard deviation of calibration counts scaled by a gain estimate for all channels (left: warm-cal, right: cold-cal)

The black lines show specs and the colored dots show actual performance on three different dates and for three scan positions. Performance generally is better than specs.

Orbital & secular trends

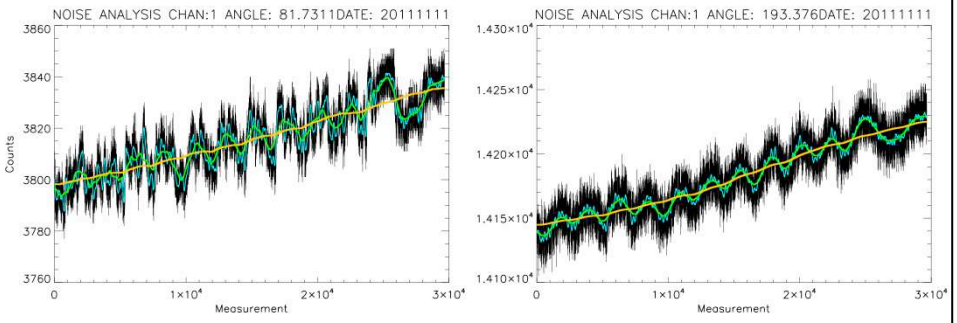

Radiometer calibration counts (left: cold-cal, right: warm-cal) exhibit substantial orbital and secular variations. This shows channel 1 as an example.

This is expected, but ***some channels show signs of abnormal behavior and will be further investigated***. Such analysis of Aqua/AMSU data revealed anomalous correlated noise in channel 7, which made that channel largely unusable. The analysis of channel 9 revealed occasional "popping" noise (sudden shifts in radiometer output), but this is mostly calibrated out and does not disable that channel from use. This analysis needs to be completed for ATMS.

Orbital variability

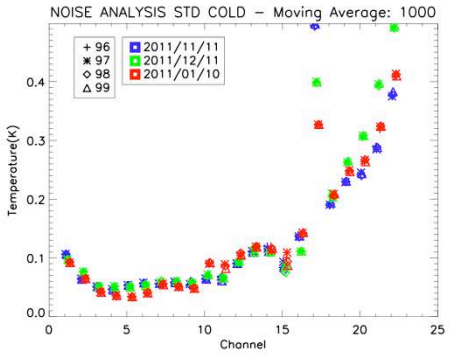

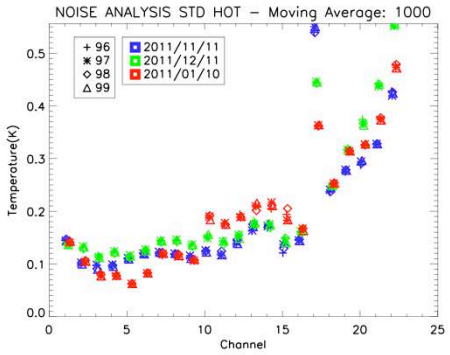

These plots show the standard deviation of the orbital component from the preceding plots, again for the calibration points (left: cold-cal, right:warm-cal)

Channel 17 is anomalous and must be further analyzed

Channels 19-22 exhibit unexpectedly large day to day variability and must also be further analyzed

Secular variability

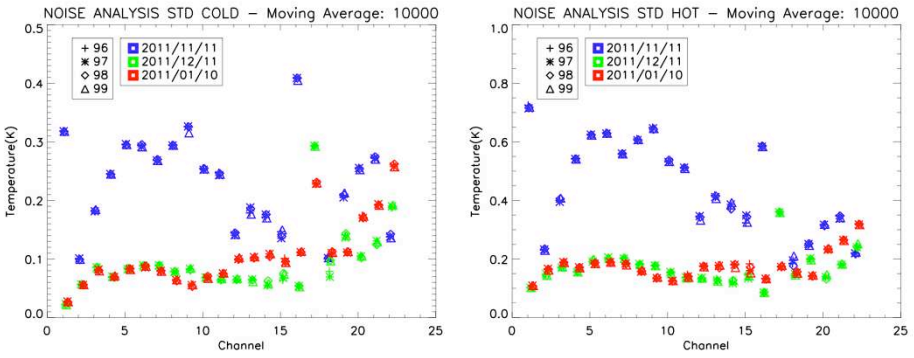

These plots, which focus on the longer term variations in the calibration signal, reveal unexpected large day to day changes. It may that one of the three days used in this comparison has invalid data – to be investigated.

Cold-cal is expected to be scene dependent due to radiation received through sidelobes that view the Earth

Warm-cal should only be dependent on cal-target and instrument temperatures. Such correlations must be established to explain the observed variability

Further analysis should also be done to determine the receiver noise temperature, which can only depend on (slowly varying) instrument temperatures and can be averaged over long periods and therefore determined quite accurately.

Optimal cold-cal position

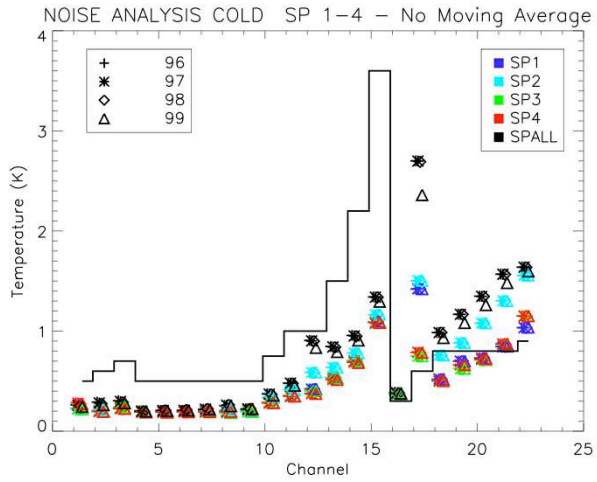

The optimal cold-cal scan position is the one that yields the lowest variability and lowest output (i.e. the position that has the cleanest view of space and smallest reception of Earth radiation through sidelobes)

This plot shows that this is generally SP4

The figure also shows that the standard deviations of the four readings for a given SP are not equal but is generally lowest for reading #99, while the other three readings are largely equal but higher. This suggests that these readings should not be averaged in the calibration processing and that only #99 should be used. This should be further investigated to determine if calibration performance would improve.

This plot also shows channel 17 to be anomalous

Scan bias: Why worry?

- **Operational users usually apply "tuning coefficients"**
  - Typically tuned against limited-scope ground truth (e.g., raobs from time t)
  - Accounts for global-mean bias
  - Data where 'obs-calc' is too great can simply be rejected and not assimilated with only minor consequences
- **But: Research users have different needs**
  - Need valid error characterization at all times, including accuracy (= bias)
  - Need valid data covering all weather/climate regimes of interest
  - Must avoid empirical tuning against a particular weather/climate state
- **Therefore: Scan bias must be fully characterized & modeled**
  - Global mean is not good enough
  - Empirical tuning against limited 'truth' is not good enough
  - Bias correction must be based on broadly valid physics

Scan bias will probably represent the greatest potential uncertainty in the context of ESDR/CDR production.

The baseline approach until now, for both NASA and NOAA, has been to tune out the scan bias. This is done by training a regression system against a set of raobs (or even model output in some cases) covering a relatively short time period. This essentially locks in the weather/climate state that existed during those raobs measurements, and the result may be a state bias.

Some have extended the training period to cover multiple years, but it is still possible to lock in a mean climate state. This approach also typically results in an improved mean but a larger variability around that mean – i.e. a reduced bias is traded for increased random uncertainty

This tuning approach is adequate for operational users, who typically do additional short-term tuning, since their time horizon generally extends only to a couple of weeks.

For climate research this approach is inadequate. We must avoid regression techniques and instead develop a physically based method to at least characterize the bias and uncertainty and preferably model the effect and correct for it. That is the goal of this analysis

Scan bias: Origin

- **MW antennas are imperfect**
  - Gaussian-shaped main "beam" receives 95-99% of energy
  - But: sidelobes outside main beam receive non-negligible 1-5%
- **Antenna sidelobes see some cold space at all times**
  - This results in effective antenna temperatures < primary scene temperature
    - → ***zeroth order effect: negative bias***
- **Sidelobe amplitude generally declines away from the main beam**
  - This results in a cold bias that grows with scan angle
    - → ***first order effect: scan angle dependent bias***
- **Instrument sits at edge of S/C → obstructed view of space on one side**
  - This results in a cold bias that is asymmetric
    - → ***second order effect: asymmetric scan bias***
- **MLI surfaces reflect/scatter extraneous radiation into sidelobes**
  - This results in scan bias depending on orbit location and sun angle
  - Polarization mixing effects may also play a role
    - → ***third order effect: orbit dependent bias – can be positive!***

As part of the post-launch Aqua AMSU assessment we developed a model that explains much of the observed scan bias. Here we list a hierarchy of effects that together make up the scan bias. The last one is particularly difficult to model and predict, but it is likely possible to model the others and make bias corrections to reducethem

We note that the zeroth order effect, an overall generally negative bias, also exists at nadir and contributes to the overall radiometric accuracy (bias) and therefore needs to be considered when calibration accuracy is assessed and validated. Some refer to this bias as the "beam efficiency bias"

Scan bias: Theoretical model

- **Measured antenna temperature is a composite integrated over all radiation sources**

  $T_{obs} \approx \langle f_e T_e \rangle + \langle f_c T_c \rangle + \rho \langle f_s T_s \rangle$

  - *<..> is mean over all solid angles*
  - *f is antenna amplitude (efficiency)*
  - *sources: e=earth, c=space, s=S/C*
- **Mean f's can be estimated from antenna pattern measurements**
  - But quality & density of measurements may not be adequate
  - Alternative is to estimate these parameters from on-orbit obs
- **Model was developed for Aqua 10 years ago**
  - Verified for AMSU

Example →

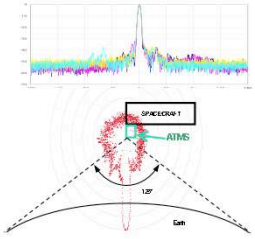

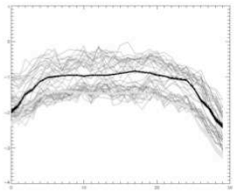

This slide summarizes the scan bias model that was developed for Aqua AMSU. The lower-right plot shows an example for one channel of the model (solid line) compared to observations (family of grey lines)

The example shows the result of implementing a mean bias correction that is linearly dependent on the mean scene temperature. It also illustrates that there is a residual error (represented by the spread of observations around the bias correction function), but it is seen to account for scan bias asymmetry quite well

The model needs to be fully implemented and must account for variability within the Earth disc visible from the instrument at any given time

The third order effect noted on the previous page also accounts for sizable variability at certain orbit locations and certain times and are difficult (but not impossible) to model and account for

We note that for a given scan position, a zeroth order scan bias correction could simply be a fixed value. This is the approach that has often been taken by operational users; it results in large residual bias errors that appear random

A zeroth-order correction could also consist of a linear correction with a fixed term plus a term that is proportional to the mean scene temperature, which is the next level of approximation to the equation shown above. This is likely the approach that JPSS will implement. As we show in subsequent pages, there are large residual errors resulting from this approach as well, and this method is not adequate for NASA climate use.

Scan bias: Data analysis

- **We use simulations to estimate observed scan bias relative to nadir**
  - Compute Tb from reanalysis fields
    - *OSS and MIT RTMs; CRTM coming*
  - Eliminate unknown overall bias by computing relative to nadir
    - *Nadir bias = calibration accuracy; to be determined by other means*
- **Analysis is not yet definitive**
  - Models produce unexpected left-right asymmetry
    - *Due to asymmetry in geophysical fields? TBD*
  - RTMs do not agree
    - *Resulting uncertainties need to be assessed*

The next few pages how examples of ATMS scan bias analysis

Scan bias - Model comparisons

Comparison of observations to simulations at nadir

MIT

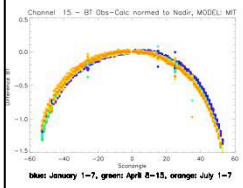

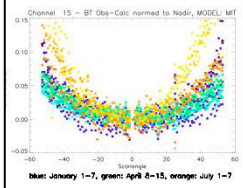

Example: Channel 15

Mean difference (upper panels):

- **Similar Scan bias form for both simulations**
- **But different magnitudes**
- **Only small seasonal differences**

Stddev of differences (lower panels):

- **Lower magnitude of variation forOSS models**
- **Slight increase on edges**
- **Stronger seasonal variation for MIT**

OSS

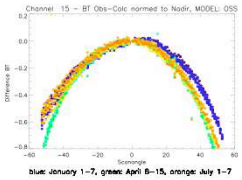

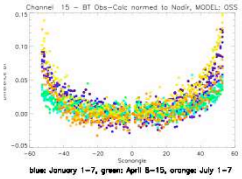

On this and following pages we show results of scan bias analysis

Much of this analysis uses model fields as a reference, to account for the normal zenith angel effect, i.e. we assume that the modeled scan profile correctly represents the normal limb brightening or darkening, which is of course also represented in the observations. By differencing the two we get an estimate of the anomaly in the observations caused by the scan bias.

We should note that these analyses are not definitive, due to uncertainties associated with the RTM. Comparisons between the two models the Sounder PEATE currently has access to (MIT and OSS), reveals significant differences between the two models. An example of that is shown above

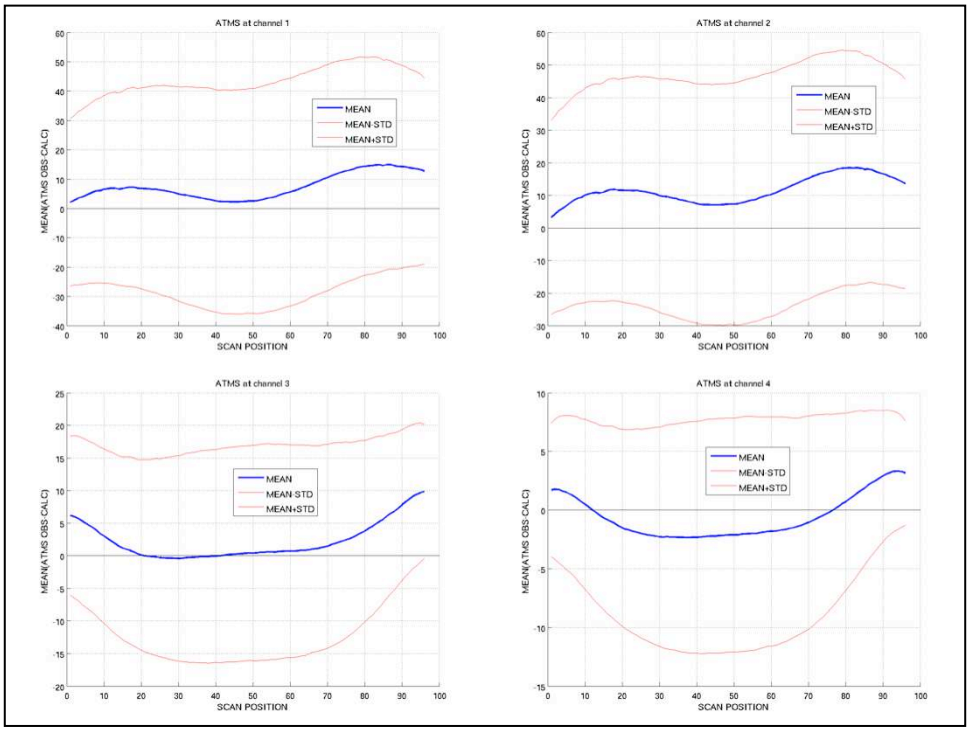

On this and the following 5 pages we show the results for each of the 22 ATMS channels of scan bias determined by comparing with modeled data, computed with a forward model (RTM) operating on ECMWF forecast fields.

The 4 pages following that shows in comparison equivalent analysis for Aqua AMSU

In each case we show plots of (obs-calc) vs. scan position number using three weeks of data; the blue line is the mean and the red lines denote the ±standard-deviation limits

Nadir bias (scan positions #47-48) should be ignored – this analysis is useful to determine relative scan bias only, i.e. to determine the shape of the bias

It should be noted that these results are only as good as the model, i.e. any unreal left-right bias or asymmetry in the model cannot be distinguished from instrument bias

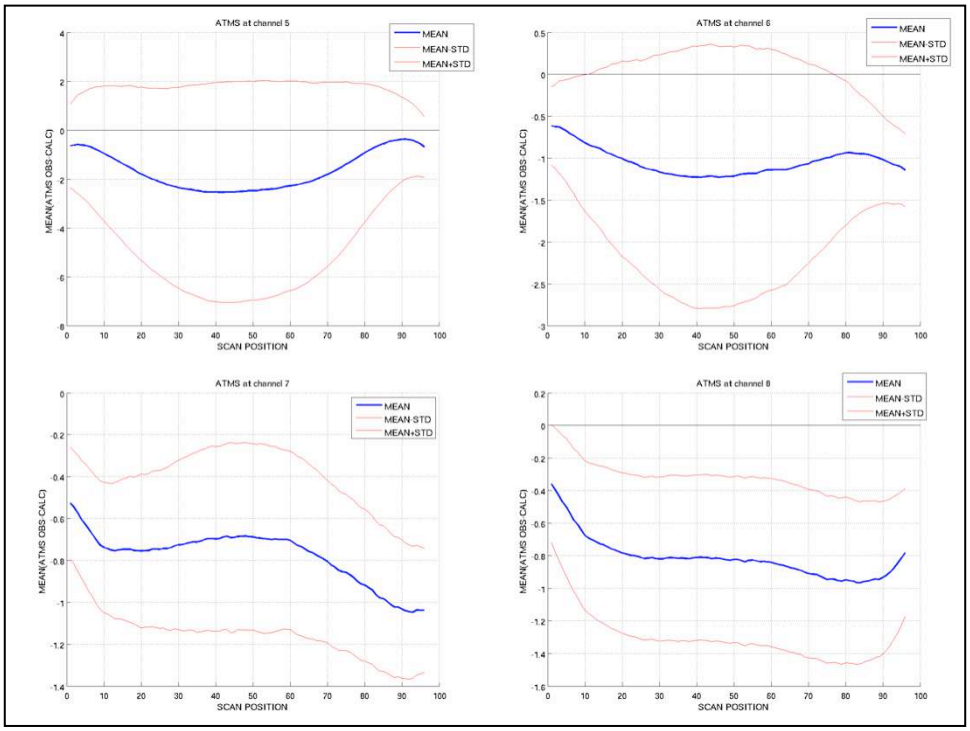

ATMS channels 5-8

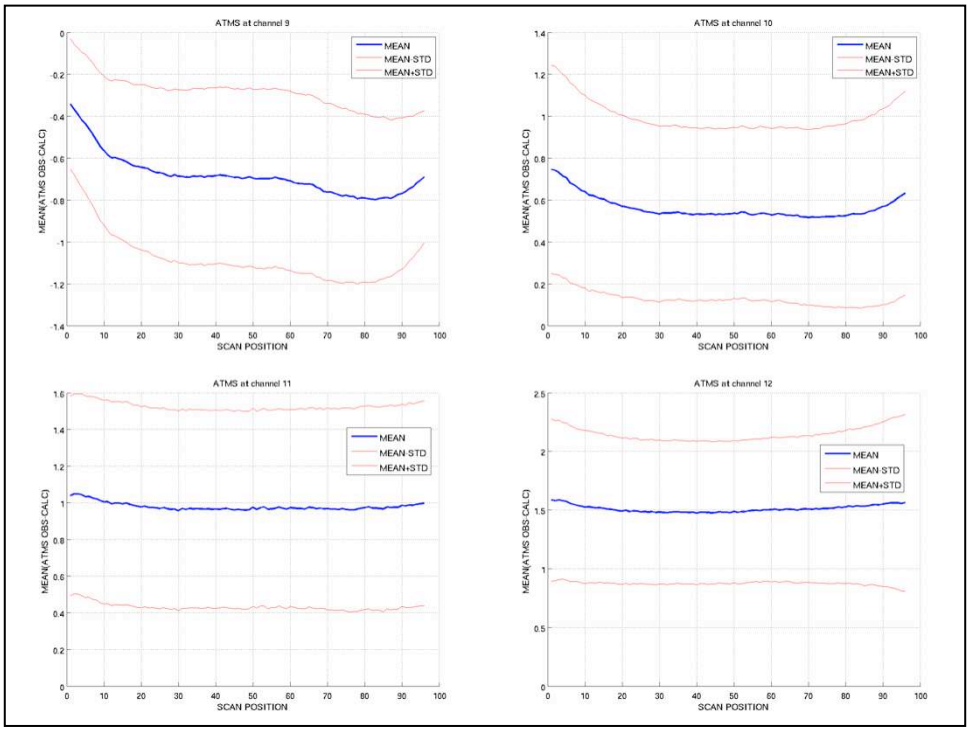

ATMS channels 9-12

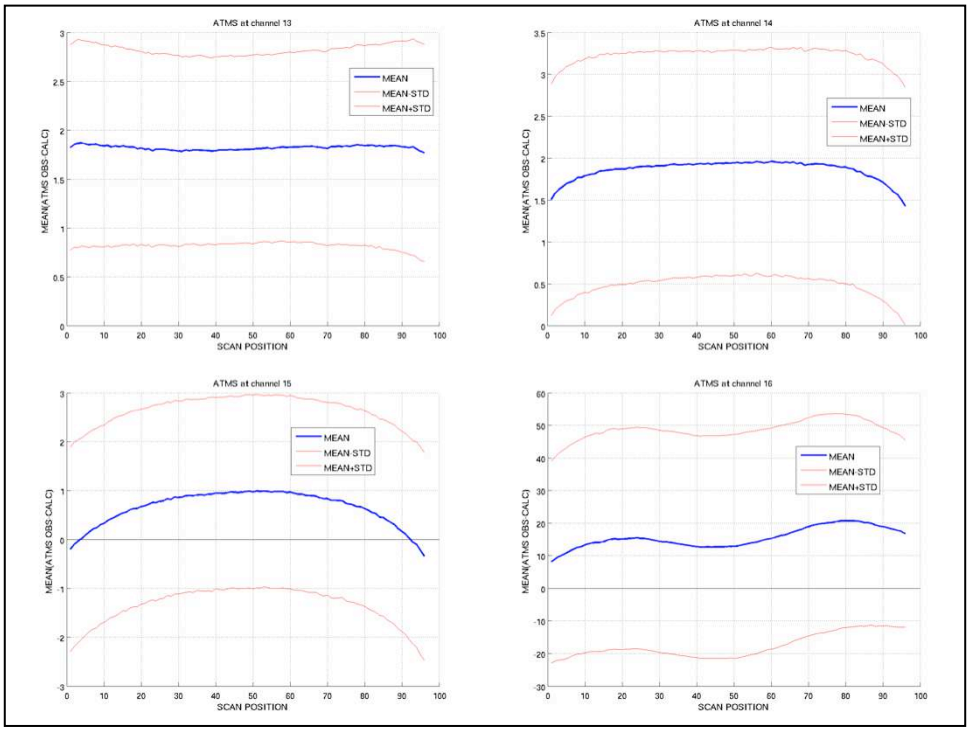

ATMS channels 13-16

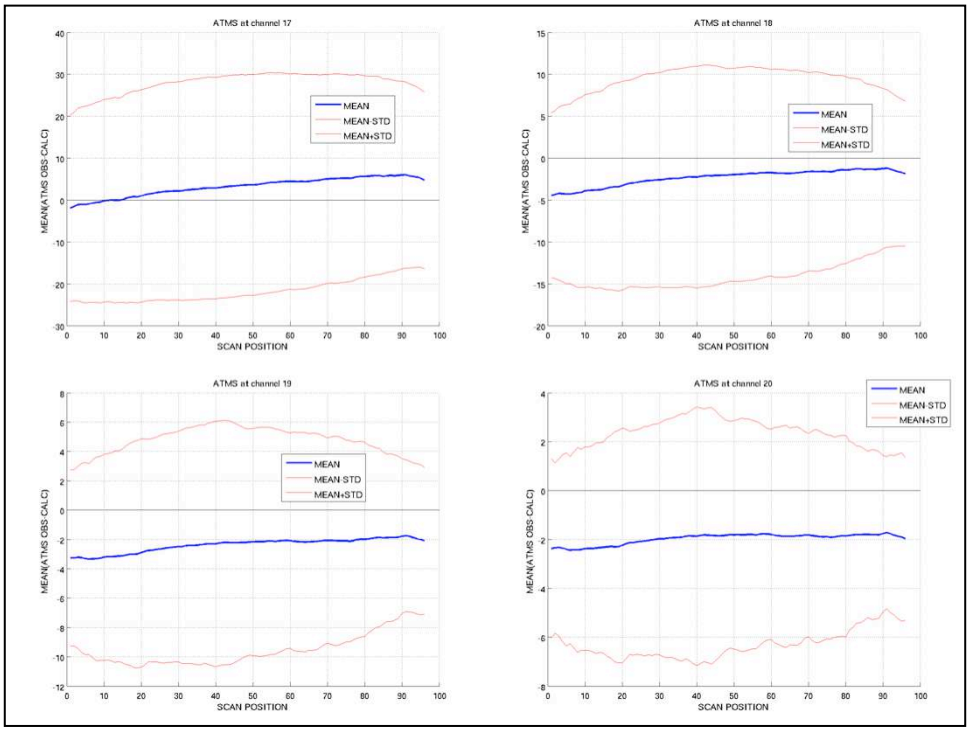

ATMS channels 17-20

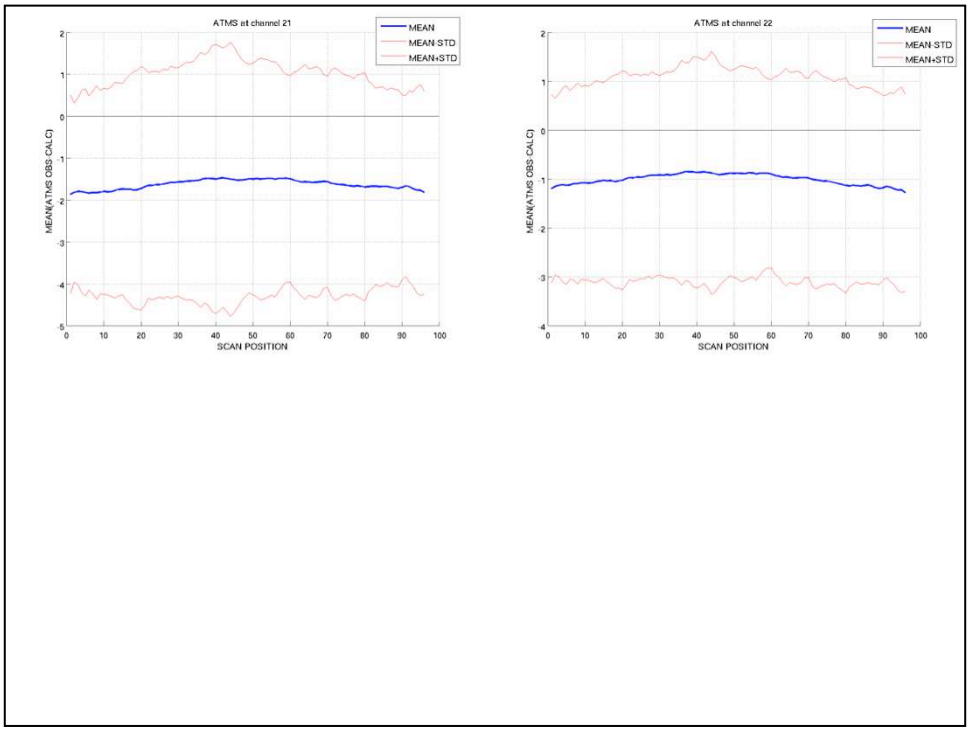

ATMS channels 21-22

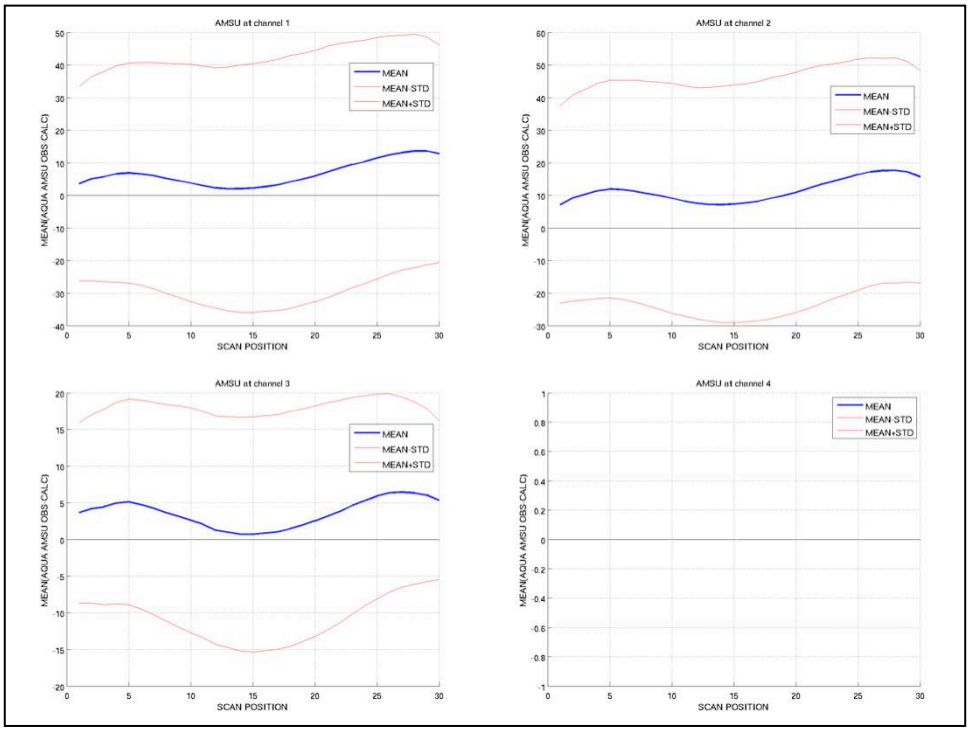

This and the following 3 pages shows the same analysis method applied to Aqua AMSU

An obvious difference is that Aqua AMSU has considerably more scan bias asymmetry in many channels than ATMS

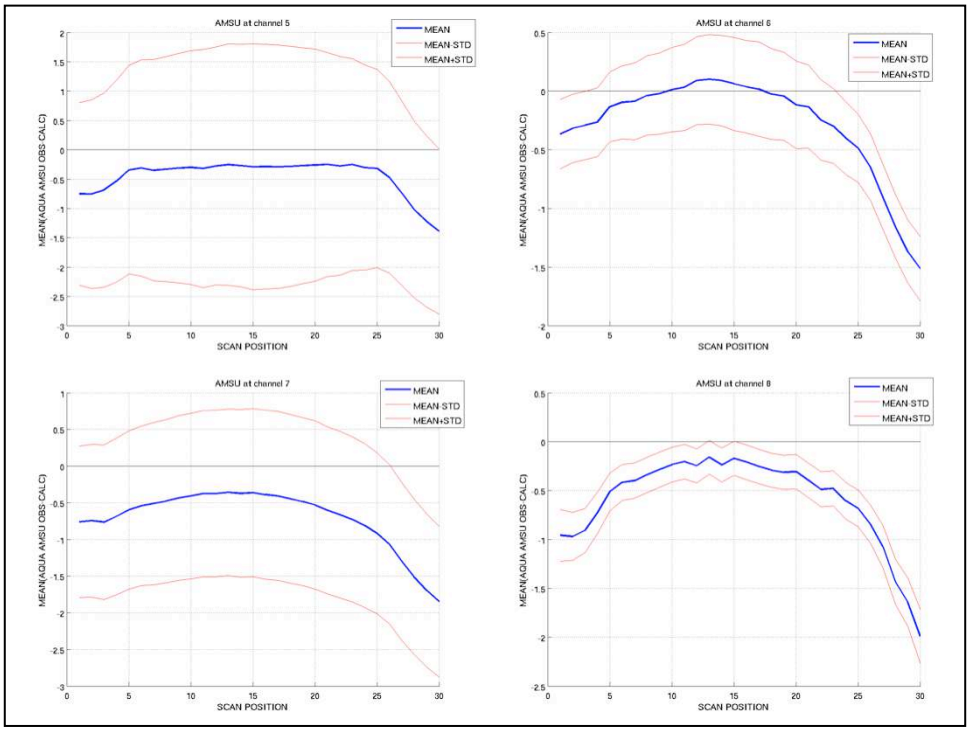

AMSU channels 5-8

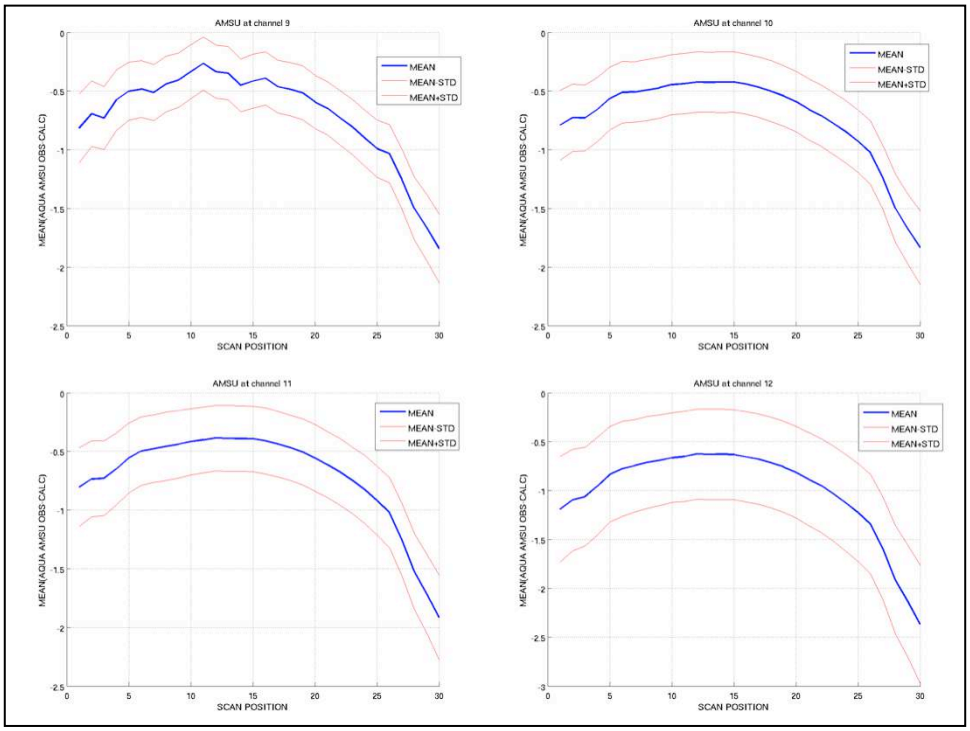

AMSU channels 9-12

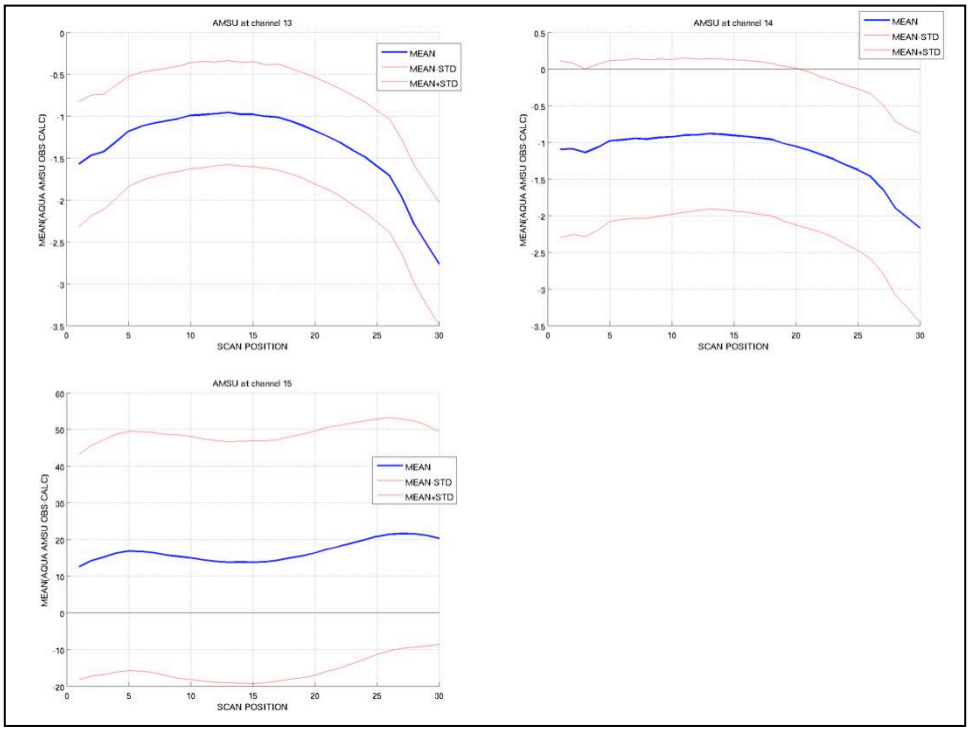

AMSU channels 13-15

Scan bias: Asymmetry

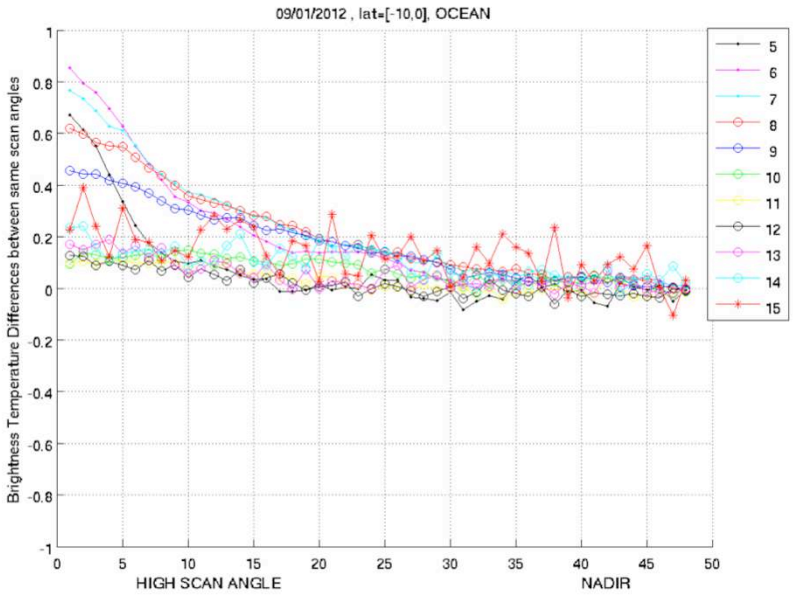

On this and the following pages we highlight the scan bias asymmetry
These results are not entirely self consistent, and further analysis is required

Above: Left-right difference relative to model (results are preliminary)

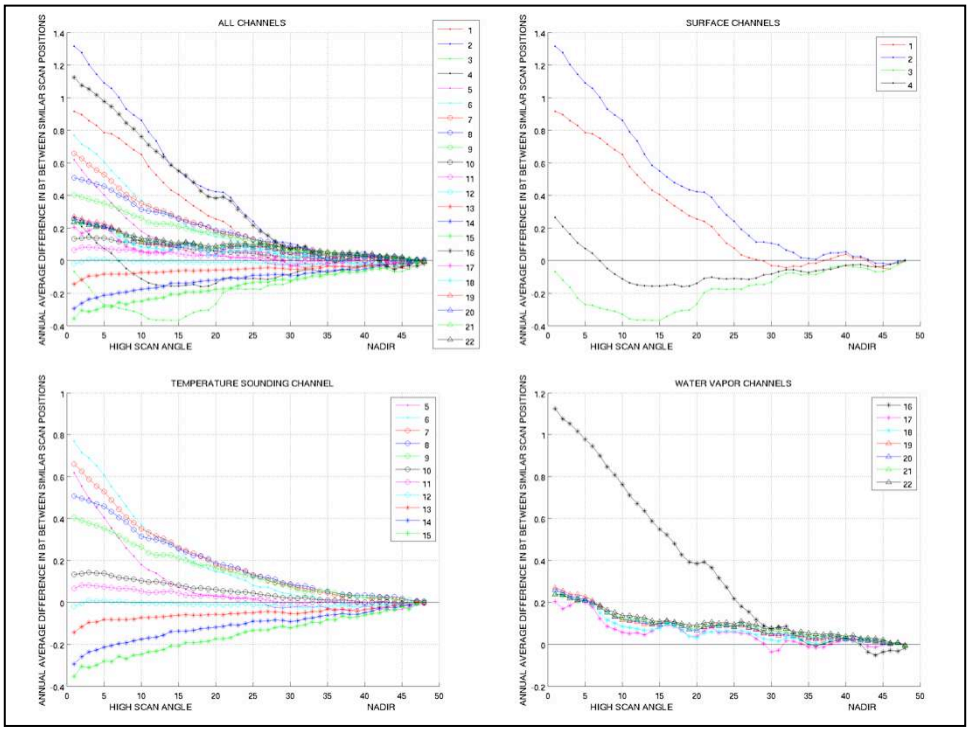

These plots show scan bias asymmetry entirely derived from the observations

The plots represent the annual average bias relative to nadir, i.e. left-right differences, corrected for latitude differences across the scan – which is done by interpolating along-track to the nadir latitude. This is expected to take out almost all of the apparent bias that would be due to latitudinal gradients (which can be substantial and amount to a large fraction of a Kelvin). We do not account for longitudinal gradients, since we expect those to be largely weather related and will average out. Diurnal gradients across the scan swath are assumed to be negligible – the swath is less than an hour wide in local time.

SNO analysis

NPP and NOAA-19 are nearly in the A-train

- **Therefore, SNOs between NPP, NOAA-19 and Aqua occur at all latitudes**
- **This allows for a much broader SNO analysis than usual**

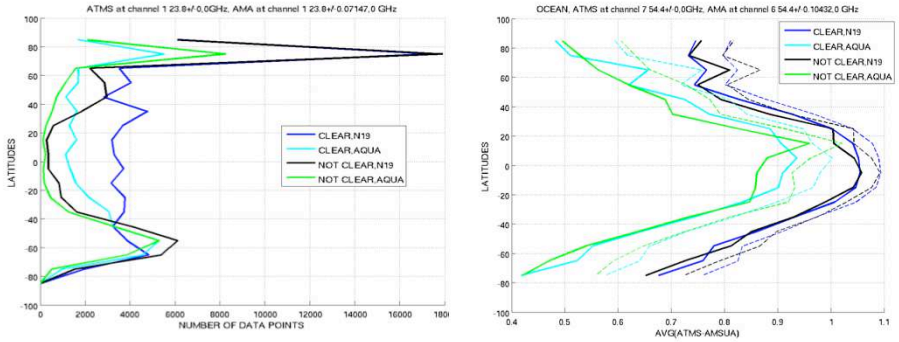

On the following pages we show analysis based on Simultaneous Nadir Observations (SNO). The analyses are largely based on NPP/ATMS-NOAA19/ AMSU SNOs, but we have also analyzed NPP/ATMS-Aqua/AMSU SNOs. The se are unusual in the sense that SNOs occur at all latitudes, since the NPP, NOAA-19 and Aqua orbit planes are nearly identical and the equator crossing times are close as well. Orbit altitudes are sufficiently different that the SNOs do not occur continuously but tend to be periodic.

The left curves above show the frequency distribution of NOAA-19 and Aqua SNOs by latitude and separated into clear and not-clear

The right curves show the corresponding brightness temperature differences for ATMS channel 7 (AMSU ch. 6). Our working hypothesis for the shape of those curves, where the difference between ATMS and the AMSUs is maximum at the equator, is that most of the relative bias with ATMS is caused by far sidelobe effects, which we referred to as the zeroth order scan bias effect. In other words, the observed nadir Tb is depressed due to sidelobe views of space.

The plots indicate that ATMS is less depressed than AMSU, and that is expected because ATMS presumably has smaller far sidelobes

Thus, the latitudinal dependence can be explained by the expectation that the scan bias is largest for the largest contrast between scene temperatures and space, which occurs at the equator for this channel.

Further analysis is need to verify this quantitatively

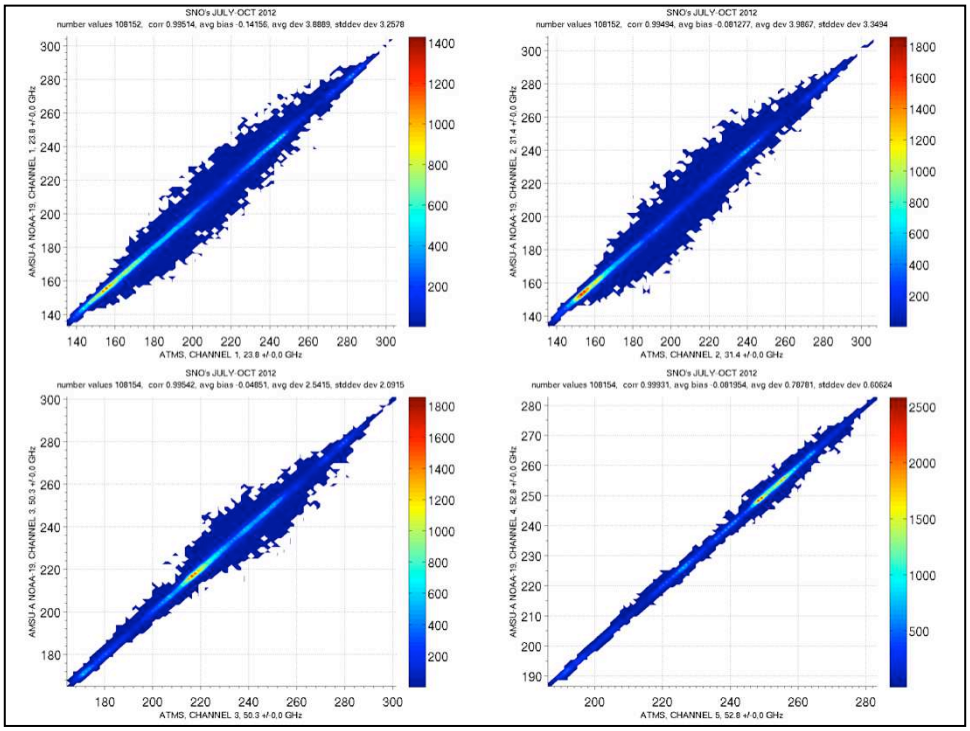

On this and following pages we show 2-dimensional histograms of ATMS vs. NOAA-19 AMSU SNOs. Some of the spread reflects slight SNO mismatches, for example where there are coast lines nearby. That is most apparent in the surface channels but becomes very small for the more opaque channels.

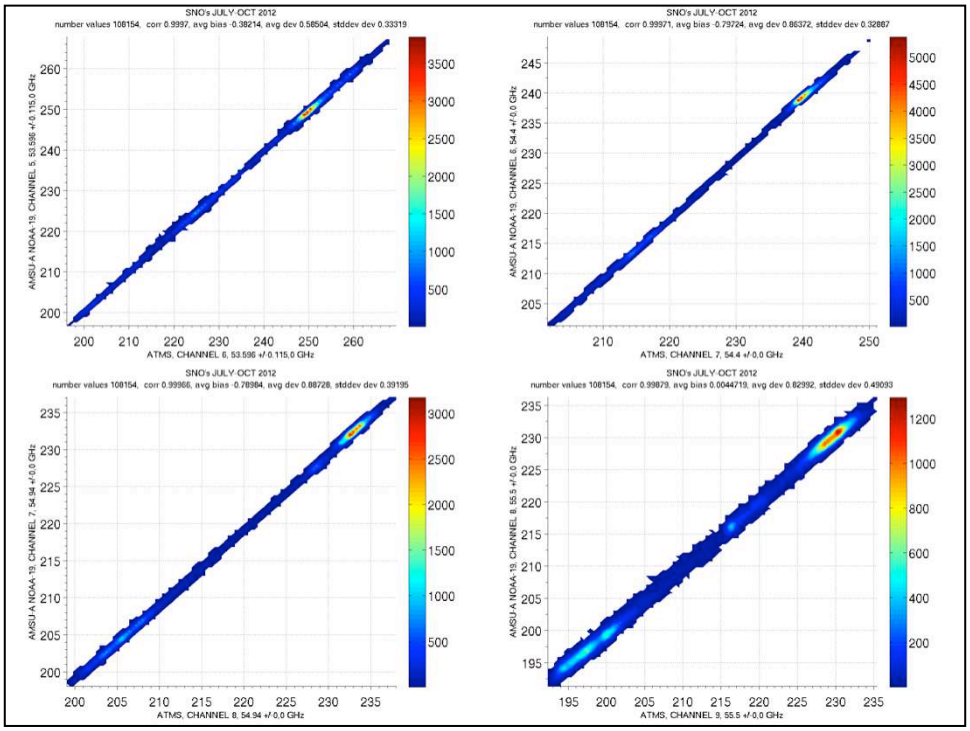

Note the change in scale from the previous plots

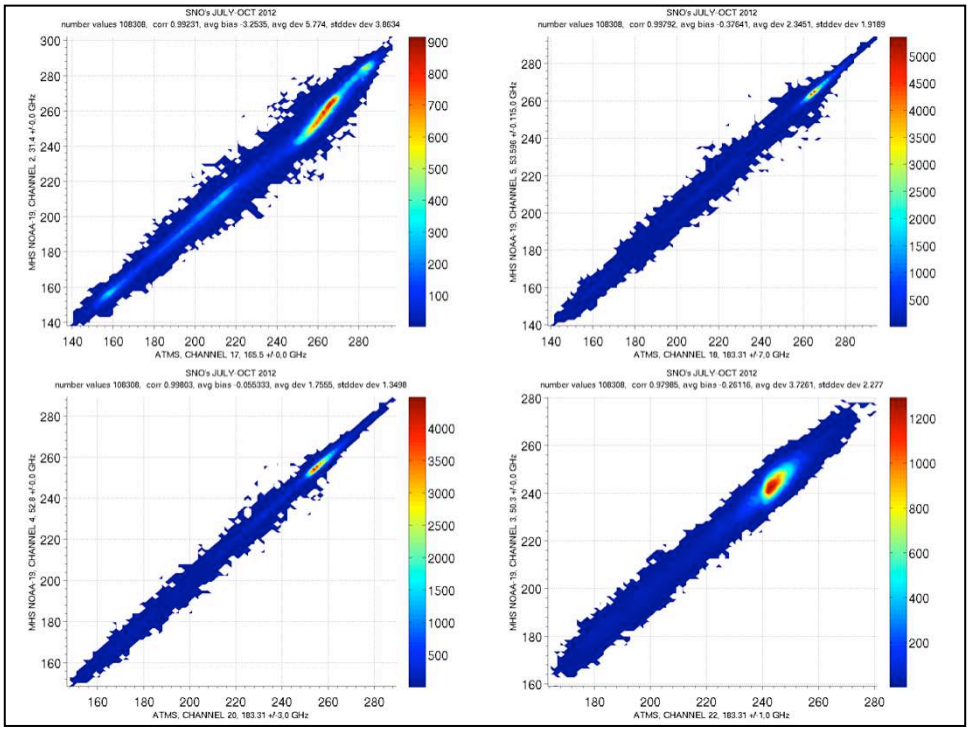
SNO's JULY-OCT 2012
number values 108308, corr 0.99231, avg bias -3.2535, avg dev 5.774, stddev dev 3.8634
MHS NOAA-19, CHANNEL 2, 31.4 +/-0.0 GHz
ATMS, CHANNEL 17, 165.5 +/-0.0 GHz
SNO's JULY-OCT 2012
number values 108308, corr 0.99792, avg bias -0.37641, avg dev 2.3451, stddev dev 1.9189
MHS NOAA-19, CHANNEL 5, 53.596 +/-0.115 0 GHz
ATMS, CHANNEL 18, 183.31 +/-7.0 GHz
SNO's JULY-OCT 2012
number values 108308, corr 0.99803, avg bias -0.055333, avg dev 1.7555, stddev dev 1.3498
MHS NOAA-19, CHANNEL 4, 52.8 +/-0.0 GHz
ATMS, CHANNEL 20, 183.31 +/-3.0 GHz
SNO's JULY-OCT 2012
number values 108308, corr 0.97985, avg bias -0.26116, avg dev 3.7261, stddev dev 2.277
MHS NOAA-19, CHANNEL 3, 50.3 +/-0.0 GHz
ATMS, CHANNEL 22, 183.31 +/-1.0 GHz

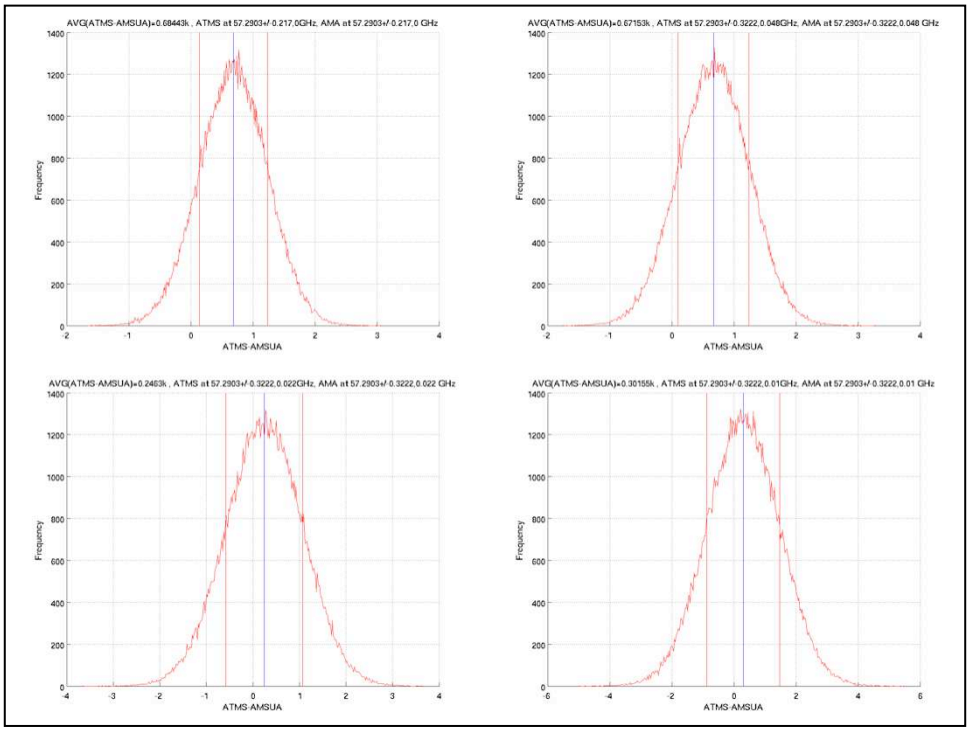

On this and the following pages we show histogram plots of the mean bias between ATMS and NOAA-19 AMSU for a subset of channels. The value of the mean bias can be found in the upper left of each plot

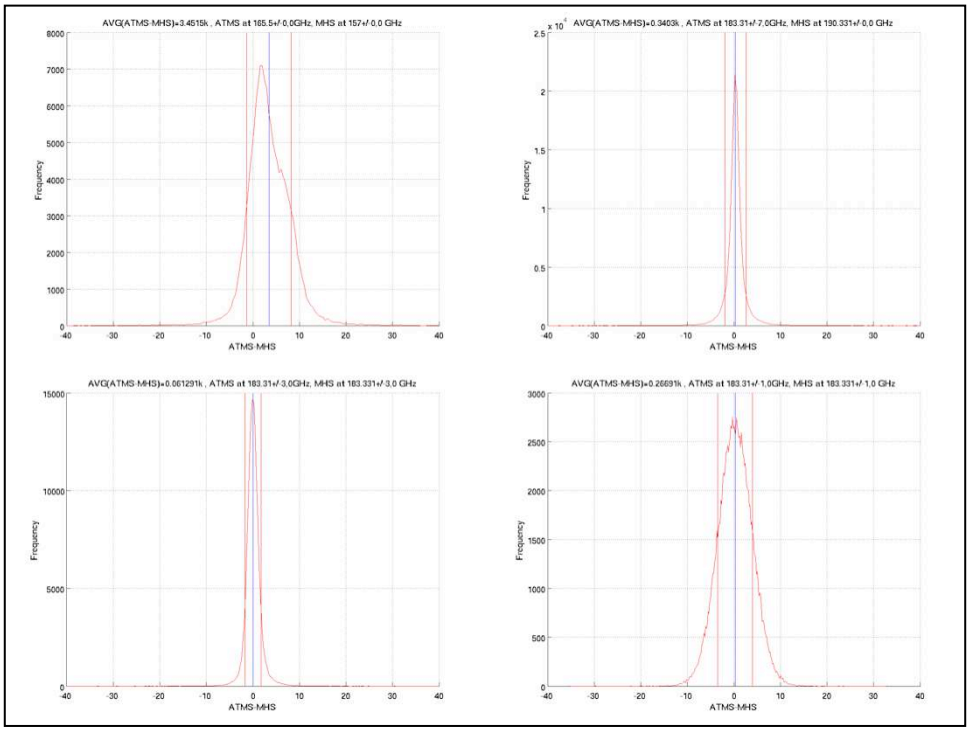

Water vapor channels

Scan bias: Putting it all together

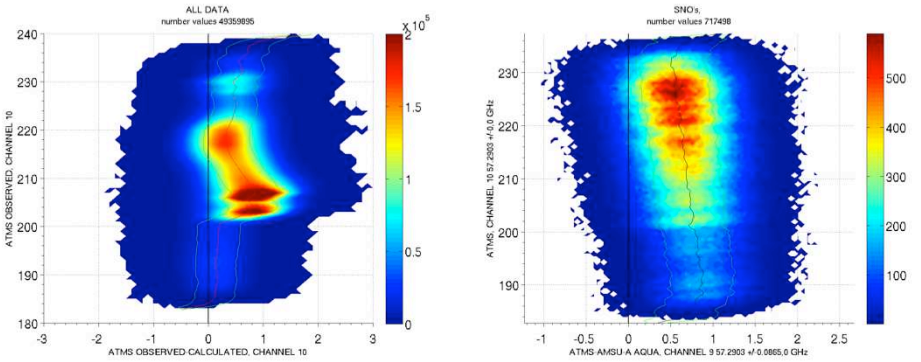

The left plot shows nadir obs-calc for ATMS ch. 10 at nadir, plotted against the nadir Tb. It exhibits the zeroth-order linear relationship that our scan bias model predicts (as discussed earlier), with a negative slope of about -0.046 K/K.

The right plot shows SNOs between ATMS and Aqua/AMSU for the same channel. It also exhibits a negative slope, but it is only about -0.0075 K/K

From these two results we would infer that the slope for Aqa/AMSU is about -0.038 K/K.

However, these results should not be taken at face value and are only shown to illustrate our methodology, although it seems likely that the apparent confirmation of the linear model can be trusted.

The uncertainty in the quantitative results arises from uncertain forward modeling ('calc'). On the next page we show an example.

Scan bias: Dubious results

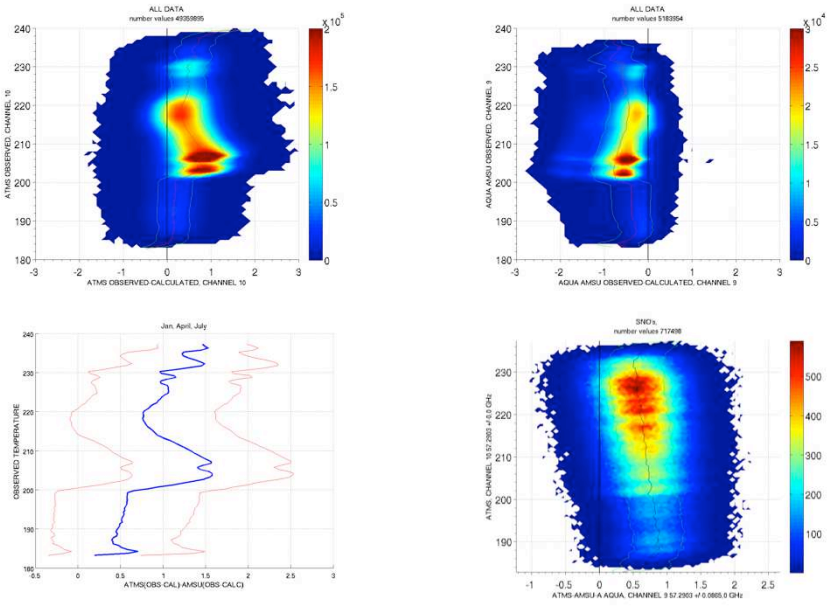

Here we show the same plots as on the previous page (upper-left and lower-right). In addition, the upper-right shows obs-calc for Aqua/AMSU (channel 9, corresponding to ATMS channel 10). It is the equivalent of the upper-left plot for ATMS. However, it exhibits a positive slope (about 0.023 K/K), i.e. the opposite of what we expect.

The lower-left plot shows the difference between the two obs-calc cases and represents what the model comparisons predict for the ATMS-Aqua/AMSU SNO comparisons. The model slope is clearly the opposite of the observed SNO slope. This is probably indicative of a model problem, which could be due to the RTM or the forecast fields.

There are additional "issues" at high latitude, which is where the anomalous values nears 230 K and below 200 K in the upper-left plot come from. These also differ significantly from the SNO observations.

The bottom line is that further analysis is needed with regard to scan bias

Calibration accuracy

- **Results based on comparison with model "truth"**
  - Computed from reanalysis fields
  - OSS and MIT models (CRTM pending)
  - There are issues with both truth fields and RTMs
- **Definitive estimates of calibration accuracy are pending**
  - Will account for beam efficiency (sidelobe bias)

Absolute calibration accuracy is difficult to determine on-orbit. In addition to the SNO analysis, we have done some preliminary analysis against models, but that is only relative to those sources, which are likely biased in various ways. This problem needs more work.

Overall bias against "Truth Fields"

MIT

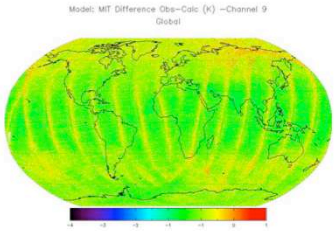

OSS

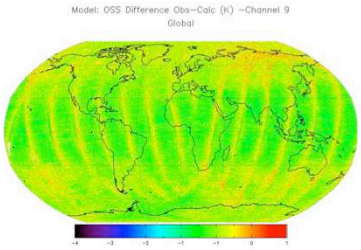

Here the "truth" is represented by simulations from forecasts. It can be seen that the observations appear to be uniformly unbiased near the tropics, where we have the most confidence, but the observations have not been corrected for the nadir "scan bias" referred to preciously.

Example, Channel 9:

- Small differences between model and observations
- Slight scan angle difference (see before)
- Slight latitude dependence
- Bias over Siberia

Overall bias for different areas/seasons

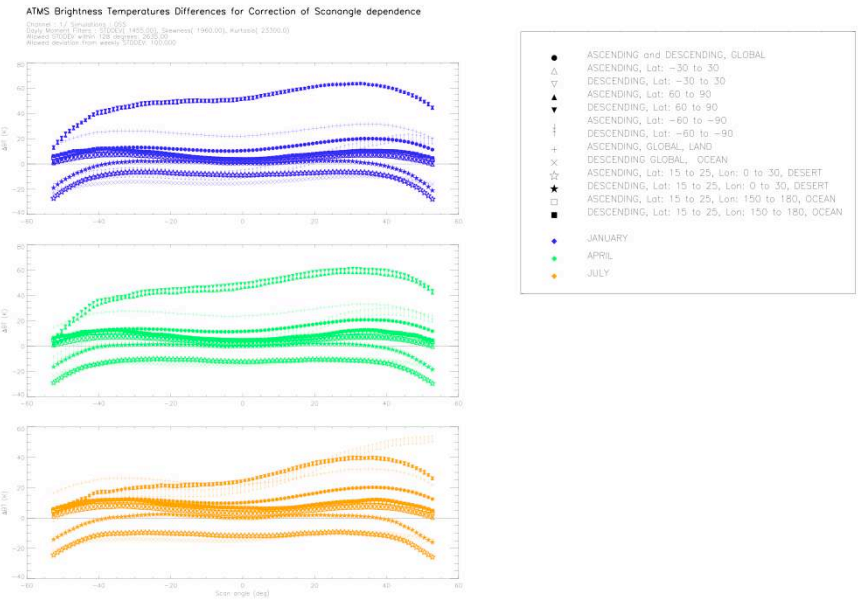

Example : Channel 1

- Small variation ascending/descending
- Slight Seasonal variation
- Strong Latitudinal Variation
- Strong Difference Land/Ocean

Calibration processing

- **Calibration algorithm will be updated by JPSS**
  - To eliminate "striping"
    - *Caused by noisy on-board calibration measurements*
    - *Cal-noise gets "frozen" into complete scan line → "striping"*
  - JPSS solution is to average cal-obs over wider time window
  - Could be problematic for channels with prominent 1/f-noise
- **Need to assess whether striping or JPSS mitigation is OK in climate context**
  - If not, we will explore alternative calibration algorithms
    - *Several possibilities exist*
- **For now: Wait until JPSS has reconfigured; then reanalyze**

The official calibration algorithms and coefficients are still somewhat in flux

This has been caused by the appearance of "striping" in some channels

Striping is not an unexpected effect and is likely caused by the fact that each scan results in updated calibration coefficients that are used to convert radiometer counts to brightness temperatures. Since the per-scan calibration measurements are noisy, there will also be noise in the resulting coefficients, and that noise is "frozen" into the scan line. Next scan line will have a different instantiation of the noise. This then appears as striping, i.e. a random jump in bias between the scan lines. It is perfectly normal, and the only issue is how to minimize the effective noise in the calibration coefficients.

The NOAA approach seems to be to widen the window that is used to compute the calibration averages. However, that approach can be defeated by the presence of 1/f-noise

1/f-noise is certainly present in ATMS in varying degree from channel to channel. It has the effect of preventing a reduction of the effective noise in an average beyond a certain number of averaging points, and we must analyze the revised calibration with that in mind. That analysis is pending definitive algorithms.

Optimal Averaging

Try to find the minimum of N for the averaging window, by using the RMS(counts)

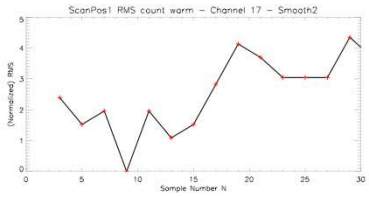

Minimum calculated by fitting a inverse Gaussian function to the measured data:

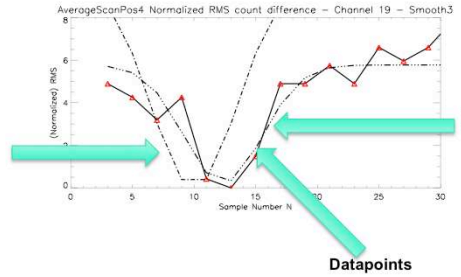

Furst Guess Gaussfunction

Resulting Gaussfunction

Datapoints

While we wait for NOAA to revise the calibration algorithms, we have done some preliminary analysis of the optimization problem

1/f-noise analysis

Tested for:
a) Calibration Targets (and their difference)
b) Different calibration positions (position 1-4 and average)
c) Different smoothing functions (Box function, Triangle, Gaussian)

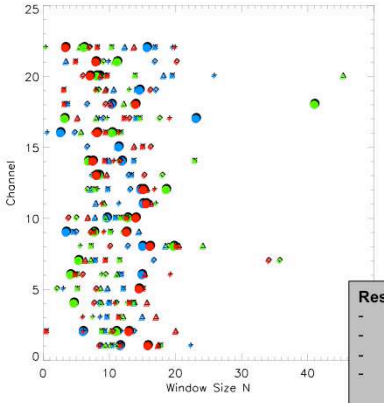

Shown: Minima for warm Target RMS(noise)

Results:
- Minima seems to be below N=20 in most cases
- Huge spread between Targets
- Averaging of Targets keeps minimum for N higher
- Box-Function or Gaussian have usually higher N

This page shows the results of preliminary 1/f-noise analysis